PNC TN8410 91-082

公開資料

The Third International Conference on Nuclear Fuel Reprocessing and Waste Management

RECOD '91 論文集（東海事業所）

1991年4月

動力炉・核燃料開発事業団
東海事業所

Ⓢ

公　開　資　料
PNC　TN 8410 91-082
1　9　9　1　年　4　月

The Third International Conference on Nuclear Fuel Reprocessing and Waste Management

RECOD '91 論文集（東海事業所）

編集担当者　松田　　瑛*

要　　旨

1991年4月14日～18日に宮城県仙台市で開催されたＲＥＣＯＤ'91に，東海事業所から発表した20件について，その発表論文を収録したものです。

なお，本論文集は，事業所の研究開発成果として，関係者の日常業務及び教育用資料として，広く活用されるものと考える。

* 技術開発推進部　技術管理室

目　　次

題　　名	CORROSION RESISTANCE OF SEVERAL METALS IN PLUTONIUM NITRATE SOLUTION		
発表先	RECOD'91		
発表地	仙　　台	発　表 年月日	平成3年　4月14日 ～ 4月18日
発表者 (○印口頭発表者)	所　属　名	再開部　CMS室	
	○武田誠一郎，永井　崇之，小泉　　務，林　正太郎		

(要　旨)

再処理プラントにとって装置の寿命延長は，稼働率向上の観点から，重要なテーマである。再処理溶液に含まれる元素のうち，プルトニウムは比較的高い酸化還元電位を持つことから，ステンレス鋼の腐食を加速することが懸念される。

ここでは，ビーカースケールで行った硝酸プルトニウム溶液中での各種金属材料の腐食試験の結果を報告する。

資　料　番　号
(80－02－216)

資料番号 80-02-216

CORROSION RESISTANCE OF SEVERAL METALS IN PLUTONIUM NITRATE SOLUTION

Seiichiro TAKEDA, Takayuki NAGAI, Tsutomu KOIZUMI and Shotaro HAYASHI

Power Reactor and Nuclear Fuel Development Corporation
Muramatsu 4-33, Tokai-mura, Ibaraki-ken,
Japan 319-11
Phone: 0292-82-1111

Abstract

Corrosion behavior of several metals exposed in plutonium nitrate solution was studied. Plutonium nitrate solution with the plutonium concentration ranging from 0.01 to 65g/l was used as a corrosive medium. Specimens made of type 304L (304L) stainless steel, type 310Nb (310Nb) stainless steel, titanium(Ti), titanium-5% tantalum alloy (Ti-5Ta) and zirconium(Zr) were used. Corrosion behavior of these metals in plutonium nitrate solution at the boiling point was evaluated through examining electrochemical characteristics and corrosion rates which were obtained by weight loss measurement. Three immersed corrosion tests, each being 96 hours long, were performed under conditions of continuous heating, no recharge of solution, and specific volume of 8 ml/cm^2. Anodic and cathodic polarization curves were measured using a potentio-static method. Polarizaton was started from the corrosion potential of each metal up to 1.1V vs SCE at a sweep rate of 50mV/min. The surface of the specimens after undergoing immersed corrosion tests were observed through a scanning electron microscope (SEM).

From the results of the corrosion tests, it was found that the corrosion rate of stainless steel, namely 304L and 310Nb, was enhanced by co-existant plutonium in the nitric acid solution. The corrosion potential of stainless steel shifted to the noble region in proportion to the increase of plutonium concentration. It is thought that the shifts in corrosion potential of the stainless steel to the noble region caused an increase in anodic current which brought about an incremental increase in corrosion rate. Valve metals, namely Ti, Ti-5Ta and Zr, showed good corrosion resistance regardless of plutonium concentration. The stainless steel specimen surfaces observed by SEM became rough due to grain boundary corrosion in accordance with increases in plutonium concentration, whereas valve metals showed no signs of corrosion. The corrosion rates of stainless steel depended on the concentration of nitric acid only in the region of low plutonium concentration.

1. Introduction

For a reprocessing plant it is important to prolong the lifetime of equipment to improve plant availability. Plutonium, which is one of the distinctive elements in the reprocessing process, has a high redox potential. There is some concern that such elements with high redox potential such as plutonium could accelerate the corrosion rate of stainless steel in the transpassive region.

In order to better understand the influence of plutonium on the corrosion behavior of metals, corrosion tests in plutonium nitrate solution were performed .

2. Experiment

(1) Test Specimens

304ULC, 310Nb, Ti, Ti-5Ta and Zr were tested as candidate materials for reprocessing equipment. Platinum (Pt) was used to measure the redox potential of the solutions.

(2) Test Solution

Plutonium nitrate solution consisting of 3M or 8M free nitric acid with a plutonium concentration ranging from 0.01 to 65 g/l was prepared as the corrosion medium.

(3) Test Procedure

Three immersed corrosion tests were performed continuously for 96 hours per test under boiling conditions with continuous heating, no recharge of solution, and specific volume of 8 ml/cm². Anodic and cathodic polarization curves under boiling conditions were measured using potentio-static methods. Polarization was started from the corrosion potential of each metal initially to the less noble region up to ca.200 mV (vs. SCE) and finally to the noble region up to ca.1000mV (vs. SCE). The surface of the specimens exposed in the corrosion solutions were observed by SEM occasionaly.

3. Results and Discussion

The influence of plutonium concentration on the corrosion rate of materials under boiling 3M free nitric acid conditions is shown in Fig.1. The corrosion rate of 304ULC is enhanced by increasing plutonium concentration, but Ti-5Ta and Zr, which are unaffected by plutonium concentration, show good corrosion resistance. Grain boundary corrosion was observed by SEM on the 304ULC specimens exposed in plutonium nitrate solutions.

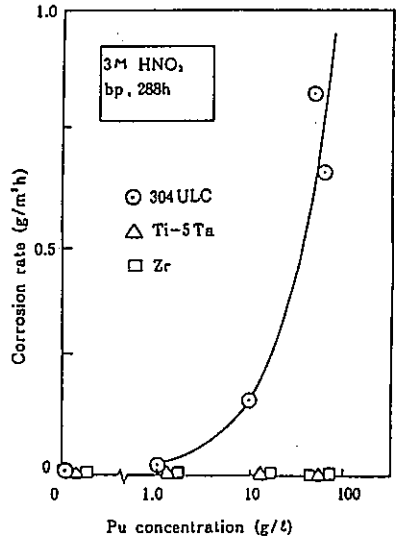

Fig.1 Influence of Pu concentration on corrosion rate of metals

This behavior was supported by the results of polarization measurements as shown in Figs. 2 and 3. Anodic polarization curves of 304ULC show the dependence on plutonium concentration. Corrosion potential shifts from the passivation region to the noble direction as plutonium concentration increases (Fig.2). On the other hand, Ti-5Ta shows no depndence on plutonium concentration in the anodic polarization curves and maintains a broad passivation region (Fig.3) .

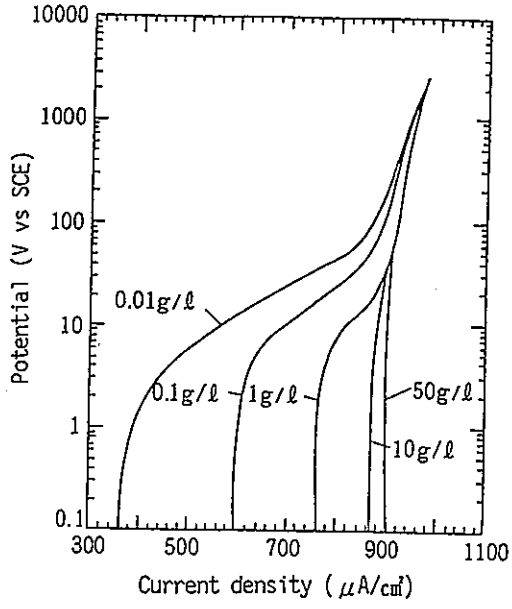

Fig.2 Anodic polarization curves of 304ULC measured in plutonium nitrate solution

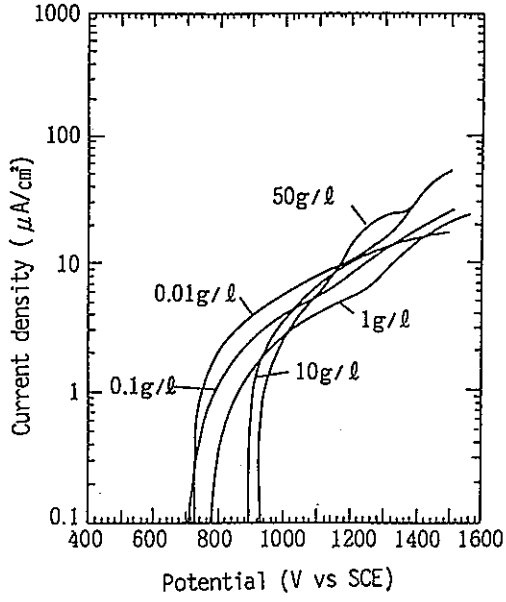

Fig.3 Anodic polarization curves of Ti-5Ta measured in plutonium nitrate solution

Corrosion potential of 304ULC shifts to noble direction in proportion to increases of plutonium concentration in 3M and 8M nitric acid solution. Corrosion potential seems to be influenced by plutonium ions more heavily in 3M nitric acid than in 8M nitric acid (Fig.4).

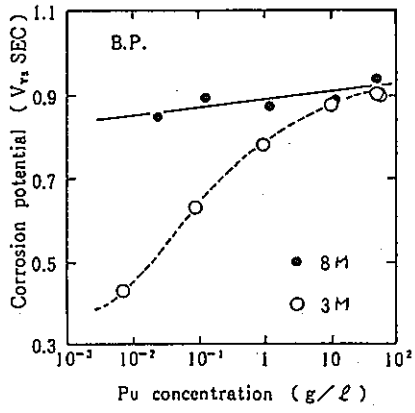

Fig.4 Relation between Pu concentration and corrosion potential of 304 ULC

4. Conclusion

It has been found that the corrosion rate of stainless steel, namely 304L and 310Nb, was enhanced by co-existant plutonium in nitric acid solution. The corrosion potential of stainless steel shifted to noble potential in proportion to the increase in plutonium concentration. It is believed that the shifts in corrosion potential of the stainless steel to the noble region caused a rise in anodic current which brought about an incremental increase in corrosion rate. Valve metals, namely Ti, Ti-5Ta and Zr, showed good corrosion resistance regardless of plutonium concentration. The surface of stainless steel specimens observed by SEM became rough due to grain boundary corrosion in accordance with increases in plutonium concentration, whereas valve metals showed no signs of corrosion. The corrosion rates of stainless steel depended on the concentration of nitric acid only in the region of low plutonium concentration.

題　　名	DEVELOPMENT OF FBR FUEL REPROCESSING TECHNOLOGY IN PNC		
発表先	RECOD'91		
発表地	仙　　台	発　表 年月日	平成3年　4月14日 ～ 4月18日
発表者 (○印口頭発表者)	所　属　名	再開部　CMS室	
	○河田東海夫，林　正太郎，武田　　宏，富樫　昭夫， J. G. Stradley		

(要旨)

過去20年間，動燃はＦＢＲシステムとその燃料サイクル技術の確立に向けて広範囲にわたるＲ＆Ｄを実施してきた。この中で，Ｆ再に関するＲ＆Ｄは関連する主要なＲ＆Ｄ施設を持つ東海事業所を中心に進められてきた。これらには，ＥＤＦ－Ⅰ，Ⅱで行われているプロセス機器開発のためのフールド及びウラン試験や，ＣＰＦでの燃焼度最大約 100,000 MWd／tまでの燃料の溶解抽出挙動を調べるホット再処理試験ＥＤＦ－Ⅲでの遠隔技術開発等がある。また，日米協力でＯＲＮＬとの共同により，連続溶解槽や遠心抽出器の開発等も進められている。これら新型の機器やプロセスの工程規模でのホット試験を行う新しい施設の設計が現在進められている。

資料番号
TN8100　91－002 (80－02－224)

資料番号 TN8100 91-002

DEVELOPMENT OF FBR FUEL REPROCESSING TECHNOLOGY IN PNC

T. Kawata, H.Takeda, A.Togashi, S.Hayashi, and J.G.Stradley*

Reprocessing Technology Development Division
Tokai Works
Power Reactor and Nuclear Fuel Development Corporation
Tokai-mura, Ibaraki-ken, Japan 319-11
Telephone: 0292-82-1111, Facsimile: 0292-87-0534

*Consolidated Fuel Reprocessing Program
Oak Ridge National Laboratory
P.O.Box 2008, Oak Ridge, TN 37831-6305 USA
Telephone: 615-574-7067, Facsimile: 615-574-4624

ABSTRACT

For the past two decades, a broad range of R&D program to establish fast breeder reactor(FBR) system and its associated fuel cycle technology has been pursued by the Power Reactor and Nuclear Fuel Development Corporation (PNC). Developmental activities for FBR fuel reprocessing technology have been primarily conducted at PNC Tokai Works where many important R&D facilities for nuclear fuel cycle are located. These include cold and uranium tests for process equipment development in the Engineering Demonstration Facilities (EDF)-I and II, and laboratory-scale hot tests in the Chemical Processing Facility (CPF) where fuel dissolution and solvent extraction characteristics are being investigated with irradiated FBR fuel pins whose burn-up ranges up to 100,000 MWd/t. An extensive effort has also been made at EDF-III to develop advanced remote technology which will provide increased plant availability and decreased radiation exposures to the workers in future reprocessing plants.

The PNC and the United States Department of Energy (USDOE) entered into a joint collaboration in which the US shares the R&Ds to support FBR fuel reprocessing program at the PNC. Several important R&Ds on advanced process equipment such as a rotary dissolver and a centrifugal contactor system are in progress in a joint effort with the Oak Ridge National Laboratory (ORNL) Consolidated Fuel Reprocessing Program (CFRP).

In order to facilitate hot testing on advanced processes and equipment, the design of a new engineering-scale hot test facility is now in progress aiming at the start of hot operation in late 90's. This facility features a large remote cell which accommodates both head-end and chemical process areas and will serve as a test bed for newly developed process or equipment by using actual spent FBR fuel assemblies.

INTRODUCTION

Recent growth of the concern for global change of the climate calls for a worldwide effort to reduce CO_2 emission into the atmosphere. In this light the importance of the nuclear energy utilization is being re-emphasized. Recycling plutonium in fast breeder reactor (FBR) system allows maximum use of uranium resources, and it has been regarded as one of the key elements in the long-term energy strategy in Japan which has to import virtually 100 % of its energy resources. In this regard, a broad range program for developing fast breeder reactors and associated fuel cycle technology has been pursued by the Power Reactor and Nuclear Fuel Development Corporation (PNC) for the past two decades.

The development of FBR fuel reprocessing technology is one of the most important elements to close a complete FBR fuel cycle. The technology is based on the combination of a chop-and-leach type head-end process and the Purex process for chemical separation, which is now very common in commercial reprocessing of light water reactor (LWR) fuels in the world. In Japan, a pilot scale reprocessing of LWR fuels has been continuing for more than fifteen years at the Tokai Reprocessing Plant (TRP) and an accumulated amount of the fuel processed in the plant exceeded 500 tons in November, 1990.

Since the basis for reprocessing technology had already existed, the R&Ds conducted so far have been aimed at following two objectives;

(1) Develop or improve the systems and components so as to overcome the problems due to the fact that FBR spent fuels have a hexagonal tube wrapping their fuel pin bundle and contain much more fissile materials and fission products than LWR fuels have.

(2) Improve efficiency and economy by introducing both advanced process technology with higher performances and advanced remote technology which leads to the increase of the plant availability and the decrease of the radiation exposures to the workers.

In order to achieve these goals, a variety of R&D works are in progress in PNC Tokai Works where many important R&D facilities are located.

GENERAL R&D FRAMEWORK

There are three Engineering Demonstration Facilities (EDFs) in Tokai Works devoted to FBR reprocessing technology development; the EDF-I for chemical components development and their uranium testing, the EDF-II for head-end components development, and the EDF-III for remote technology development. Also located in the same site is the Chemical Processing Facility (CPF) where laboratory-scale hot dissolution and flowsheet studies are being conducted with irradiated fuel pins from the experimental fast reactor Joyo and others.

In addition to the R&D activities at these facilities, the PNC entered in 1987 into a joint collaboration with the United States Department of Energy (USDOE) to enhance the developmental program in this field, and since then, many important activities have been in progress as joint efforts at the Oak Ridge National Laboratory (ORNL) Consolidated Fuel Reprocessing Program (CFRP).[1]

As near-term objectives, most of these R&D efforts are oriented towards the demonstration of key technologies in engineering-scale hot testing, and the design of the Recycle Equipment Test Facility (RETF) is in progress to provide the space for such experiments. The RETF features a large process cell which accommodates both head-end and chemical equipment areas and will serve as a test bed for newly developed processes or equipment by using actual spent fuel assemblies. The prototype FBR Monju

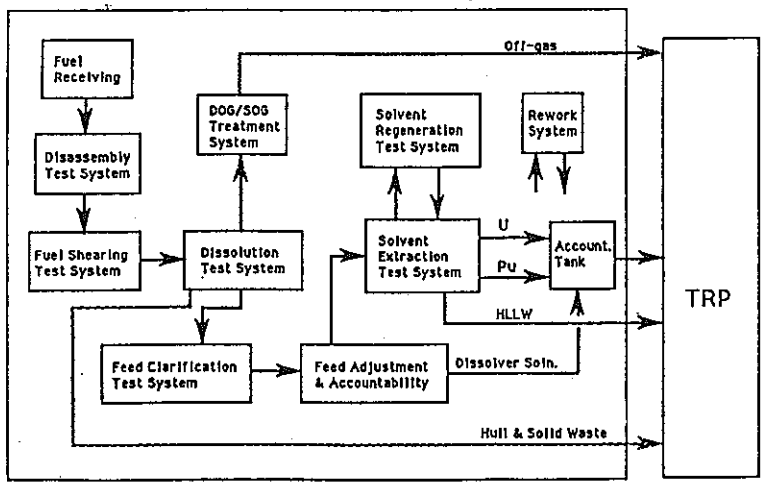

Fig. 1 RETF BLOCK FLOW DIAGRAM

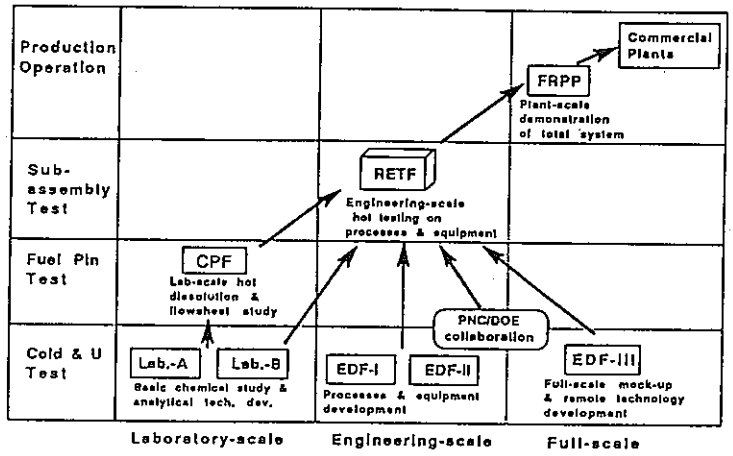

Fig. 2 DEPLOYMENT SCENARIO FOR FBR FUEL REPROCESSING TECHNOLOGY

which is scheduled to achieve initial criticality in 1992 will become the main source to supply such spent fuel assemblies.[2] The RETF is planned to be built adjacent to the TRP so that all the wastes and the intermediate products generated by the experiments can be further processed in the existing facilities. The major test systems planned to be installed in the RETF are shown in the block diagram in Fig. 1. The majority of the chemical equipment will be mounted on the racks arranged along either cell wall. The maintenance on these chemical components as well as mechanical components in the head-end area will be conducted by using an overhead crane and bilateral servo-manipulator (BSM) systems. The data and experiences gained from the RETF project and other R&Ds will become the basis for design of the pilot plant and future industrial plants with improved performance, reliability and economy. An overall strategy for the deployment of the FBR fuel reprocessing is illustrated in Fig. 2.

STATUS OF MAJOR R&D ACTIVITIES

Head-End Process Development

As for the removal of the hexagonal wrapper tube prior to fuel chopping, a disassembly system with a CO_2 laser has been developed and tested. A reference cutting scenario has been established from a series of laser cutting experiments with dummy fuel assemblies performed both at the EDF-II and the Integrated Equipment Test Facility (IET) at the ORNL. Based on these test results and experiences, a design of the RETF prototype system is in progress. Experiences on a fuel bundle shear gained at both PNC and ORNL are also fed to the design of the system to be used in the RETF.

For a fuel dissolution system, a geometrically safe rotary dissolver has been developed as a part of PNC/DOE collaboration. The design is based on the past experiences accumulated at the ORNL and the criticality control requirement set by PNC. As shown schematically in Fig. 3, the internal of the dissolver drum is separated into 8 stages by a spiral separator and the chopped fuel pieces are fed from one end and the heated nitric acid solution from the other end to form a counter-current flow. The nitric acid solution of 8 to 8.5 molar will be fed to produce dissolver solution with 3 to 3.5 molar acid concentration. The high acidity in feed nitric acid solution is favorable for enhanced dissolution of the mixed oxide with high Pu content used for typical FBR core fuels. The system sized to an hourly throughput of 10 kg is about 50 cm in outer diameter and 4 m long. Following the conceptual design, a plastic model of full scale in diameter but with only 4 stages was fabricated and a series of tests were conducted to verify the hull transfer capability in both normal and off-normal conditions. The results were reflected to the next phase of the design for RETF and the full-scale prototype

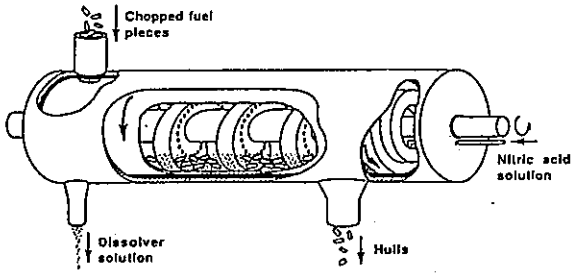

Fig. 3 SCHEMATIC VIEW OF CONTINUOUS ROTARY DISSOLVER

dissolver unit was fabricated for use in uranium testing. The prototype dissolver has been installed in the IET facility of the ORNL to make full use of existing peripheral systems. This dissolver unit was designed for full remote maintenance, and the test conducted on the prototype unit has demonstrated that the remote assembling or disassembling with the servo-manipulator system and the crane can be done within an hour or two. The preparation to start uranium test is now in progress.

Effective removal of the sludge in the dissolver solution is one of the key elements in the reprocessing of highly burned FBR fuels, and the development of a back-flushable centrifugal clarifier system has been continuing at the EDF-II. The latest version of the clarifier unit has a rotating bowl of 50 cm in diameter made of a light-weight alloy which can rotate at 6000 rpm.

In parallel with such components development, an effort is continuing at the CPF to further investigate the dissolution behavior of the mixed oxide and the characteristics of the insoluble residues in various conditions. The results are reported in the accompanying paper in this meeting.[3]

Chemical Process Development

In the chemical separation process in FBR fuel reprocessing, the solvent degradation due to radiation will be enhanced because of much higher level of fuel burnup than in LWR fuels. This problem will be best solved by utilization of centrifugal contactors which have significantly shorter residence time for the solvent in the system than conventional contactors such as mixer-settlers or pulsed columns have. The centrifugal contactors will also contribute to the improvement of the economy thanks to their remarkably small size and space requirement as well as their excellent operational flexibility due to very short startup/shutdown time.

An extensive effort had been made in early days for developing pulsed column and the technology was established through various experiments including those with full-scale test systems. Then the development of centrifugal contactors was initiated 5 years ago, and following early phase of basic studies and improvements, an engineering test system which consists of 34 contactor units was installed in the EDF-I in 1987. This system represents the extraction, scrub, strip and solvent wash sections. An extensive study has been conducted with the system not only to verify steady state behavior but to investigate the response to various upset conditions such as an abrupt reduction of solvent feed rate. A typical uranium concentration profile obtained in the

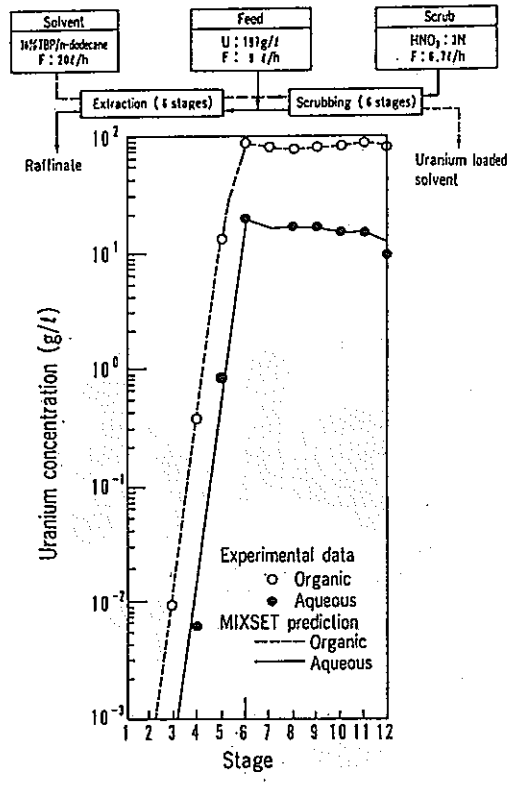

Fig.4 URANIUM CONCENTRATION PROFILES IN CENTRIFUGAL CONTACTORS

steady state operation is shown in Fig. 4 where an excellent agreement with the prediction by the "MIXSET" code is indicated. It has been demonstrated in the test that the centrifugal contactors also work very efficiently as a solvent washer.[4]

The ORNL has a long history in developing centrifugal contactors which has lead to many aggressive improvements in the design and performances.[5] Since the start of the collaboration, developmental efforts at both ORNL and PNC merged and the design of the prototype RETF contactor unit has been completed in a joint effort. A program to build and conduct uranium test with an experimental system which represents a portion of the RETF solvent extraction test rack is in progress. The system, named Chemical System Test, is being fabricated by the ORNL for installation at the IET facility. The outer view of the RETF prototype contactor unit is shown in Fig. 5. The unit was designed in a 4-stage pack for which the replacement of each driving motor unit can be easily done by remote handling.

As a part of the effort to eliminate the generation of secondary salt-bearing waste in the Purex process, a series of basic studies on solvent cleanup with salt-free reagents such as hydrazine oxalate and hydrazine carbonate have been carried out.[6] The feasibility of salt-free solvent cleanup process has been also demonstrated using 4-stage centrifugal contactor system.[4,7] The Pu reoxidation process is another point for which the salt-free process is addressed. An electro-oxidation technique was investigated for this purpose in a beaker-scale tests with actual Pu solution.[7] An engineering-scale electro-oxidation cell has been fabricated and installed at the EDF-I for uranium testing. The test will also be conducted with this electrolytic cell to decompose residual hydrazine oxalate in a spent solvent wash solution.

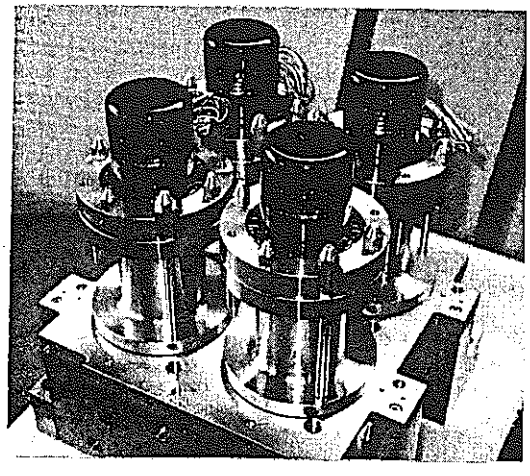

Fig. 5 PROTOTYPE RETF CONTACTOR UNIT

REMOTE TECHNOLOGY DEVELOPMENT

An improvement of the remote maintenance capability is the key element to increase plant availability and to decrease radiation exposures to the workers. A bilateral servo-manipulator (BSM) system combined with the rack concept is the main part of the solution to this challenge. The development of the "Prototype-II" servo-manipulator system (Fig. 6) has been completed and is being tested in the EDF-III.[8] The system utilizes radiation hardened electronic components and the slave arms are modularized so that the failed parts can be easily replaced by remote operation. Radiation hardened TV camera has also been developed as an in-cell viewing system.[9]

As described in the previous section, most of the chemical components in the RETF are mounted on the racks so that they can be removed or replaced as an unit when necessary. Since so many line connections are involved for each rack, a "roll-in rack" concept has been developed to make the tie-in of all the connectors easy. In this concept, each rack has special rollers attached on its bottom and can travel back and forth for approximately 50 cm towards the cell wall. Both male and female ferrules of the remote connectors are grouped and arrayed to form connector banks, and the engagement or the disengagement of all ferrules can be done simultaneously as the rack rolls in or out. The feasibility of this concept has been demonstrated in the tests jointly performed with the ORNL team on the full-scale experimental rack installed in the EDF-III.

In the RETF, an automated sampler will be used to retrieve sample bottles from sampling stations mounted on the top of the rack arrays. A prototype model of the remote sampling vehicle had been fabricated by the ORNL and transferred to the EDF-III. Remote operation and maintenance tests are in progress with this model there.

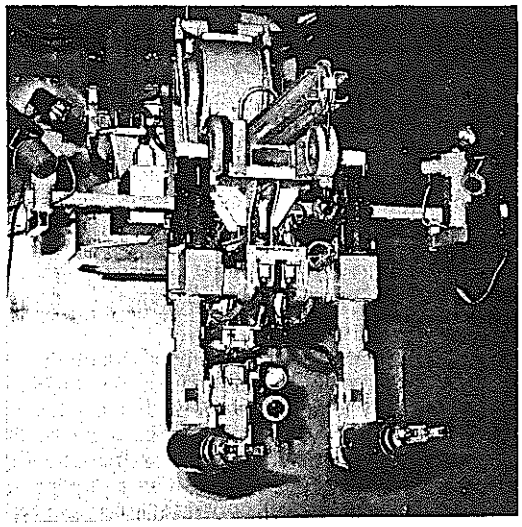

Fig. 6 PROTOTYPE-II BILATERAL SERVO-MANIPULATOR SYSTEM

CONCLUSION

Recent status of R&D activities with regard to FBR fuel reprocessing technology has been reviewed. A significant progress is being made especially for advanced process equipment such as a continuous dissolver and centrifugal contactors, and for advanced remote technologies. The collaboration with the ORNL has been largely contributing to the enhancement of the R&D programs in many aspects. The design of the RETF is in progress where the hot demonstration tests with actual spent fuel assemblies are planned for advanced processes and equipment currently being developed. The data and experiences gained from the RETF project and other R&Ds will become the basis for design of the pilot plant and future industrial plants with improved performance, reliability and economy.

REFERENCE

1. W. D. Burch, K. Matsumoto et al., "Technical Collaboration between the United States and Japan in the Field of Liquid Metal Reactor Reprocessing", Trans. Am. Nucl. Soc., **56**, 71, (June 1988)
2. T. Takahashi et al., "Construction of the Monju Prototype Fast Breeder Reactor", Nuclear technology, **89**, 162, (Feb 1989).
3. S. Nemoto et al., "Dissolution of Mixed Oxide Fuel from FBR", Proc. RECOD'91, April 1991, Sendai.
4. H. Takeda et al., "Development of a Centrifugal Contactor", Proc. ISEC'90, July 1990, Kyoto.
5. R. T. Jubin et al., "Recent Development in Centrifugal Contactor Technology", Proc. ISEC-90, July 1990, Kyoto.
6. M. Ozawa et al., "Solvent Cleanup Mechanism with Salt-Free Reagents", Proc. RECOD'91, April 1991, Sendai.
7. M. Ozawa et al., "Salt-Free PUREX Process Development", Proc. RECOD'91, April 1991, Sendai.
8. T.Koizumi et al.,"Remote Maintenance Test of Two-Arm Bilateral Servo-Manipulator System", Proc. 37th Conf. on Remote systems Technology, Nov. 1989, San Francisco.
9. S. Hayashi et al., "Development of Radiation Hardened High Definition TV system", Poc. Third Topical Meeting on Robotics and Remote Systems, March 1989, Charleston.

題　　名	Review of Melter Technology and Vitrification Process for TVF		
発表先	RECOD'91		
発表地	仙　　台	発　表 年月日	平成3年　4月14日 ～ 4月18日
発表者 (○印口頭発表者)	所　属　名	環開部　HTS室	
	○吉岡　正弘，狩野　元信，遠藤　　昇，本橋　昌幸，高橋　武士		

(要旨)

動燃では，1993年にホット運転開始を予定しているＴＶＦに向けたプロセス開発を進めてきた。固化プロセスは廃液供給直接通電型溶融炉方式に基づいたもので，最適なメルタ構造および運転性の観点から，多くのメルタシステムに関する開発が動燃独自の改良を加えることによって行われた結果，ＴＶＦメルタは45°の炉底勾配をもつこと，そして焼結型ガラスファイバーカートリッジをガラス原料として使用すること等に特徴をもっている。動燃でこれまでに開発されてきたメルタ技術の経緯およびＴＶＦのプロセスについてレビューする。

資料番号
TN8100　91－003 (80－02－226)

資料番号 TN8100 91-003

REVIEW OF MELTER TECHNOLOGY AND VITRIFICATION PROCESS FOR TVF

M.Yoshioka, M.Karino, N.Endo, M.Motohashi, and T.Takahashi

Power Reactor and Nuclear Fuel Development Corporation
Tokai-Works
4-33 Muramatsu, Tokai-mura, Ibaraki-ken, Japan 319-11
phone : 0292-82-1111

ABSTRACT

Power Reactor and Nuclear Fuel Development Corporation (PNC) has carried out many developmental works on the liquid fed joule-heated ceramic melter (LFCM) process focussed on the Tokai Vitrification Facility (TVF) which is now under construction aiming at the start of test operation in 1992. The melter technology developed in PNC and the vitrification process for the TVF are reviewed in this paper.

The vitrification technology based on the LFCM process has been developed since 1977. Many activities on LFCM process development have been carried out in the engineering-scale or the full-scale cold tests through the operations of Engineering Test Facility (ETF) and Mock-up Test Facility (MTF) since 1980 and 1982, respectively, and have provided the design basis for the process design of the TVF. Technologies ever developed in PNC include design of the melter bottom structure in order to avoid the operational problems caused by accumulation of electroconductive sludge, glass fiber cartridge and its feeding system, bottom freeze valve with two-zone induction heating, and associated monitoring instruments.

INTRODUCTION

The joule-heated ceramic melter, which is based on the glass melter commercially used in the glass industry, is the main equipment in the LFCM process. In the developmental work, PNC's own improvements and modifications were added to the glass melter to be more suitable for TVF. And other process technologies such as an off-gas clean-up system have also been modified to reduce the release of radioactive nuclides.

The ground preparation for the TVF was started in mid 1988 after getting the license from the government. The construction of TVF building was completed in February of 1991. Subsequently, the installations of process equipment to the cell are now being carried out aiming at its completion in early 1992.

The capacity of the TVF is designed to be equivalent to the capacity of 0.7 tons U/day in Tokai Reprocessing Plant (TRP) which treats the LWR fuels burned up 28,000 MWD/MTU in average. The capacities of the high-level liquid waste (HLLW) treatment rate, glass production rate, and canistered waste production rate are 0.7 m^3/day, about 9 kg/h, and 140 canisters/year (200 days operation) respectively. The TVF employs fully remote operation and maintenance in a large vitrification cell with low flow ventilation system. All equipment in the cell are placed in standardized rack-mounted modules.

DESCRIPTION OF MELTER DEVELOPMENT FOR TVF

Many developmental works were carried out on the melter system in order to get reliable melter operability of the TVF. Several glass melters with different structures and materials were tested to compare their process characteristics in earlier stage of the development. The melter design was then modified to improve the melter process performance. A melter bottom structure with sloped floor, a continuous feed system for glass fiber additive, a bottom freeze valve with two-zone induction heating, and glass level detection are the major results being adopted in the first melter of the TVF.

The Mock-up Melter-III which has the same structure and system as the TVF melter was constructed in late 1987 following the design improvement of the TVF, and has been operated with the complete system of process equipment to ensure the melter performance and operability of the TVF. Figure 1 shows the structure of TVF melter(1).

Glass additive form

In the development of glass frit feed technology, use of powdered and granular(beads) additives was tested in the earlier stage of LFCM process development. To maintain stable melter operation, the glass fiber cartridge was chosen which has less particulates. This approach was expected to prevent the off gas line pluggage and maintain good glass product quality. Sintered formed glass fiber additive and continuous feed system were developed to replace ground or beaded frit. After the continuous operation tests using these types of glass additives, the continuous glass frit feed system using cylindrical cartridges of fiber glass was adopted with high reliability for the TVF process.

In the stable feed operation, entrainment of particles in the off gas stream was reduced to 1/10 compared with that of the feed operation using beaded frit. The glass fiber additive also made the glass melting stable without pressure surge by the release of significant amounts of steam from glass pool to the melter plenum space.

Melter structural design and operation

Melter structure is very important to temperature distribution, heat balance, glass flow, and also the behavior of immiscible deposits in LFCM operation that are electroconductive. Melter bottom refractory design especially should be optimized to avoid the operational problems caused by accumulation of electroconductive sludge.

Several experiments were performed using laboratory-scale melters in order to look into the effect of melter bottom slope on the melter operation and discharge of electroconductive deposits that consist of noble metals. The result showed that a melter bottom slope of 45° would eliminate the operational difficulties by facilitating the discharge of deposits.

In addition to the improvement of melter structure, tests to operationally prevent the accumulation of noble metals and to discharge them more effectively from the melter were carried out through the operations of Mock-up Melter-III with 45° sloped bottom over a long period. One of the methods to make this attempt operationally was to keep the melter bottom at a low temperature. It is also expected in this method to discharge the noble metals settled on the melter bottom efficiently by the low flow rate of glass pouring.

The melter operation with a low bottom temperature kept the resistance between main electrodes stable. No significant change was observed during the operation using this method. It was confirmed by removing the glass left in the melter after the feed of noble metals of 116 kg, and by evaluating the balance of noble metals that the amount of noble metals discharged from the melter was more than 99% of the total amount fed into the melter as shown in Figure 2(2).

The cold bottom mode of operation is one of the promising methods to eliminate the operational difficulties caused by noble metals based on long melter operation experience.

Other melter related technologies development

The drain system has been developed to have good operation and maintenance ability. From the standpoint of simplicity, operation and especially of expected long lifetime of the drain nozzle, the freeze valve with induction heating has been further developed and modified.

A freeze valve with two-zone induction heating with aircooling system for emergency, which heats the lower or upper part of drain valve independently, was found to be effective in eliminating the formation of glass string. This was applied to the TVF melter.

The glass melter is equipped with several instruments to monitor the operation status, including temperature, pressure, and electrical conditions. Instrumentation which is typical for PNC melter is the molten glass level detection system based on electrical resistance measurement between the common probe and the detection probes. The system has been developed and improved to get enough reliability in measuring the glass level within 10 mm.

Many R&D activities have been carried out on the glass melter and process technology to attain the most suitable LFCM process for the TVF. As a result, the present melter for the TVF was designed and will be operated without the operational difficulties in feed and glass melting operation.

VITRIFICATION PROCESS

The HLLW is transferred from the Tokai Reprocessing Plant to a receiving tank of the TVF. Elemental and radioactive analysis are carried out for process and product quality control. The HLLW is pretreated to adjust the composition by the addition of chemicals like a sodium and/or by concentration using an evaporator when required. Denitration of HLLW with formic acid was discarded in the vitrification plant because of the difficulty of HLLW feed system by deposits in the evaporator.

After the pretreatment, HLLW is transferred to a melter continuously using a two-stage airlift. Glass fiber cylinders are used as a glass additive for melting. The HLLW transferred to a melter is soaked into the cylinder just before it is fed into the melter pool. The glass melted at the temperature of 1150°c is discharged periodically through a metallic nozzle located at the bottom of the melter into a canister. During the discharge, the weight and volume of the glass in the canister are successively measured by load cells and by the gamma-ray method, respectively. The filled canister is subsequently cooled, and transferred to the welding position, and a lid is welded by a TIG welder to seal the canister. After being decontaminated by high-pressure water jet spray and wire brushing and being inspected, packages are

stored in forced-air cooling storage pits.

Melter off-gas is cleaned by submerged bed scrubber venturi scrubber, perforated plate type water scrubber, high efficiency mist eliminator and subsequent filtration process such as a ruthenium adsorber(silica gel), iodine adsorber and HEPA filter.

SPECIFICATION AND FEATURES OF TVF

Plant description

The TVF consists of two buildings which consists of a process building and an administration building, and a stack. The process building has two stories underground and three above ground, with 58m length, 42.5m width, 19m depth and 26m height, floor space totalling 2600m^2.

The process building has two main cells. One is the vitrification cell shown in Figure 3. This cell has about 1.6m shielding wall and 13m height, 27m length, 12m width and about 4200m^3 volume. The vitrification process area and the cutup area are arranged, and most of vitrification process equipment such as a glass melter, the off-gas treatment equipment which were improved through the cold operation tests are installed in this cell.

Most equipment in this cell are placed in standardized modules with the dimensions of 3m by 3m by 6.5m which are ordered along both side of walls of this cell. The TVF incorporates 7 racks which we call standardized module rack, and a melter.

For maintenance, over head systems are disposed above the rack. These systems consist of two manipulators and two cranes. There is a passageway with 5m width between the rack. This is used for maintenance work, for movement of the replaced rack and the remote maintenance equipment.

And another cell is the storage cell, which is for temporary storage of the waste package. This has the storage capacity of 420 packages by forced air cooling in the 70 pits with each dimension of about 560mm O.D, 15mm thick.

Fully remote maintenance

The TVF incorporates a new concept of remote maintenance for process equipment so that the plant availability is increased and personnel exposure decreased. In order to carry out a new concept, most equipment in the cell are arranged in standardized rack-mounted modules which are ordered along both sides of the cell wall.

The failured equipment is maintenanced using the remote maintenance tools like in-cell cranes and two-armed servo-manipulators equipped in the cell from the control room viewing the industrial televisions.

Low-flow ventilation system

The TVF equips the low-flow ventilation system as a cell exhaust treatment in accordance with the adoption of large vitrification cell. This contributes to compact the ventilation system. Also this system is expected to reduce the release of radionuclides from the vitrification cell to atmosphere in the case of release from the equipment to the cell.

As the heat of process is not removed by this ventilation system, the in-cell coolers are installed on the module rack for remote maintenance. Exhaust from the vitrification cell for keeping the negative pressure of -80mm of water in the cell is provided by allocating 500m^3/hr for cell exhaust in the vessel off-gas system. It is also

possible to maintain the negative pressure through in-cell coolers.

REFERENCE

1.Yoshioka,M.,Torata,S. et al.Glass melter and process development for the PNC Tokai Vitrification Facility. In:Proc.of 1989 Joint International Waste Management Conference, Kyoto, Japan, October 22-28, 1989, p.13-19;1989, American Society of Mechanical Engineers(1989)

2.Yoshioka,M. and Takahashi,T. Evaluation of glass melter operation using nighly simulated waste for TVF. In:Proc.of International Topical Meeting on the Nuclear and Hazardous Waste Management, Knoxville, TN(USA), September 30-October 4, 1990, p.296-298;1990, American Nuclear Society(1990)

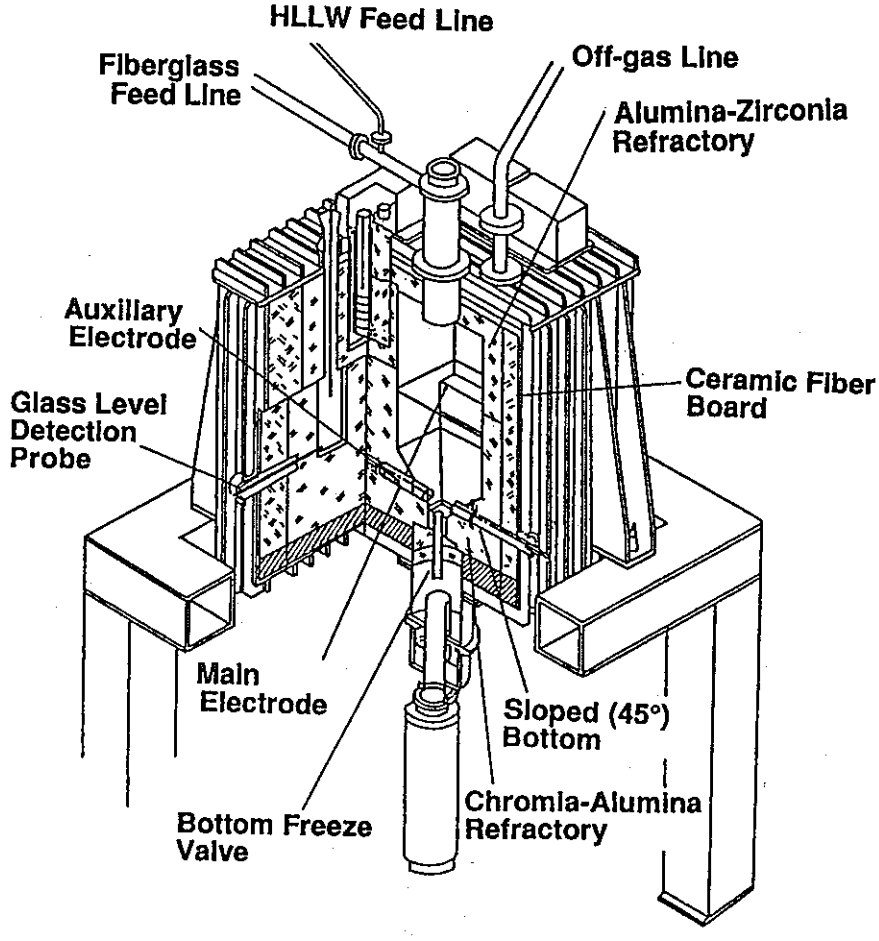

Figure 1. Structure of TVF Melter

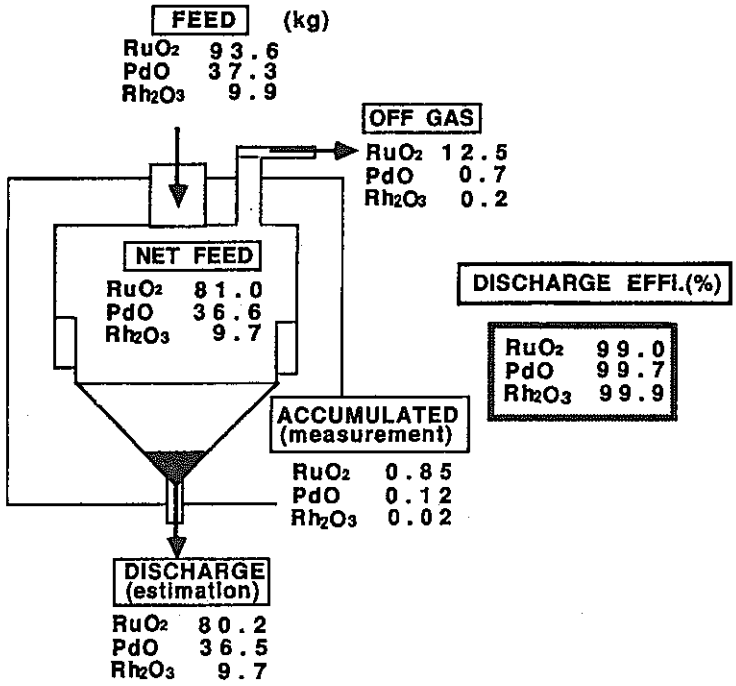

Figure 2. Noble Metals Balance in Melter

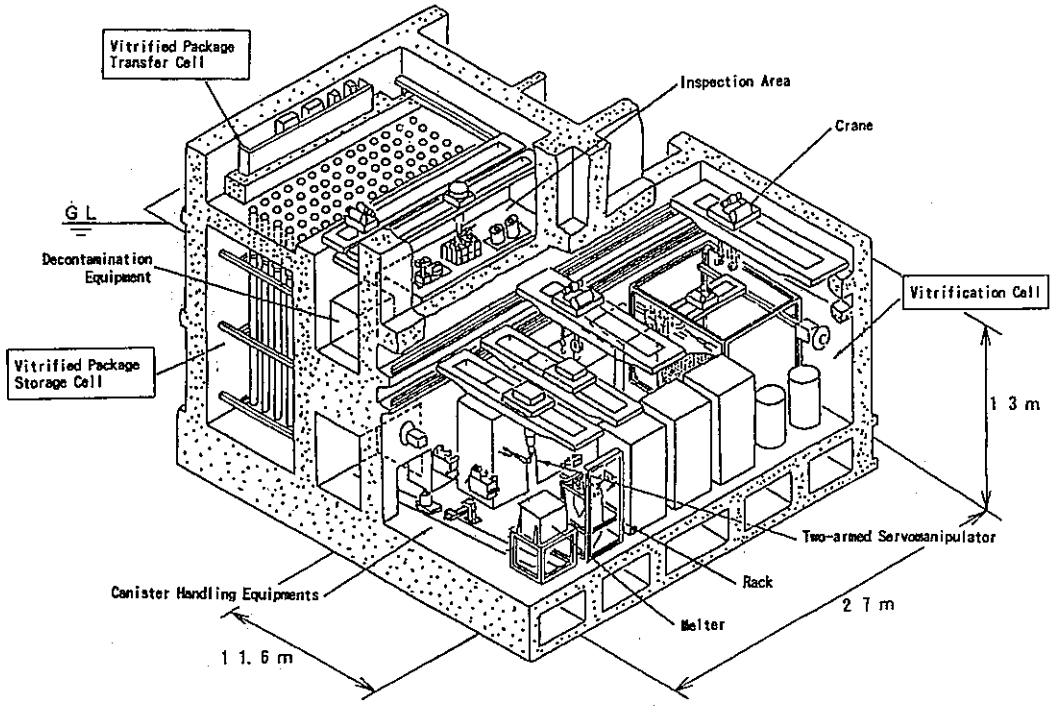

Figure 3. Vitrification cell in TVF

題　　名	SOLVENT CLEANUP MECHANISM WITH SALT-FREE REAGENTS		
発表先	RECOD'91		
発表地	仙　　台	発　表 年月日	平成3年　4月14日 ～ 4月18日
発表者 (○印口頭発表者)	所　属　名	再開部　CMS室	
	○小沢　正基，河田東海夫，清水　　亮，田村　伸彦， 中村　友隆*，深沢　哲生*，植竹　直人*，近藤　賀計*　*日製		

(要　旨)

ソルトフリー溶媒洗浄剤であるシュウ酸ヒドラジンと炭酸ヒドラジンの持つ洗浄メカニズムを推定するために，ＨＤＢＰ，Ｚｒ，Ｒｕ等を含む模擬劣化溶媒を用いて洗浄試験を行った。本実験結果からは，

(1)　ＨＤＢＰはＤＢＰ$^-$ に解離して水相側に移行する。

(2)　ＺｒはＺｒ－ＤＢＰ錯体の解離によって水相側に移行し，それにはシュウ酸の効果が認められる。

(3)　Ｒｕは加水分解により水溶性の錯体を形成し水相側に移行する。

等が推定された。

また，同時に中間クラッドの生成挙動が洗浄剤のｐＨ値に依存することが観察された。

資料番号
TN8100　91－004 (80－02－223)

資料番号 TN8100 91-004

SOLVENT CLEANUP MECHANISM WITH SALT-FREE REAGENTS

M.OZAWA, N.TAMURA, R.SHIMIZU, T.KAWATA
Tokai Works, Power Reactor and Nuclear Fuel Development Corporation
Muramatsu, Tokai-mura, Naka-gun, Ibaraki-ken, Japan 319-11, phone : 0292-82-1111
T.NAKAMURA, T.FUKASAWA, N.UETAKE
Energy Research Laboratory, Hitachi, Ltd.
1168, Moriyama-cho, Hitachi-shi, Ibaraki-ken, phone : 0294-53-3111
Y.KONDO
Hitachi Works, Hitachi, Ltd.
3-1-1, Saiwai-cho, Hitachi-shi, Ibaraki-ken, Japan 316, phone : 0294-21-1111

ABSTRACT

In order to determine the mechanisms of reprocessing solvent cleanup with salt-free reagents of hydrazine oxalate [$(N_2H_5)_2C_2O_4$)] and hydrazine carbonate [$(N_2H_5)_2CO_3$)], a series of basic cleanup tests were carried out for simulated solvent contained dibutyl phosphate (HDBP), Zr and Ru as impurities. The cleanup of HDBP must be accomplished by its dissociation to DBP^-. The Zr was probably removed by dissociation of its extractable complex with HDBP, particularly oxalate ion which forms a strong complex with Zr could enhance the dissociation. The cleanup efficiency of Ru was lower than other impurities, but increased with alkalinity of cleanup reagent. The cleanup of Ru mainly occurred with changing its extractable complex to certain water-soluble form by hydrolysis.

The formation behavior of interfacial crud was also investigated with salt-free reagents and sodium carbonate [Na_2CO_3] for comparison. The apparent volume of the formed interfacial crud in a mixer-settler test using hydrazine carbonate was almost the same as that using sodium carbonate. And the hydrazine oxalate remarkably suppressed the crud formation. The results of separation funnel tests using hydrazine carbonate and sodium carbonate showed that the crud formation occurred at pH= 5 to 7 and became a maximum at pH=6.

INTRODUCTION

The 30% tributyl phosphate (TBP)-70% dodecane mixture used as the extraction solvent in spent nuclear fuel reprocessing undergoes degradation by exposure of nitric acid and intensive radiation, then mainly produces dibutyl phosphate (HDBP). In the first cycle extraction of reprocessing process, HDBP forms strong complexes with U, Pu and certain fission products such as Zr[1] which are retained into the solvent phase and are not stripped out with dilute nitric acid. These degradation products, fission products and complexes must be removed from the solvent in solvent cleanup process prior to its recycle.

Ordinarily, Na_2CO_3 solution is used as solvent cleanup reagent, but the principal drawback of this method is production of the large quantities of $NaNO_3$ which eventually must be handled as radioactive waste (100Kg for every tonne of fuel reprocessed[2]). Accordingly, the salt-free cleanup reagents such as hydrazine[2)3)], hydroxylamine[4)], tetrametylammonium[5)] which can be decomposed to water and gases have been proposed.

The authors have already confirmed by the solvent cleanup tests using various types of salt-free reagents that hydrazine carbonate and hydrazine oxalate were available on a purpose of removing the impurities from the solvent[6)]. However, the cleanup mechanisms of the impurities were not clarified yet. In this study, the cleanup mechanisms were investigated based on some cleanup tests.

The formation of interfacial crud should be also considered in evaluation of the cleanup reagent because it causes the poor phase separation and occasionally the failure in operation of the solvent cleanup unit[7)]. The formation mechanism of interfacial crud has not inquired. In this study, the formation mechanism was also estimated.

EXPERIMENTAL METHODS

1.Sample preparation

Simulated solvents

At first, a 30 % TBP-70 % dodecane mixture was

washed once with 0.5M Na_2CO_3 and thrice with pure water. The Zr was extracted from its nitric acid solution into a potion of the mixture to which HDBP was added before. The Ru and U were extracted from their nitric acid solutions into other potions of the mixture without HDBP. The simulated solvent was prepared by mixing those three. The solvents which contained only HDBP or Ru and DBP were also used.

Cleanup reagents

The Na_2CO_3 solution was obtained by dissolving the reagent Na_2CO_3 into distilled water. The $(N_2H_5)_2C_2O_4$ solution was prepared by the addition of oxalic acid $[H_2C_2O_4 \cdot 2H_2O]$ solution to hydrazine hydrate $[N_2H_4 \cdot H_2O]$ solution. The $(N_2H_5)_2CO_3$ was obtained by bubbling CO_2 through the hydrazine hydrate solution.

2. Procedures

Batchwise test

The simulated solvent and the cleanup reagent of equal volumes (50ml) were put into the separating funnel and mechanically shaken. After settling, the aqueous phase and the organic phase were collected separately. In order to determine the cleanup efficiency of impurities, their residual concentrations in the solvent were analyzed by ICP emission spectroscopy or ion chromatography. The pH value of the cleanup reagent was measured by pH meter.

Continuous flow test

$(N_2H_5)_2C_2O_4$ and $(N_2H_5)_2CO_3$ were compared with Na_2CO_3 on the formation behavior of interfacial crud in continuous flow condition using a small mixer-settler which constitution and operation condition were shown in Fig.1 The concentration of impurities in the simulated solvent was established to about three times as much as the expected concentration in practical solvent.

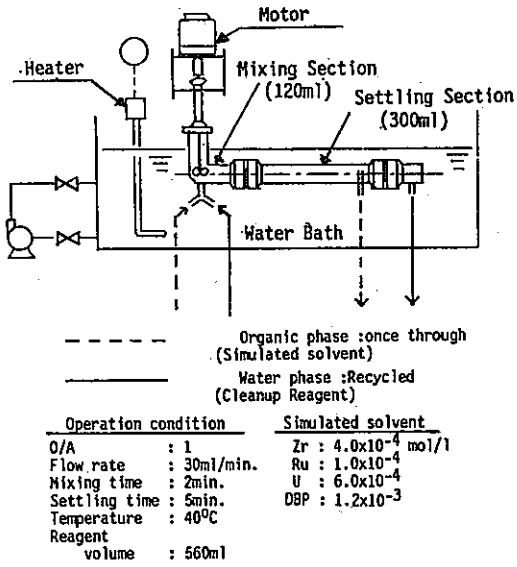

Fig.1 Apparatus for the coutinuous flow test (1 stage of mixer-settler)

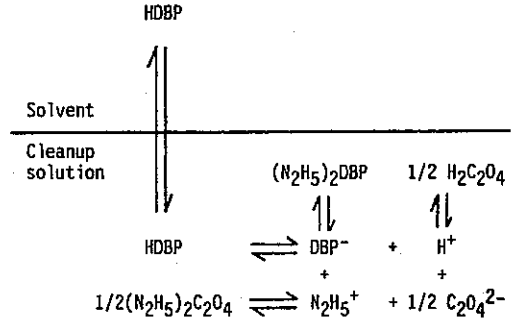

Fig.2 Estimated cleanup process for HDBP

RESULTS AND DISCUSSION

The cleanup mechanism for dibutyl phosphate (HDBP)

The cleanup mechanisms of HDBP was suggested as following reaction equations in the past[2];

$$(HDBP)_{org} + (NaOH)_{aq} \longrightarrow (NaDBP)_{aq} + H_2O \quad (1)$$

$$(HDBP)_{org} + (N_2H_5OH)_{aq} \longrightarrow (N_2H_5DBP)_{aq} + H_2O \quad (2)$$

Fig.2 shows the estimated cleanup process for HDBP in case of using $(N_2H_5)_2C_2O_4$ as an example. The partition coefficient of HDBP molecular, K, the dissociation constant, Ka, and the complex formation constant between $N_2H_5^+$ and DBP^-, Kf, were defined as follows;

$$K = [HDBP]_{org}/[HDBP]_{aq} , \quad (3)$$

$$Ka = ([DBP^-]_{aq}[H^+]_{aq})/[HDBP]_{aq} , \quad (4)$$

$$Kf = [N_2H_5DBP]aq/([N_2H_5^+]_{aq}[DBP^-]_{aq}) . \quad (5)$$

The constant K and Ka can be quoted as 17 and 0.1, respectively. The K was measured in 30% TBP-70 % dodecane / 3M HNO_3 system on which the dissociation of HDBP can be negligible[8], and the Ka was measured in $HClO_4$-$NaClO_4$ solution[9].

On the other hand, a distribution ratio of dibutyl phosphate is described by Eq.(6);

$$D = \frac{[HDBP]_{org}}{[HDBP]_{aq}+[DBP^-]_{aq}+[N_2H_5DBP]_{aq}} \quad (6)$$

Transforming Eq.(1)-(3) and substituting into Eq.(6) deduce the following equation;

$$D = \frac{K[H^+]/Ka}{[H^+]/Ka+1+Kf[N_2H_5^+]} \quad (7)$$

$$\log D = \log\{k[H^+]/Ka\}-\log\{[H^+]/Ka+1+Kf[N_2H_5^+]\}. \quad (8)$$

At pH>2 ,which was the pH region in this study, $[H^+]/Ka$ value is <0.1. Assuming of $Kf[N_2H_5^+]>>1$ and rearranging Eq.(8) gives the following approximate equation;

$$\log D + pH = \log\{K/(Ka\cdot Kf)\}-\log[N_2H_5^+] . \quad (9)$$

Based on this equation, (logD + pH) versus $\log[N_2H_5^+]$ should be linear with a slope -1. A plot of the experimental data from the cleanup tests using $(N_2H_5)_2C_2O_4$ and $(N_2H_5)_2CO_3$ is shown in Fig.3 (In data treatment, complete dissociation of $(N_2H_5)_2C_2O_4$ and $(N_2H_5)_2CO_3$ was assumed for simplicity). The result indicates that the data do not satisfy a relation in Eq.(9) and that $N_2H_5^+$ can not interact with DBP^-. This observation supports a fact that ^{31}P-NMR analysis for dibutyl phosphate dissolved in N_2H_5OH solution indicated no interaction between $N_2H_5^+$ and DBP^-[10].

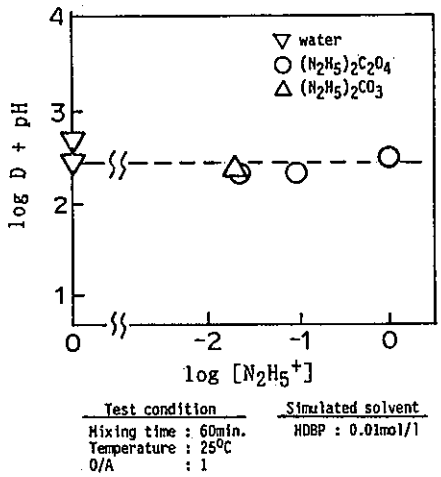

Test condition	Simulated solvent
Mixing time : 60min.	HDBP : 0.01mol/l
Temperature : 25°C	
O/A : 1	

Fig.3 Relationship of log D for HDBP and log $[N_2H_5^+]$

Therefore, it seems that DBP^- is the final formin the cleanup process. In this case, a distribution ratio of dibutyl phosphate can be described as Eq.(10);

$$D = \frac{[HDBP]_{org}}{[HDBP]_{aq} + [DBP^-]_{aq}} \quad (10)$$

Eq.(10) can be transformed to Eq.(11) by using Eq.(3) and (4);

$$D = \frac{K[H^+]}{[H^+] + Ka} \quad (11)$$

Rearranging in logarithmic form approximately in pH>2 gives a Eq.(12);

$$\log D = \log K/Ka - pH . \quad (12)$$

A calculated result for pH versus logD as a solid line and a plot of the experimental data which were rearranged to the relation between logD and pH value of cleanup solutions are shown in Fig.4. The pH value for each data point is equal to equilibrium value after the cleanup operation. The experimental data agree well with the calculated result. This fact proves that the cleanup of HDBP is accomplished by its dissociation to DBP^-.

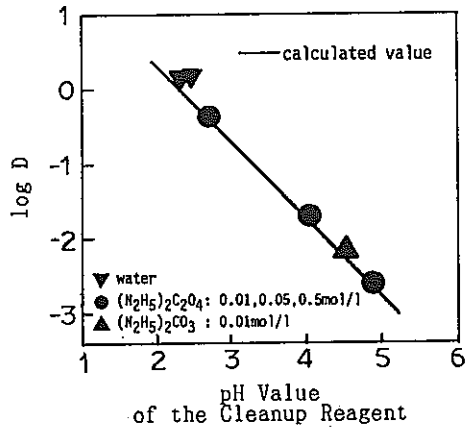

Test condition	Simulated solvent
Mixing time : 60min.	HDBP : 0.01mol/l
Temperature : 25°C	
O/A : 1	

Fig.4 Relationship of log D for HDBP and pH

The cleanup mechanism for Zr and Ru

Figure 5 shows the cleanup efficiency of Zr and

Ru as a function of pH from the batchwise tests for which the reagent concentration and mixing time were varied. The variation of the reagent concentration gives different pH value. The Zr probably exists as a $Zr(DBP)_2(NO_3)_2$ complex[1] in the simulated solvent. As it is not water-soluble, Zr would be removed into creanup reagent solution by its dissociation. In $(N_2H_5)_2CO_3$ test, the cleanup efficiency of Zr remarkably decreased with decrease of pH value of reagent solution. The pH has to be kept high for the dissociation of Zr complex when using $(N_2H_5)_2CO_3$. On the other hand, in soite of the lower pH value of $(N_2H_5)_2C_2O_4$ solution than that of $(N_2H_5)_2CO_3$, the cleanup efficiency by $(N_2H_5)C_2O_4$ was remarkably high. Its influence is probably that oxalate ion enhanced the dissociation of the Zr-DBP complex by forming certain water-soluble complex with Zr.

The cleanup of Zr attained to the equilibrium in about 5 min apparently, but Ru did not attain to the equilibrium in this test condition. The cleanup efficiency of Ru was especially lower than that of Zr, U and DBP in the low pH condition. The cleanup efficiency was also related to pH.

The tri-nitrate nitrosylruthenium, $RuNO(NO_3)_3$, has been known to expose hydrolysis by exchanging NO_3 with OH in water[11]. It was estimated that the certain Ru complex, $RuNO(NO_3)_a(DBP)_b$ (a+b=3), in simulated solvent also was hydrolyzed by contacting with cleanup reagent solution as following reaction;

$$RuNO(NO_3)_a(DBP)_b + eH_2O \rightleftharpoons \{Ru(NO_3)_c(DBP)_d(OH)_e\}^{(3-c-d-e)-} + (a-c)NO_3^- + (b-d)DBP^- + eH^+ . \quad (13)$$

In this case, the distribution ratio of Ru was described by Eq.(14);

$$D = \frac{[RuNO(NO_3)_a(DBP)_b]_{org}}{[\{Ru(NO_3)_c(DBP)_d(OH)_e\}^{(3-c-d-e)-}]_{aq}} . \quad (14)$$

A plot of experimental data as log D for Ru and DBP versus pH from another cleanup test which uses the solvent containing only Ru and DBP is shown in Fig.6. The distribution ratio decreases with the increase of pH and the distribution ratio of DBP behaves in almost the same manner as that of Ru. This fact suggests that the main cleanup reaction of Ru is the transformation of its extractable complex to water-soluble complex by hydrolysis.

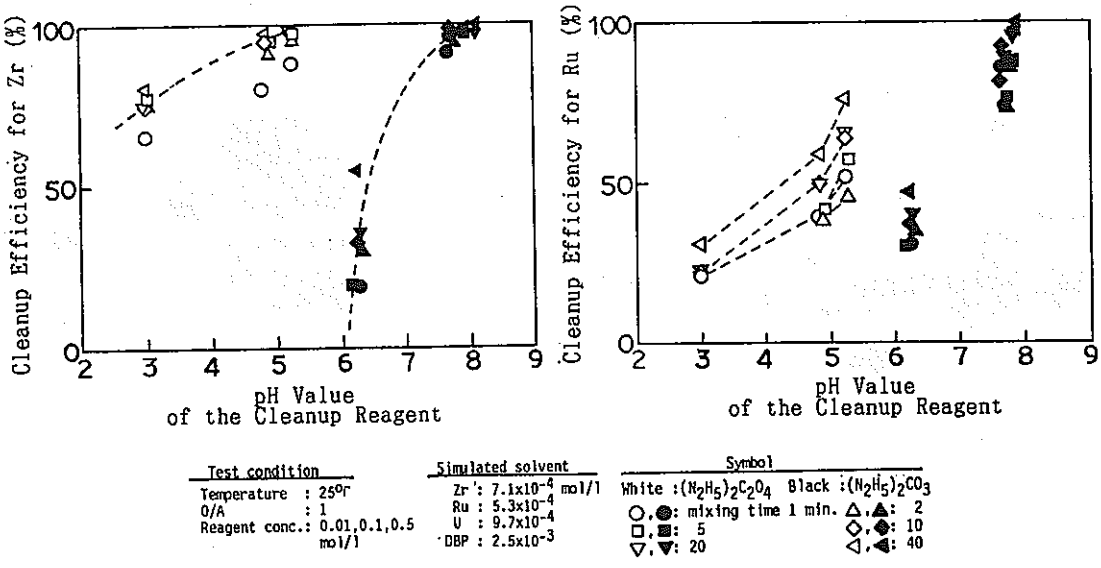

Fig.5 Cleanup efficiency of Zr and Ru in batchwise test

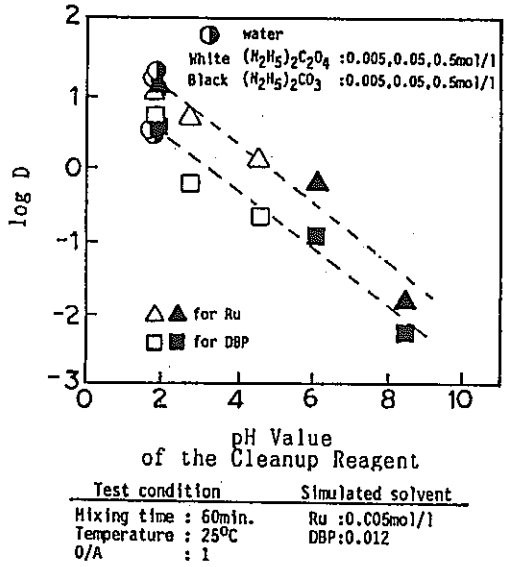

Fig.6 Relationship of log D for Ru and DBP and pH

Interfacial crud formation

Figure 5 shows the appearance of interfacial crud in case of using $(N_2H_5)_2C_2O_4$ and $(N_2H_5)_2CO_3$. It was observed that $(N_2H_5)_2C_2O_4$ remarkably suppressed the crud formation compared with Na_2CO_3. On the other hand, $(N_2H_5)_2CO_3$ formed almost equal crud volume to Na_2CO_3.

The collected interfacial crud was sufficiently washed with pure solvent and water, and dried at 180°C for 8 hours. The sample was dissolved into the alkaline solution and analyzed to determine its component. On the other hand, O-H bond in the crud was discovered by FT-IR spectroscopy analysis. The interfacial crud formation probably occurs by polymerization of Zr-DBP complex containing OH group as bridge species [13]. Accordingly, it was estimated that $(N_2H_5)_2C_2O_4$ could suppress the crud formationdue to the formation of certain Zr-oxalate complex prior to polymerization.

In order to confirm the relationship between the pH and crud formation, the batchwise cleanup tests using the separating funnel were carried out with $(N_2H_5)_2CO_3$ and Na_2CO_3. The pH value was varied by adding nitric acid. The concentration of impurities in the simulated solvent is about three times higher than that in mixer-settler test. Figure 8 shows the crud volume which is normalized with a maximum value as a function of pH. The result indicated that crud formation occurred at pH=5 to 7 and the volume became a maximum at pH=6 in this condition. Even though the concentration of impurities was raised still more, crud volume maximum at pH=6 was unchanged. In the continuous solvent cleanup, maintaining the pH value of $(N_2H_5)_2CO_3$ or Na_2CO_3 solution higher than 8 must be effective on suppressing the crud formation as well as removing the impurities.

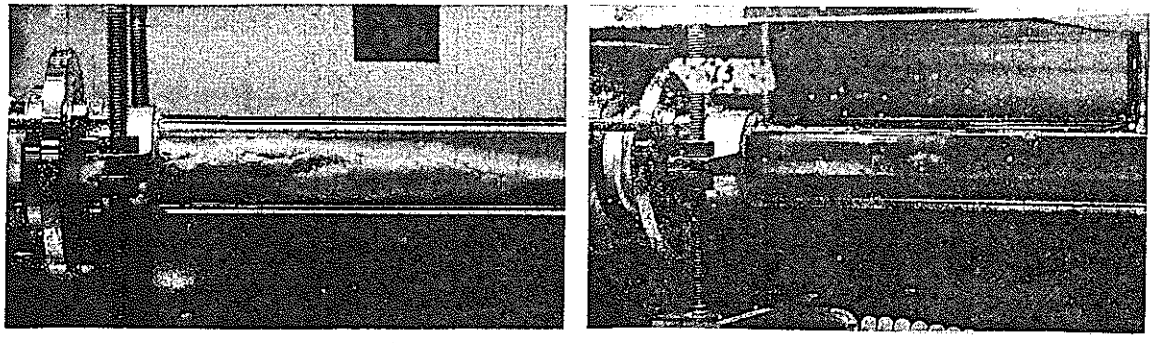

Cleanup regent :Na_2CO_3 Cleanup reagent :$(N_2H_5)_2C_2O_4$

Fig.7 Photograph of interfacial crud in the mixer-settler (at 390 min. since stared)

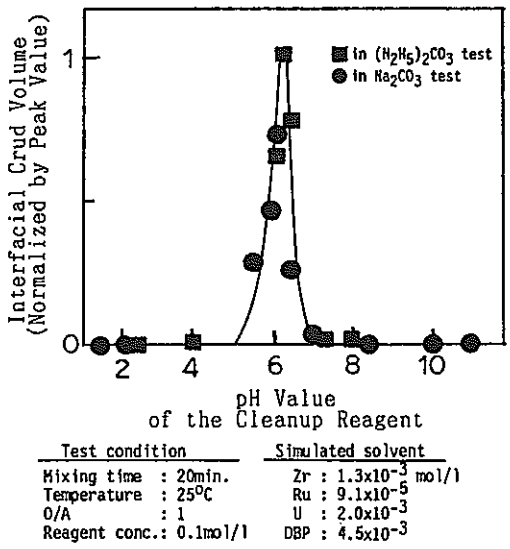

Test condition		Simulated solvent	
Mixing time	: 20min.	Zr	: 1.3×10^{-3} mol/l
Temperature	: 25°C	Ru	: 9.1×10^{-5}
O/A	: 1	U	: 2.0×10^{-3}
Reagent conc.	: 0.1mol/l	DBP	: 4.5×10^{-3}

Fig.8 Effect of pH upon the volume of interfacial crud (in batchwise test)

CONCLUSIONS

Based on experimental results, it was concluded that:

(1)The cleanup of HDBP would be accomplished by its dissociation to DBP^- which is a stable form in aqueous phase.

(2)The Zr was probably removed by dissociation its extractable complex with DBP. Oxalate ion which forms strong complex with Zr could enhance the dissociation.

(3)The cleanup efficiency of Ru was lower than that of other impurities. The main reaction of Ru cleanup was probably the transformation of extractable complex to certain water-soluble form by hydrolysis.

The most important observation in this study was that pH of cleanup reagent was closely related to the cleanup efficiency of HDBP, Zr and Ru as well as interfacial crud formation. As a result, an effective solvent cleanup could be maintained by the continuous pH control in system operation.

REFERENCE

1. TUJINO T., "Chemical and Radiation Damage of Reprocessing Solvent", JAERI-memo, number 3229 (1967).

2. GOLDACKER H. et. al., "A New Developed Solvent Wash Process in Nuclear Fuel Reprocessing Decreasing the Waste Volume" , Kerntechnik, 18, 426 (1976).

3. TALLENT O.K. and MAILEN J.C., "An Alternative Solvent Cleanup Method using a Hydrazine Oxalate Wash Reagent", Nucl. Technol., 59, 51 (1982).

4. MAILEN J.C. and TALLENT O.K., "Assessment of Purex Solvent Cleanup Method using a Mixer-Settler System", ORNL-TM-9118 (1984).

5. UETAKE N., KAWAMURA F. and YUSA H., "Alternative Solvent Wash Process using Tetrametylammonium Hydroxide Solution as Salt-Free Reagent", J. Nucl.Sci. Technol., 26[2], 270 (1989).

6. OZAWA M, et. al., "Application of Salt-Free Technology to the Purex Process for FBR Fuel Reprocessing", ISEC 1990, Kyoto.

7. ORTH D.A. and OLCOTT T.W., "Purex Process Performance Versus Exposure and Treatment", Nucl. Sci. Eng., 17, 593 (1963).

8. OCHSENFELD W., et. al.,"Experience with the Reprocessing of LWR, Pu Recycle, and FBR in the MILLI Facility", ISEC 1977, Tront.

9. OYRESSEN D. et. al., "Distribution and Dimerization of Dibutyl-n-phosphate (DBP)", Acta. Chem. Scand., 11, 1771 (1957).

10. OZAWA M. et. al., "Scrubbing Behavior and Mechanism of Dibutyl Phosphate", 1990 Annual Meeting of the Atomic Energy Society of Japan.

11. NIKOL'SKILL B.P. and IL'ENKOl E.I., "Hydrolysis of Nitrate Complexes of Nitroso Ruthenium", Radiokhimiya, 8, 189 (1966).

12. ZIMMER E., and BORCHARDT J., "Crud Formation in Purex and Thorex Process", Nucl. Technol., 75, 332 (1986).

13. MIYAKE C., et. al., "The Third Phase of Extraction Process (I)", J. Nucl. Sci. Technol., 27[2], 157 (1990).

題　　名	Salt-Free PUREX Process Development		
発表先	RECOD'91		
発表地	仙　　台	発　表 年月日	平成3年　4月14日 ～ 4月18日
発表者 (○印口頭発表者)	所　属　名	再開部　CMS室	
	○小沢　正基，根本　慎一，上田　吉徳，鷲谷　忠博， 宮地　茂彦，河田東海夫，林　正太郎		

(要旨)

ＦＢＲ燃料再処理技術開発の一環として再開部を中心として進められてきたＰｕｒｅｘプロセスへのSalt-Free 技術の適用の成果を総合論文として発表する。

まず，Ｐｕｒｅｘプロセスのうち，Salt-Free 技術の適用可能な箇所として化学反応が関与するところ，すなわちU／Ｐｕ分配工程，Ｐｕ再酸化工程及び溶媒洗浄工程をとりあげ，U／Ｐｕ分配工程では，Acid-split技術の適用性の検討結果，Ｐｕ再酸化工程では，ＯＴＬで実施したＰｕ^{Ⅲ}／HAN／Ｈｄｚの電解酸化の結果，溶媒洗浄ではシュウ酸ヒドラジンによる遠心抽出器を用いた溶媒洗浄結果を述べる。また，将来への取り組みとしてＰｕｒｅｘプロセスにとって邪魔な核種であるルテニウム，パラジウムなどの白金族元素を溶解液中から電解析出法により除去する試みについて報告する。

資　料　番　号
TN8100　91－005 (80－02－222)

資料番号 TN8100 91-005

SALT-FREE PUREX PROCESS DEVELOPMENT

M. OZAWA, S. NEMOTO, Y. UEDA, T. WASHIYA, S. MIYACHI, T. KAWATA, S. HAYASHI
Power Reactor and Nuclear Fuel Development Corporation
Muramatsu 4-33, Tokai-mura, Ibaraki-ken
Japan 319-11
phone: 0292-82-1111

ABSTRACT

One of the major concerns of the conventional Purex process is secondary salt-bearing waste which is generated in the main solvent extraction process. To settle such a problem, application of electrochemistry as a means of achieving a Salt-Free Purex process was considered. An "acid-split" flowsheet was also investigated to fit in with the centrifugal contactor cycle. Electrooxidation results from a galvanostatic study on mixtures of Pu (III)/Hydroxylammonium nitrate(HAN)/Hydrazine(Hdz) in nitric acid proved that not only plutonium ion but also co-existing nitrogen compound could be oxidized in different manners. The fact that the presence of HAN lowered the apparent Pu(III) oxidation rate indicated that tri-valent plutonium ion itself likely acts as a mediator in HAN oxidation reaction paths. The Salt-Free solvent cleanup process was successufully demonstrated using engineering scale 4 -stage centrifugal contactors. The series of results supports the prospect for application of a Salt-Free method to the Purex process. Beyond this attempt, a new effort is being directed toward expanding the traditional function of the Purex process.

INTRODUCTION

The recent requirement to realize lower reprocessing costs, especially in the future FBR spent fuel cycle, is receiving greater emphasis and importance worldwide. Nevertheless, at the same time, the requirement to adequately address safety still exists. The secondary salt-bearing waste which is generated in the main solvent extraction process is considered to be one of the constituents to cause higher reprocessing costs. In that sense, improvements in both process flowsheet and hardware are essential, and both will be desirably developed in harmony. In the process flowsheet aspect, the solvent extraction process which constitutes the "core" of the Purex process, particularly, the U/Pu partitioning, Pu reoxidation and solvent cleanup processes which involve major chemical reactions should be simplified and improved by avoiding the generation of secondary salted liquid waste. The in -situ electrochemical redox method, for example, is recognized as one of the key technologies to respond to such process requirements. In the equipment aspect, utilization of centrifugal contactors was judged by the PNC to save costs by contributing to reduced plant size. The in-situ electrooxidation cell also offers an advantage by simplifying the complicated make-up system because only a simple electric current supply system can cause preferable reaction without any chemical reagents.

Ideally, the Purex process should be functional enough to positively handle the minor actinides, i.e., Np like U and Pu in the solvent extraction process. It is also desirable to improve solvent extraction performance by getting rid of troublesome fission products, i.e., Pd, Rh and Ru, before conducting solvent extraction. The platinum group elements such as Pd, Rh and Ru are of course worthy to recover if marketing demands will increase reasonably. These objectives will hopefully be achieved by Salt-Free methods.

This paper describes the state of the art in the PNC on achieving a "Salt-Free Purex" process basically by incorporating centrifugal contactors, and a suggested method for recovering platinum group elements from purex solutions for technical development in the future. Fig. 1 shows the concept of an advanced reprocessing system based on a "Salt-Free Purex" process.

RESULTS AND DISCUSSIONS

U/Pu Partitioning

U/Pu partitioning by hydrazine-stabilized HAN and/or pure HAN, one of the typical applications of Salt-Free techniques, were both successfully demonstrated with only a small amount of uranium leakage to the plutonium stream using FBR spent fuel in small scale mixer-settlers as reported in ISEC'90 (1). Elimination of hydrazine will contribute significantly to reduce the necessary reoxidation capability in the successive reoxidation step as well as to avoid being involved in a cycle to generate azide compounds.

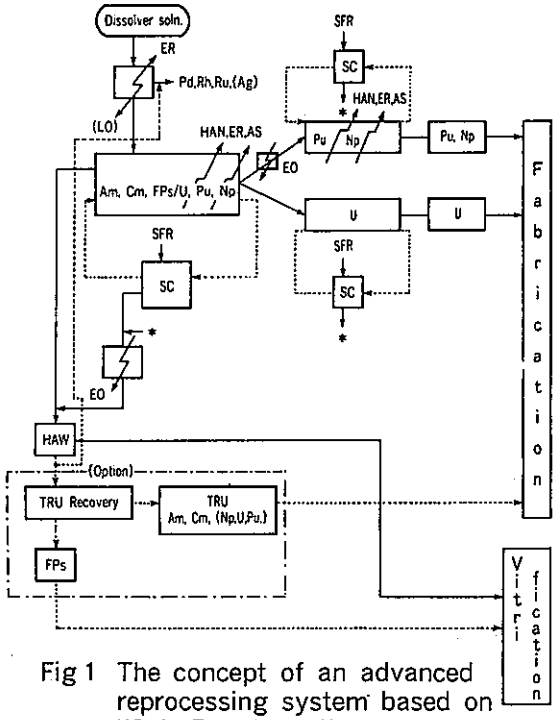

Fig 1 The concept of an advanced reprocessing system based on "Salt-Free Purex" Process

AS : Acid-Split
ER : Electrolytic Reduction
EO : Electrolytic Oxidation
SFR : Salt-Free Reagent
SC : Solvent Cleanup

Further needs to simplify the process necessitate the adoption of other kinds of partitioning techniques; One method uses lactic acid as a Pu-complexing agent. Another one takes advantage of conditions which increase the difference between distribution ratios of Pu and U such as decreasing the temperature in low nitric acid solution known as "acid-split" proposed by Campbell, et al(2). Both methods are characterized by no change of plutonium valency throughout the process.

"Hot" demonstration of lactic acid split(3) showed sufficient partitioning of Pu from U to the expected values, but questions on recycling or decomposition of spent lactic acid still remained. Preliminary tests on direct electrooxidative decomposition of lactic acid(4) indicated that under a higher anodic current density, e.g., 100mA/cm2, in nitric acid, the lactic acid could be destroyed to gaseous meterials, carbon dioxide and nitrogen, but accompanied by a large amount of hydrogen and oxygen as a result. Although the decomposition rate approached 90% in 10 hrs oxidation, a considerable amount of acetic acid was generated at the same time. The acetic acid was fairly stable for direct electrooxidation in nitric acid solution. This result indicated that consideration of another approach, possibly using some kind of mediator, might be necessary for complete destruction of such materials.

The acid-split process fundamentally depended on no chemical reaction, so that both the make-up and reoxidation units seemed to be rationalized. Before entering the demonstrative laboratory test, flowsheet conditions were evaluated to determine the feasibility of this process. In a simulation study (5) conducted with the Revised MIXSET code, calculation conditions included 30%TBP in n-dodecane as a solvent, heavy metal concentration corresponding to typical FBR spent fuel composition, a residence time corresponding to that in a series of centrifugal contactors, and 5 ℃ as a initial assumption temperature. The evaluated parameters and results are summarized in Table 1.

Table 1 Effect of parameter change on product quality in an acid-split process.

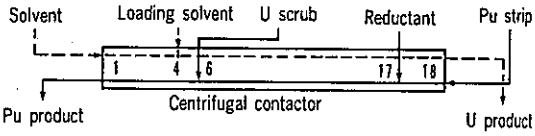

Parameter		Change	Pu in U product	U in Pu product	Third-phase formation	Pu conc. factor
U back scrub injection point		Shift to right	+ − (Exist optimum point)	+ +	− −	(−)
U back scrub flow rate		Increase	+ +	+	− −	−
Pu strip flow rate		Increase	+ +	− −	+ +	−
Loading solvent injection point		Shift to left	+ +	(−)	(−)	(+)
Addition of a little amount of reductant	HAN	Addition	+ +	(+)	+	(+)
	U(IV)	Addition	+ +	−	+	(+)

+ Positive effect − Negative effect ( ) Slight effect

As this process deals only with Pu(IV) with U(VI) at lower temperatures, it is necessary to select a proper temperature to avoid Pu(IV) third phase formation under any conditions, because the solubility of Pu(IV) solvate is reported to be strongly limited by a temperature decrease(6). From an engineering point of view, achieving lower process temperature requires the provision of interstage coolers at the proper locations with special kinds of coolant. Especially, in the case where the centrifugal contactor cycle is placed in a large cell with other heat generating equipment, it will be harder to achieve such a low temperature. As shown in Fig. 2, calculations indicated that the combination of a small quantity of reductant tended to improve the partitioning efficiency(Pu content in U product) even at a low temperature. And, as the temperature is increased up to 15℃, for example, adding only ca. three percent of reductant to Pu can keep the U product quality level which was obtained in an acid-split process without reductant at 5℃, as shown in Fig. 3.

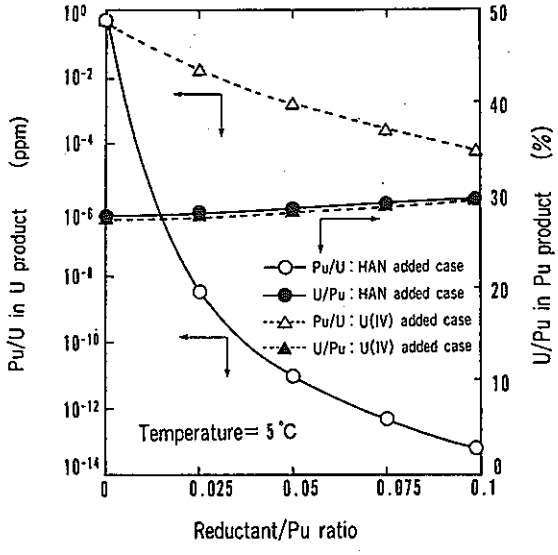

Fig. 2 Effect of addition of reductant on the product quality in an acid-split process.

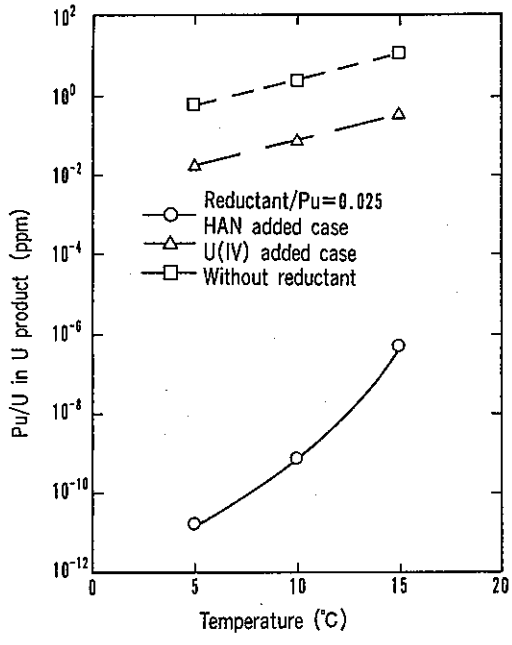

Fig. 3 Temperature effect on the product quality in an acid-split process with reductant.

Therefore, satisfying the required partitioning efficiency in a limited number of the stages might necessitate the combination of a small quantity of reductant in a realistically higher process temperature environment. Nevertheless the calculation showed that only a small quantity of reductant will function as a "alpha barrier" at lower process temperatures. Whether or not HAN will always act more effectively than U(IV) should be verified by experiments.

Pu Electrooxidation

As the incorporation of in-situ electroreduction into the centrifugal contactor cycle is an idea at PNC, reductive partitioning using HAN/Hdz is a reasonables choice. While the acid-split process seems to be more attractive, the combination of a small quantity of reductant seemed to be inevitable as mentioned above. Therefore, reoxidation of Pu(III)/HAN/Hdz is still necessary.

The batch electrolysis tests of Pu(III)/HAN/Hdz in a nitric acid system were conducted with a beaker scale electrolysis cell. Plutonium solution was supplied from refined Pu-product in the Tokai reprocessing plant, so metalic impurities in the tested solution were negligible. The systematic electrolysis test was performed using a small scale filter-press type electrolysis cell. Neither the beaker scale nor the filter-press type cell were equipped with a diaphragm. The anode was made of a thin platinum coating on a titanium base, and the cathode was a smooth platinum wire. The electrolysis was based on galvanostatic condition, then the effect of anodic current density, acidity, temperature and stirring rate on the electrooxidation rates were evaluated respectively.

As shown by run a and b in Fig. 4 from the beaker scale electrolysis tests, electrooxidation of Pu(III) stabilized by hydrazine showed an apparently very simple time dependency, that is, Pu(III) oxidation was observed to be accelerated by an increase of anodic current density. After the end of oxidation of Pu (III) to Pu(IV), further oxidation to Pu(VI) occasionally occurred, but it did not exceed ca. 2% of initial Pu(III).

In the case of the presence of HAN with Pu(III) /Hdz, electrooxidation behavior of Pu(III) was considerably different, especially in a low anodic current density condition, as shown by run d in Fig. 4. Pu(III) oxidation behavior could be explained as follows; In the initial oxidation step, a very low oxidation rate occurred which produced Pu(IV) which immediately reacted with HAN to regenerated Pu(III). Thus HAN was oxidized by electrolytically produced Pu(IV). In sufficiently low concentration of HAN in the next step, Pu(III) oxidation proceeded quickly without any reductive consumption of Pu(IV). As anodic current density increased, shown as run c, such a oxidation "circle" was accelerated. In the presence of HAN, there was no Pu(VI) at all observed. On the contrary, oxidation of HAN and hydrazine proceeded irreversibly. These results indicate, an increase of Pu/HAN ratio, temperature and current density will accelerate the oxidation rate of Pu(III)/HAN/Hdz system in the nitric acid. Current efficiency of these oxidation results are summerized in Table 2. In the case of HAN, calculations were made on the assumption that one mole of Pu(IV) generated by electrode reaction might

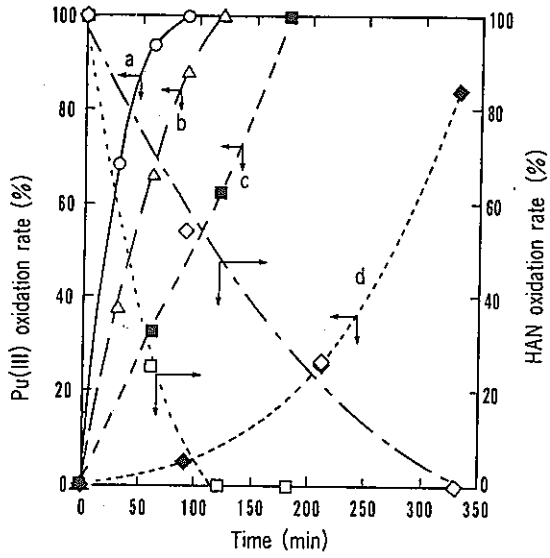

Fig. 4 Electrooxidation of Pu(III) and HAN in nitric acid solution.

—○— ia : 20mA/cm², Pu/Hdz/HNO_3
—△— ia : 10mA/cm², Pu/Hdz/HNO_3
—■— ia : 20mA/cm², Pu/HAN/Hdz/HNO_3
-◆- ia : 10mA/cm², Pu/HAN/Hdz/HNO_3
-□- ia : 20mA/cm², Pu/HAN/Hdz/HNO_3
—◇- ia : 10mA/cm², Pu/HAN/Hdz/HNO_3

Table 2 Results of electrooxidation of Pu(III), HAN, Hydrazine in HNO_3.

RUN	Current efficiency, η(%)				NH_4^+ formation (mM/Ah)	HN_3 formation (mM/Ah)	Pu(VI) formation (mM/Ah)
	$\eta_{Pu(III)}$	η_{HAN}	η_{Hdz}	$\Sigma\eta$			
Pu/Hdz[a]	11.5	—	45.3	56.8	0.04	ND[e]	ND[e]
Pu/Hdz[b]	20.1	—	68.2	88.3	0.20	ND[e]	ND[e]
Pu/HAN/Hdz[c]	1.6	104.2	93.2	199.0	ND[f]	2.6	ND[e]
Pu/HAN/Hdz[d]	4.4	4.3	19.0	27.7	ND[f]	0.5	ND[e]

Sa/Sc=20, Temp.=25°C
a, ia=20mA/cm², v=0.01cm/s, Soln.: Pu(III)22.3g/ℓ, Hdz 2.6g/ℓ, H^+ 2N
b, ia=20mA/cm², v=0.02cm/s, Soln.: Pu(III)20.7g/ℓ, Hdz 2.0g/ℓ, H^+ 2N
c, ia=10mA/cm², v=0.01cm/s, Soln.: Pu(III)222g/ℓ, Hdz 2.9g/ℓ, HAN 15.0g/ℓ, H^+ 1N
d, ia=50mA/cm², v=0.02cm/s, Soln.: Pu(III)18.2g/ℓ, Hdz 2.9g/ℓ, HAN 8.3g/ℓ, H^+ 3N
e, Not Detected
f, No Data

consume a half mole of HAN in the bulk solution when the presense of HAN was in a small concentration. Although low current efficiency was obtained on Pu (III) oxidation in general, higher current efficiencies on hydrazine were obtained with lower anodic current densities. In low anodic current density, 10 mA/cm2, the total current efficiency exceeded the theoretical one.

The average yield of ammonium ion, in cases a and b, were almost the same as that from another experiment(7). Although hydrogen azide was negligible in runs a and b, small amounts of it was recognized in runs c and d, the case where HAN existed in the Pu/Hdz system. The results from this series of experiment supported a similar mediator function of Pu(III) ion to that of Fe(II) and Ce(III) ions in previous experiment(1).

As taking a new turn, electrooxidation of Np ion to its extractable form, Np(VI), should be studied.

Solvent Cleanup

In a preliminary study, cleanup tests with beaker scale laboratory equipment and a centrifugal contactor were performed to consider the applicability of a centrifugal contactor to the Salt-Free process. In these tests, 30%TBP/n-dodecane containing DBP and hydrazine oxalate were used as the simulated degraded solvent and Salt-Free cleanup reagent, respectively.

The beaker scale tests were conducted under various concentrations to collect basic scrubbing data. The test conditions were as follows; the mixing time was 10 minutes, the ratio of organic to aqueous phase was 1.0. After cleanup, the concentration of DBP in the organic phase was analyzed. The result is shown in Fig. 5.

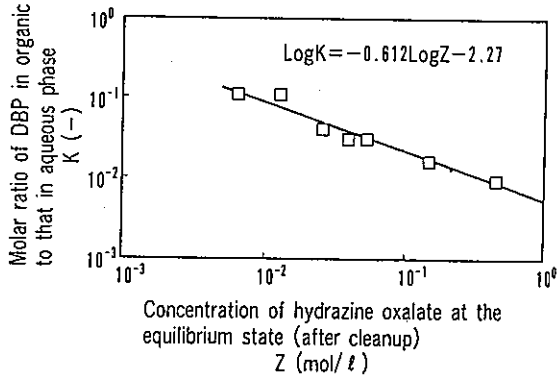

Fig. 5 Result of cleanup tests in beaker scale laboratory equipment.

The y-axis is the molar ratio of DBP in organic to that in aqueous phase (this ratio is expressed as K in this paper); as the value of K decreases scrubbing efficiency increases. The x-axis is the concentration of hydrazine oxalate at the equilibrium state (after cleanup) assuming that one mole of hydrazine oxalate relates to the clean up of one mole of DBP (this value is expressed as Z in this paper). This figure indicates that the scrubbing efficency increases as Z increases. From these data, under the above assumption, an empirical equation was derived to express the relation between K and Z in the range of $K < 0.1$ as shown in Fig. 5.

Solvent cleanup tests using a 4-stage contactor developed at PNC(8) were conducted. The contact time (residence time in a mixing section) per one stage was about 5 seconds. The concentration of DBP in the organic phase was analyzed in this test. Fig. 6 shows the test flowsheets and the results. Black and white symbols show the experimental and calculated data based on beaker scale test, respectively. The concentration of DBP dropped from 1340ppm to less than 10 ppm (which was the analytical limitation in this test) within 4-stages. In the case of run 1, the feed molar ratio of hydrazine oxalate to DBP was 1.6. The prediction agrees well with the concentration profile obtained.

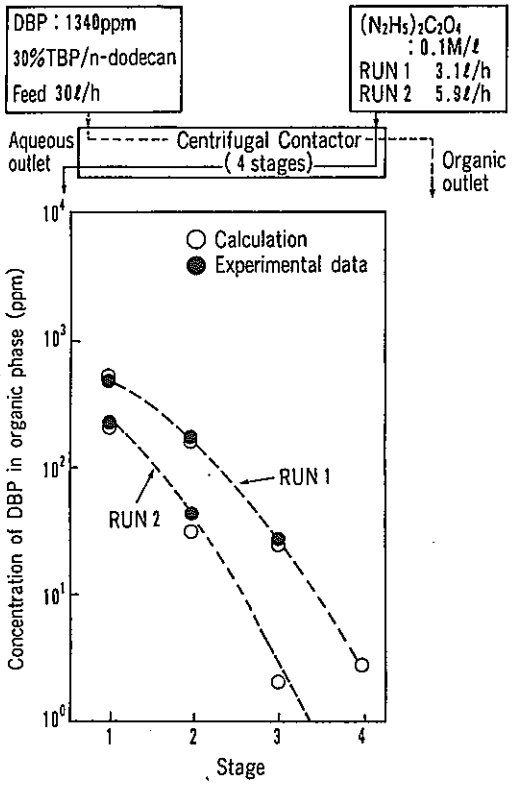

Fig. 6 Solvent cleanup characteristics by Salt-Free reagent using centrifugal contactors.

Good agreement of the prediction with the profile obtained showed that the scrubbing efficiency in the centrifugal contactor for DBP is almost the same as that in beaker scale tests in spite of the shorter residence time in this particular system. This result also gives the prospect to design improved solvent cleanup systems based on Salt-Free reagents with a short residence time if DBP is the dominant material to the solvent cleanup process design, whereas the conventional solvent cleanup processes have been designed with longer residence times and alkaline-salts reagents using mixer-settlers.

Removal of Platinum Elements

Even in the existing Purex process Ru and Np are recognized to be noticeable elements for understanding their extraction behaviors and thus improving the Purex process itself. Various existing kinds of ionic states and the difficulties of identifying those complexes in actual purex solution complicated detailed evaluation of in-plant behavior(9). Ru (one of the long lived fission products) instead of Zr, became a major requisite to simplify the extraction process because recently reprocessing plants have tended to treat somewhat longer cooled spent fuel. A preliminary study of the removal of platinum group elements from nitric acid solution was newly initiated using an electroreductive method. Simulated HLLW solution, containing Ru, Rh, Pd, Ag, etc, was used as a basic electrolyte, type 304L stainless steel and smooth Pt were chosen for the working and counter electrodes, respectively, and SCE was used as the reference electrode. As electrolysis occurred, a black colored material deposited on the cathode surface, some of which was easily detached by only small vibration. Electrodepositted material was anodicaly dissolved from the electrode surface in a pure nitric acid. Fig. 7 shows electrodeposit rates of concerned metals during a 24 hour potentiostatic electrolysis.

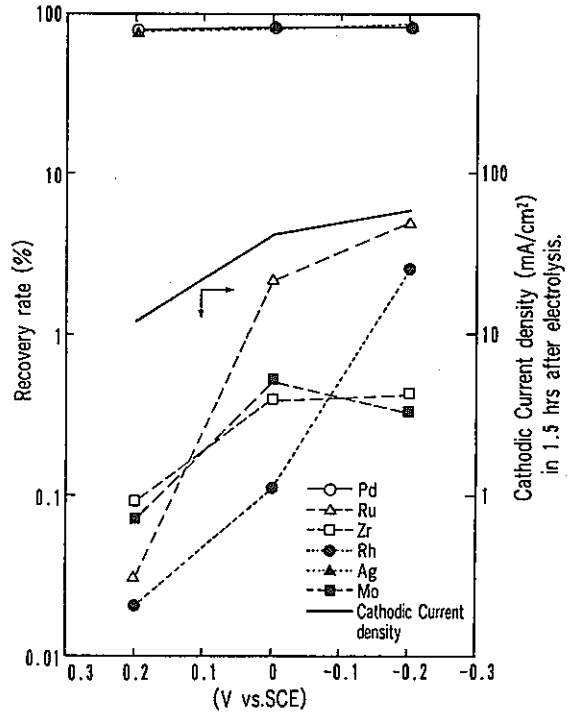

Fig. 7 The relation between deposited metal on the cathode and Polarized Potential.
Recovery rate : $M_{deposited}/M_{bulk} \times 100(\%)$
Packing density(Sc/V) : $1 \times 10^{-2} cm^{-1}$

In spite of lower packing density of the experimental cell, Pd and Ag tended to deposit in a given potential region with high rates. Ru and Rh, on the contrary, resulted in a very small amount of deposition in comparison with predicted values by a standard redox potential corresponding to a simple metal ionic discharge system, while the tendency that their deposition increased as polarized potential became more negative was observed. The current program is focused on finding out the proper electrodeposition conditions on the effect of co-existing U and Pu ions and improving current efficiency. Possible future experiments could focus on electroreduction conditions for converting nitrosylruthenium nitrate complexes to their less extractable species.

CONCLUSIONS

- In the acid-split process with centrifugal contactors, calculations support that a very small quantity of reductant would be useful in improving plutonium stripping from the uranium product stream.
- Pu(III)/Hdz and Pu(III)/HAN/Hdz could be oxidized quantitatively by electrolysis. The power of Pu(III) as a mediator in the HAN oxidation system was confirmed.
- In a DBP/hydrazine oxalate cleanup system, expected cleanup efficiency was obtained for very short residence time corresponding to mixing in a four-stage contactor.
- An attempt to remove troublesome platinum elements by electrodeposition from dissolver solution appeared to be feasible for palladium and silver. Futher research is being planned.

ACKNOWLEDGEMENT

The authors wish to acknowledge the valuable advice of Dr. D.O.Campbell.

REFERENCES

1. M.Ozawa, N.Tamura, R.Yamamoto, T.Kawata and S.Hayashi, "Application of Salt-Free Technology to the PUREX process for FBR Fuel Reprocessing" ISEC '90 (1990).
2. D.O.Campbell and A.L.Mills, "Non Reductive Partitioning of Uranium and Plutonium in the PUREX Process" ISEC '86 (1986).
3. T.Yasu, O.Toyoda, S.Ohtake, A.Todokoro and Y.Kishimoto, "U/Pu Partition Process with Lactic Acid" 1989 Annual Meeting of the Atomic Energy Society of Japan.
4. M.Ozawa, T.Washiya and Y.Kishimoto, "Fundamental study on Electrooxidation of Salt-free Reagents(II), 1989 Annual Meeting of the Atomic Energy Society of Japan.
5. M.Ozawa, T.Washiya, K.Ohki and T.Kawata, "Flowsheet Study on Acid-Split" 1989 Fall Meeting of the Atomic Energy Society of Japan.
6. R.Thompson, C.Mason and A.C.Tolchard, I. CHEM.E. SYMPOSIUM SERIES No.103.
7. H.Schmieder, H.Goldacker, "Experiences with Electroredox Equipment for the Separation of Plutonium" AIChE SYMPOSIUM SERIES No.254, Vol.83.
8. H.Takeda, T.Kawata, Y.Ueda, R.Shimizu, S.Nemoto and S.Hayashi, "Development of a Centrifugal Contactor" ISEC '90 (1990).
9. T.Yamanouchi, N.Sasao, M.Ozawa and H.Yamana, "Extraction Behavior of some Noticeable Nuclides in the Tokai Reprocessing Plant" RECOD '87.

題　　名	Study on the Behavior of Radionuclides in Marine Environment Under the Monitoring Program of the TOKAI Reprocessing Plant		
発表先	RECOD'91		
発表地	仙　　台	発　表 年月日	平成3年　4月14日 ～ 4月18日
発表者 (○印口頭発表者)	所　属　名	安管部　環安課	
	○林　　直美，篠原　邦彦，片桐　裕実，圓尾　好宏		

(要旨)

再処理施設から海洋に放出される処理済廃液による周辺公衆の被ばく線量当量評価に必要な放射性核種の移行パラメータについて操業前モニタリング以来の海洋モニタリングデータ並びにプルトニウム-239，240 及びアメリシウム-241の水準調査で得られたデータを基にサイト・スペシフィックな移行パラメータとして検討し，算出した。得られたパラメータは，海産生物への濃縮係数（Ｓｒ，Ｚｒ，Ｎｂ，Ｒｕ，Ｃｓ，Ｃｅ，Ｐｕ，Ａｍ），海岸砂の汚染係数（Ｓｒ，Ｚｒ，Ｎｂ，Ｒｕ，Ｃｓ，Ｃｅ）及び海底土と海水間の分配係数（Ｓｒ，Ｃｓ，Ｐｕ）である。

これらのパラメータは海洋環境での平衡状態を仮定して，海水中の放射性核種濃度に対する海産生物，海岸砂及び海底土中の放射性核種濃度の比と定義されている。平衡状態を仮定するためにこの研究では，海洋環境での放射性核種濃度が対数正規確率分布を取ることから，算術平均濃度と幾何学的平均濃度を用いた。各パラメータに対して算術平均濃度の比及び幾何学的平均濃度の比として，それぞれ算出した値は，ほとんど同等の値であった。これは海洋試料中の各核種濃度の確率分布が類似しているためと考えられる。なお，海洋モニタリングデータ等には再処理施設に起因する有意な濃度レベルの上昇は見られず，大気圏内核実験による世界的なフォールアウトと同じレベルであった。

資　料　番　号
ＴＮ８４１０　９１－００８ （８０－０２－２３１）

資料番号 TN8100 91-008

STUDY ON THE BEHAVIOR OF RADIONUCLIDES IN MARINE ENVIRONMENT UNDER THE MONITORING PROGRAM OF THE TOKAI REPROCESSING PLANT

N.HAYASHI, H.KATAGIRI, Y.MARUO and K.SHINOHARA

Environmental Protection Section, Health and Safety Division,
Tokai Works,
Power Reactor and Nuclear Fuel Development Corporation,
Tokai-mura, Ibaraki-ken, 319-11, Japan

ABSTRACT

We have studied the behavior of radionuclides in marine environment for a realistic estimation of the dose equivalent to the public caused by the discharge of low level radioactive liquid waste from the Tokai Reprocessing Plant (TRP).

In this study, we obtained the site-specific parameters on the transfer pathways of radionuclides in marine environment, such as concentration factors for marine products, sediment-sea water distribution coefficients and contamination factors for beach sand.

We used arithmetic and geometric means for concentrations of radionuclides in calculation of these parameters assuming the equilibrium condition in marine environment. The parameters calculated by using two statistical methods were on the same order of magnitude.

INTRODUCTION

The construction of TRP started in 1971 at the site of the Tokai Works, PNC, and finished in 1974. After uranium test runs, the operation of the reprocessing of spent fuels started in 1977 (1).

Environmental monitoring in marine environment started in 1971 as the pre-operational environmental monitoring to grasp the concentration levels of fission products and Pu-239,240 caused by global fallout. The routine monitoring program in marine environment started in 1977.

The simplified pathways to man from radioactive materials released to surface waters including oceans are shown in the ICRP publication 43 (2). In our case, we adopted two main pathways which were the internal exposure through the intake of marine products and the external exposure from the contaminated beach sand and fishing gears such as fishing net and a fishing boat.

The environmental parameters for assessing the effective dose equivalent to the public are concentration factors for marine products and contamination factors for beach sand and fishing gears. In the safety assessment of TRP (1969, 1977), contamination factors for fishing net and boat deck were taken into account from the literatures (3, 4). Concentration factors and contamination factors for beach sand, which are key parameters for dose estimation, were mainly based on the field data obtained around the Tokai Works in the pre-operational environmental monitoring (5).

This article describes the results of re-evaluating of concentration factors and contamination factors for beach sand, and additionally reports sediment-sea water distribution coefficients, which are based on the monitoring data from 1972 to 1986 as the study on the behavior of radionuclides in marine environment around TRP.

ENVIRONMENTAL MONITORING PROGRAM IN MARINE ENVIRONMENT

Japan Nuclear Safety Commission provides "Guideline on Environmental Radiation Monitoring" (6). The Basic objective of the environmental monitoring in this guideline is to demonstrate health and safety of the public in the vicinity of a nuclear facility.

Practical objectives are summarized as follows.

1) to estimate dose equivalents to the public, 2) to assess accumulation of radionuclides in the environment, and 3) to provide information on variations of natural background levels of radionuclides to assess un-planned

release of radionuclides from a nuclear facility and trigger a further monitoring.

Our practical monitoring program for marine environment is shown in Table 1. The observation area around TRP is within approximately 5 km from the coast, 6 km northward and southward from the discharge point. In this area, we collect various kinds of samples on the transfer pathways of radionuclides to man such as sea water, sea bed sediment, coastal sea water, beach sand and marine products.

Reference areas are located at distance of 20 km northv ard and southward from the dischage point. In these area, we monitor the concentrations of radionuclides in sea water, sea bed sediment and so on to comprehend the variation of the levels of environmental radioactivity.

To study the behavior of radionuclides, we also collect other marine products, such as cephalopods and crustaceans, and determine Am-241 in marine samples besides the routine monitoring program.

THE CONCENTRATIONS OF RADIONUCLIDES IN MARINE ENVIRONMENT

(1) Sea Water

The concentration data of sea water are very important in deriving the transfer

Table 1. Routine Environmental Monitoring Program in Marine Environment around the Tokai Reprocessing Plant.

Sample	Sampling Location and Frequency	Measuring Nuclides and Frequency
Sea Water	Discharge point and the surrounding surface: 5 (quaterly) Offshore of Tokai Works: 2 (semiannualy) 20km northward from discharge point: 1 (annualy)	Gross beta, H-3 (quaterly, semiannually or annually) Sr-90, Ru-106, Cs-134, Cs-137, Ce-144, Pu-239, 240 (annually)
Sea Bed Sediment	Discharge point and the surrounding area: 5 (semiannually) Offshore of Tokai Works: 2 (semiannually) 20km northward from discharge point: 1 (semiannually)	Sr-90, Ru-106, Cs-134, Cs-137, Ce-144, Pu-239, 240 (semiannually)
Beach Water	Beach: 5 (semiannually) 20km northward and southward from discharge point: 2 (semiannually)	Gross beta, H-3 (semiannually) Sr-90, Ru-106, Cs-134, Cs-137, Ce-144, Pu-239, 240 (annually)
Beach Sand	Beach: 5 (quaterly)	Gamma and beta dose rate (quaterly)
Marine Products	Whitebait, Fish and Shellfish: 2 (quaterly) Seaweed: 3 (quaterly)	Sr-90, Ru-106, Cs-134, Cs-137, Ce-144 (quaterly)
Fishing Net and Boat deck	Monitoring boat "Seikai" (quaterly)	Gamma and beta dose rate (quaterly)

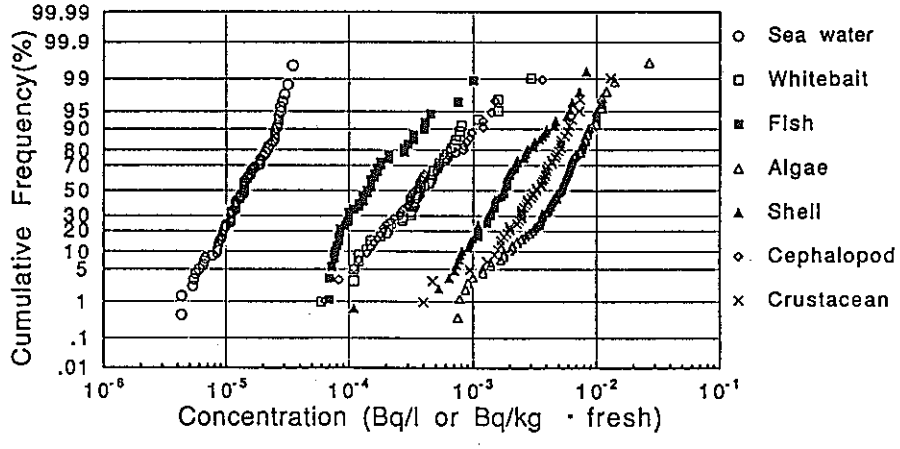

Fig.1. The distribution of $^{239,240}Pu$ concentration in sea water and marine products.

parameters such as concentration factors for marine products, contamination factors for beach sand and distribution coefficients for sea sediment. The nuclides of our concern to derive the parameters are Sr-90, Zr-95, Nb-95, Ru-106, Cs-137, Ce-144, Pu-239,240 and Am-241. The concentrations of these nuclides are compiled in Table 2. Unfiltered sea water samples were provided to determine Zr-95, Nb-95 for 1972-1977, Sr-90, Cs-137, Ce-144 and Pu-239,240 for 1980-1986 and Am-241 for 1982-1986. Undetectable values were omitted in these data (as well as in the data of marine products, beach sand and sea bed sediment). As the concentration levels of these radionuclides have been decreasing, we can now detect only long lived radionuclides such as Sr-90, Cs-137, Pu-239,240 and Am-241. No significant increase of the concentration of radionuclides in sea water due to TRP has been detected, because the total amount of the discharged gross beta activity for 1972-1988 was no more than 19 GBq (7). The concentration levels were on the same order of magnitude as the levels originated from global fallout.

(2) Marine Products

The collected marine products were whitebait (Engraulis japonica), fish (flatfish), shellfish (Gomphina (Macridiscus) melanegis), cephalopods (Decapod and Octopod) and crustacean (shrimp). In view of fisheries, Tokai offshore is one of the good fishing grounds of these marine products and their consumptions in the vicinity of the Tokai Works are greater than those of other species. Therefore we chose them as the objects of the environmental monitoring.

The concentrations of radionuclides in the edible parts of marine products are presented in Table 3. These data were measured in the samples collected for the same periods as those for the concentrations in sea water.

(3) Beach Sand and Sea Bed Sediment

Beach sand and sea bed sediment were collected at shore line and Tokai offshore, respectively. Sr-90, Zr-95,Nb-95, Ru-106, Cs-137 and Ce-144 in beach sand were analyzed to assess the external exposure to man on the beach in the monitoring area. Sr-90, Cs-137 and Pu-239,240 in sea bed sediment were also analyzed to monitor the long term accumulation of these nuclides. The sea bottom at Tokai offshore was observed to be almost covered with sand and partially with rocks. The median diameters of sand in the monitoring area were 0.1-1.3 mm.

The concentrations of these nuclides are compiled in Table 4 and Table 5.

ENVIRONMENTAL PARAMETERS DERIVED FROM THE FIELD DATA

(1) Concentration Factors for Marine Products

Concentration factors have been used extensively to estimate the accumulation of radionuclides by aquatic organisms and to predict the dose equivalent to the public from the ingestion of aquatic foodstuffs contaminated by various radionuclides. A concentration factor is defined as the ratio of the concentration of a radionuclide in edible parts of aquatic organism to that in the surrounding water under the equilibrium condition (8). It is known that the rates of both uptake and excretion in the relationship between the concentration of radionuclides in a living organism and that in the ambient sea water are affected by many factors such as body size, temperature, salinity and so on (9, 10).

The concentrations of marine environmental samples and the ratios of the concentration of marine products to that of sea water collected in almost same time follow log-normal distributions. Also, we confirmed that concentration factors of Pu-239,240 and Am-241 for marine products calculated with the three statistical methods were on the same order of magnitude. The methods were the calculations of the ratio between the arithmetic or the geometric means of the concentrations in marine products and those in sea water and the geometric mean of the concentration ratios between marine products and sea water collected in the same quarter of a given year (11).

In this article, we chose the arithmetic and geometric mean concentrations to calculate concentration factors assuming the equilibrium condition. A concentration factor is defined as a following equation.

$$C.F. = \frac{\text{arithmetic (or geometric) mean concentration in marine products (Bq/kg, fresh)}}{\text{arithmetic (or geometric) mean concentration in sea water (Bq/l)}}$$

The cumulative frequency plots of concentrations of Pu-239,240 in marine environmental samples are shown in Fig.1. The calculated concentration factors are shown in Table 6. The concentration factors for marine products calculated by the arithmetic and geometric means were almost equal. These concentration factors varied depending on radionuclides and/or the species of marine products and were almost equivalent to the previous values obtained in the pre-operational monitoring (5).

(2) Contamination Factors for Beach Sand and Distribution Coefficient for Sea Bed Sediment

Adsorption of radionuclides to solids depends on kinds of sediment, their surface condition and so on. A contamination factor for beach sand collected at shore line and a sediment-sea water distribution coefficient were defined, as well as a concentration factor for marine products, as the ratio of the concentration of a radionuclide in beach sand or sea bed sediment to that in sea water under the equilibrium condition.

The parameters were calculated by the same method for concentration factors for marine products, because the concentrations of radionuclides in beach sand and sea bed sediment also followed log-normal distributions. Contamination factors and distribution coefficients are shown in Table 7 and Table 8, respectively.

Contamination factors of Zr-95, Nb-95 and Ce-144 calculated by the geometric means tended to be higher than those calculated by the arithmetic means. Distribution coefficients of Sr-90 and Cs-137 for sea bed sediment were slightly higher than contamination factors for beach sand.

CONCLUSION

The site-specific concentration factors for marine products and contamination factors were obtained from the monitoring data to assess the dose equivalents to the public caused by the low level liquid waste discharged from TRP. Sediment-seawater distribution coefficients were also derived from the monitoring data.

The parameters based on the field data are generally reflected by all process in marine environment such as physical, chemical and biological process. We used the arithmetic and geometric mean concentrations of a radionuclide in

Table 2. Concentrations of Sr-90, Ru-106, Zr-95, Nb-95, Cs-137 and Ce-144 in Sea Water

Nuclides	n	Concentration (Bq /ℓ) Range	Arithmetic Mean:(ma)w	Geometric Mean:(mg)w
Sr-90	273	2.7 E-3 ～ 3.3 E-2	8.5 E-3	7.4 E-3
Zr-95	73	3.7 E-4 ～ 1.3 E-2	2.8 E-3	2.0 E-3
Nb-95	64	3.7 E-4 ～ 6.3 E-2	5.6 E-3	3.4 E-3
Zr/Nb-95 *	62	7.4 E-4 ～ 6.7 E-2	7.4 E-3	5.2 E-3
Ru-106	211	2.7 E-4 ～ 6.3 E-2	2.3 E-3	1.5 E-3
Cs-137	268	2.5 E-3 ～ 5.6 E-2	9.6 E-3	8.5 E-3
Ce-144	185	1.1 E-4 ～ 1.0 E-2	1.7 E-3	1.1 E-3
Pu-239, 240	109	4.3 E-6 ～ 3.5 E-5	1.5 E-5	1.4 E-5
Am-241	45	1.0 E-6 ～ 8.8 E-6	3.1 E-6	2.5 E-6

* Zr/Nb-95 means the sum value of concentrations of Zr-95 and Nb-95 detected in the same sea water samples.
** Sampling periods: Zr-95, Nb-95 : 1972 ～ 1977
Sr-90, Ru-106, Cs-137 and Ce-144; 1972～1982
Pu-239, 240; 1980～1986, Am-241; 1982～1986

Table 4. Concentrations of Sr-90, Ru-106, Zr-95, Nb-95, Cs-137 and Ce-144 in Beach Sand

Nuclides	n	Concentration (Bq / kg・dry) Range	Arithmetic Mean:(ma)b	Geometric Mean:(mg)b
Sr-90	73	2.8 E-2 ～ 4.4 E-1	1.2 E-1	9.3 E-2
Zr-95	5	1.1 ～ 1.9	1.4	1.3
Nb-95	7	3.7 E-1 ～ 2.4	8.1 E-1	6.7 E-1
Ru-106	45	8.1 E-2 ～ 1.1	4.1 E-1	3.5 E-1
Cs-137	104	2.1 E-1 ～ 1.9	7.8 E-1	7.0 E-1
Ce-144	75	7.8 E-2 ～ 1.8	6.3 E-1	5.6 E-1

* Sampling periods: Zr-95, Nb-95 ; 1972 ～ 1977
Sr-90, Ru-106, Cs-137 and Ce-144; 1972 ～ 1982

Table 5. Concentrations of Sr-90, Cs-137 and Pu-239, 240 in Sea Bed Sediment.

Nuclides	n	Concentration (Bq / kg ・dry) Range	Arithmetic Mean:(ma)s	Geometric Mean:(mg)s
Sr-90	368	2.4 E-2 ～ 1.8	1.7 E-1	1.3 E-1
Cs-137	316	1.5 E-1 ～ 5.6	1.3	1.1
Pu-239, 240	181	9.4 E-2 ～ 1.3	5.1 E-1	4.6 E-1

* Sampling periods: Sr-90 and Cs-137 ; 1972～ 1982
Pu-239, 240 ; 1980～ 1986

Table 3. Concentrations of Radionuclides in Marine Products

Marine Products / Nuclides	n	Concentration (Bq / kg・fresh) Range	Arithmetic Mean:(ma)m	Geometric Mean:(mg)m
Whitebait				
Sr-90	71	6.7 E-3 ~ 2.5 E-1	3.4 E-2	2.6 E-2
Zr/Nb-95	12	2.2 E-2 ~ 3.6 E-1	1.9 E-1	1.5 E-1
Ru-106	52	8.1 E-3 ~ 3.4 E-1	4.8 E-2	3.1 E-2
Cs-137	87	8.1 E-2 ~ 7.8 E-1	2.4 E-1	2.2 E-1
Ce-144	59	9.3 E-3 ~ 2.7 E-1	5.6 E-2	3.6 E-2
Pu-239, 240	51	6.0 E-5 ~ 3.0 E-3	5.0 E-4	3.8 E-4
Am-241	34	6.4 E-5 ~ 7.2 E-4	2.1 E-4	1.8 E-4
Fish				
Sr-90	72	6.7 E-3 ~ 1.3 E-1	2.9 E-2	2.3 E-2
Zr/Nb-95	11	3.0 E-2 ~ 5.9 E-1	2.2 E-1	1.4 E-1
Ru-106	43	5.9 E-3 ~ 8.1 E-2	2.0 E-2	1.6 E-2
Cs-137	96	4.4 E-2 ~ 5.6 E-1	2.6 E-1	2.4 E-1
Ce-144	11	5.9 E-3 ~ 6.3 E-2	2.9 E-2	2.1 E-2
Pu-239, 240	45	6.9 E-5 ~ 1.0 E-3	2.0 E-4	1.6 E-4
Am-241	41	3.2 E-5 ~ 3.0 E-4	1.1 E-4	9.1 E-5
Brown algae				
Sr-90	64	2.6 E-2 ~ 3.4 E-1	1.3 E-1	1.1 E-1
Zr/Nb-95	17	5.6 E-2 ~ 2.2	6.7 E-1	4.4 E-1
Ru-106	69	3.7 E-3 ~ 1.8	2.7 E-1	1.6 E-1
Cs-137	59	4.4 E-2 ~ 7.4 E-1	2.8 E-1	2.3 E-1
Ce-144	59	2.1 E-2 ~ 1.6	2.1 E-1	1.3 E-1
Pu-239, 240	128	7.8 E-4 ~ 2.7 E-2	5.4 E-3	4.6 E-3
Am-241	87	1.2 E-4 ~ 2.8 E-3	7.6 E-4	6.2 E-4
Shellfish				
Sr-90	59	5.9 E-3 ~ 2.6 E-1	4.4 E-2	3.3 E-2
Zr/Nb-95	8	4.4 E-2 ~ 6.3 E-1	2.7 E-1	2.1 E-1
Ru-106	85	1.8 E-2 ~ 1.3	3.3 E-1	2.5 E-1
Cs-137	75	2.2 E-2 ~ 7.4 E-1	1.0 E-1	8.5 E-2
Ce-144	91	3.0 E-2 ~ 3.2	4.4 E-1	2.9 E-1
Pu-239, 240	74	1.1 E-4 ~ 8.3 E-3	2.2 E-3	1.8 E-3
Am-241	53	3.8 E-4 ~ 4.6 E-3	2.3 E-3	2.1 E-3
Cephalopod				
Sr-90	42	6.7 E-3 ~ 1.3 E-1	2.8 E-2	2.1 E-2
Zr/Nb-95	3	7.0 E-2 ~ 5.2 E-1	3.7 E-1	2.6 E-1
Ru-106	34	8.5 E-3 ~ 8.5 E-2	2.8 E-2	2.3 E-2
Cs-137	61	1.4 E-2 ~ 2.3 E-1	9.3 E-2	7.8 E-2
Ce-144	39	9.6 E-3 ~ 1.3 E-1	3.7 E-2	3.0 E-2
Pu-239, 240	48	6.4 E-5 ~ 3.7 E-3	5.3 E-4	3.7 E-4
Am-241	29	1.3 E-4 ~ 8.5 E-4	3.9 E-4	3.5 E-4
Crustacean				
Sr-90	55	5.2 E-2 ~ 5.2 E-1	1.9 E-1	1.6 E-1
Zr/Nb-95	5	7.8 E-2 ~ 5.6 E-1	2.3 E-1	1.9 E-1
Ru-106	49	2.1 E-3 ~ 1.4	2.6 E-1	1.5 E-1
Cs-137	34	1.0 E-2 ~ 2.8 E-1	1.3 E-1	1.1 E-1
Ce-144	50	1.1 E-2 ~ 5.6 E-1	1.5 E-1	1.0 E-1
Pu-239, 240	51	4.0 E-4 ~ 1.3 E-2	3.6 E-3	3.0 E-3
Am-241	32	3.8 E-4 ~ 8.8 E-3	2.0 E-3	1.6 E-3

*Smpling periods: Zr-95/Nb-95; 1972 ~ 1977
Sr-90, Ru-106, Cs-137 and Ce-144; 1972 ~ 1982
Pu-239, 240;1980 ~ 1986 , Am-241;1982 ~ 1986

Table 6. Concentration Factor of Marine Products

Marine Products		Concentration Factor Sr	Zr/Nb	Ru	Cs	Ce	Pu	Am
Whitebait	(ma)m/(ma)w *	4.0	26	21	25	33	33	68
	(mg)m/(mg)w**	3.5	29	21	26	33	27	72
Fish	(ma)m/(ma)w *	3.4	30	8.7	27	17	13	35
	(mg)m/(mg)w**	3.1	27	11	28	19	11	36
Brown Algae	(ma)m/(ma)w *	15	91	120	29	120	360	250
	(mg)m/(mg)w**	15	85	110	27	120	330	250
Shellfish	(ma)m/(ma)w *	5.2	36	140	10	260	150	740
	(mg)m/(mg)w**	4.5	40	170	10	260	130	840
Cephalopod	(ma)m/(ma)w *	3.3	50	12	9.7	22	35	130
	(mg)m/(mg)w**	2.8	50	15	9.2	27	26	140
Crustacean	(ma)m/(ma)w *	22	31	110	14	88	240	650
	(mg)m/(mg)w**	22	37	100	13	91	210	640

* (ma)m/(ma)w is the ratio of an arithmetic mean concentration of a nuclide in marine products to that in sea water.
** (mg)m/(mg)w is the ratio of a geometric mean concentration of a nuclide in a marine products to that in sea water.

Table 7. Contamination Factors for Beach Sand

Nuclides	Contamination Factor	
	(ma)b/(ma)w *	(mg)b/(mg)w**
Sr-90	14	13
Zr-95	500	650
Nb-95	140	200
Ru-106	180	230
Cs-137	81	82
Ce-144	370	510

* (ma)b/(ma)w is the ratio of an arithmetic mean concentration of a nuclide in beach sand to that in sea water.
** (mg)b/(mg)w is the ratio of a geometric mean concentration of a nuclid in beach sand to that in sea water.

Table 8. Sediment-Sea Water Distribution Coefficients of Sr-90, Cs-137 and Pu-239, 240

Nuclides	Distribution Coefficient	
	(ma)s/(ma)w *	(mg)s/(mg)w**
Sr-90	20	18
Cs-137	140	130
Pu-239, 240	34000	33000

* (ma)s/(ma)w is the ratio of an arithmetic mean concentration of a nuclide in sea bed sediment to that in sea water.
** (mg)s/(mg)w is the ratio of a geometric mean concentration of a nuclide in sea bed sediment to that in sea water.

marine environmental samples assuming the equilibrium condition. No significant deference is observed between the parameters calculated by two statistical methods. It may be the reason why the distribution curves for concentrations of radionuclides in sea water are very similar to those in marine products, sea bed sediment and beach sand.

REFERENCES

(1) YAMANOUCHI T. et al., "DECADAL OPERATIONAL EXPERIENCE OF THE TOKAI REPROCESSING PLANT.", Proc. of Int. Conf. on Nuclear Fuel Reprocessing and Waste Management. RECOD 87, PARIS, Vol.1, pp.195-202
(2) ICRP publication 43, Principles of Monitoring for the radiation Protection of the Population.
(3) MAFF, Fisheries Radiobiological Laboratory, Radioactivity in Surface and Coastal Water of British Isles. Technical Rept. FRL-1 (1967)
(4) SAKAGISHI S. et al., Report 3 of the trial assessment subcommittee, A trial assessment of the external exposure caused by the marine discharge of the radioactive waste, Nuclear Safety Research Association of Japan (1980) (In Japanese)
(5) KURABAYASHI M. et al. "Concentration factors of marine organisms used for the environmental dose assessment", Marine Radioecology, Proc. 3rd NEA Seminar Tokyo, 1979, OECD, Paris, pp.335-345 (1980)
(6) Japan Nuclear Safety Commission, "Guideline on Environmental Radiation Monitoring", 1981, revised in1989 (In Japanese)
(7) Monthly Report of Japan Nuclear Safety Commission, Vol. 131 (1990)(In Japanese)
(8) Thompson S.E. et al., "CONCENTRATION FACTORS OF CHEMICAL ELEMENTS IN EDIBLE AQUATIC ORGANISMS", UCRL-50564, Rev.1 (1972)
(9) IAEA TECHNICAL REPORTS SERIES NO. 247, "Sediment Kds and Concentration Factors for Radionuclides in the Marine Environment." (1985)
(10) COUGHTREY D.J. et al., Radionuclide Distribution and Transport in Terrestrial and Aquatic Ecosystems, Vol. 1, A.A. Balkema, Rotterdam, 52 (1983)
(11) HAYASHI N. et al., "CONCENTRATION FACTORS OF PLUTONIUM AND AMERICIUM FOR MARINE PRODUCTS", J.Radioanal. Nuclear Chem. Articles, Vol. 138, No. 2, pp.331-336 (1990)

題　　名	Numerical Simulation for Joule-Heated Ceramic Melter to Vitrify High-Level Liquid Waste		
発表先	RECOD'91		
発表地	仙　　台	発　表 年月日	平成3年　4月14日 ～ 4月18日
発表者 （○印口頭発表者）	所属名	環開部　HTS室	
	○五十嵐　寛，正木　敏夫，高橋　武士		

(要旨)

直接通電型セラミックメルタを対象とした3次元熱流動解析コードの開発を進めている。数学モデルは電荷，質量，エネルギーおよび運動量に対する保存則の方程式から成り，有限差分法により解いた。本モデルを外寸法1.6×1.6×1.6mの工学規模溶融炉に適用し，解析結果を運転結果と比較した。

最大発熱密度は，電極前方に観察された。炉内の速度ベクトル分布から，炉内中央部に上昇流のある2つの循環流が認められた。溶融炉内の輸送現象は数学モデルにより説明でき，温度分布解析結果は複雑な構造を有する工学規模溶融炉に対して，運転結果と比較的良く一致することが判った。

資料番号
TN8410　91－009 （80－02－227）

資料番号 TN8100 91-009

NUMERICAL SIMULATION FOR JOULE-HEATED CERAMIC MELTER TO VITRIFY HIGH-LEVEL LIQUID WASTE

Hiroshi Igarashi, Toshio Masaki and Takeshi Takahashi

Waste technology development division,
Power Reactor and Nuclear Fuel Development Corporation(PNC), Tokai works
4-33 Muramatsu,
Tokai-mura, Ibaraki-ken, JAPAN, 319-11

ABSTRACT

A three-dimensional mathematical model was developed to simulate the operation of the electric glass melter to vitrify high-level liquid waste. The four differential equations are solved by finite difference method in three-dimension under the boundary conditions similar to the real operational conditions. The computational results agreed with the operations and transfer phenomena were well explained.

INTRODUCTION

The electric glass melter referred as to liquid-fed Joule-heated ceramic melter(LFCM) has been developed to vitrify the high-level liquid waste(HLLW) for the Tokai Vitrification Facility (TVF) now under construction beside the Tokai Reprocessing Plant(TRP) [1] and [2].

The requirements for the glass quality and safety need the optimization of the operational conditions and the structural design. With these requirements, the mathematical model for the melter has been developed for the LFCM.

The present paper describes a three-dimesional mathematical model for the LFCM type electric glass melter. The model is applied to the simulation for molten glass and refractory structure of the melter.

PHYSICAL DESCRIPTION OF GLASS MELTER

The melter for simulation is the nonradioactive engineering-scale test melter referred as to the Advanced B-Melter, which has been operated in the Engineering Test Facility (ETF) of PNC Tokai-works [3].

The melter is approximately 1.6x1.6x1.6m in outside dimension and has the rectangular melting cavity with the 0.53 m² of the surface area of exposed molten glass. The maximum volume of molten glass in the melter is .0.3 m³. The melter structure for computation is shown in Fig. 1 .

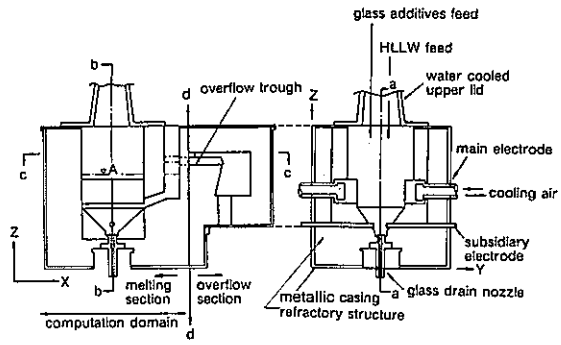

Fig. 1 Glass melter for simulation (Advanced B-melter)

The refractory structure is composed of the multilayer refractories supported in the stainless steel container. The water cooled metallic upper lid is installed on the top end of the melter.

The glass is heated by conducting alternating electric current through the glass mainly between main plate electrodes and additionally between subsidiary rod electrodes to heat the lower part of the cavity. The glass additives used in the operation are cylindrically formed glass fiber, into which the

HLLW is soaked[2]. The glass composition melted in the operation is P0730 glass which is boro-silicate glass containing 25 wt% of nonradioactive simulated waste.

MATHEMATICAL MODEL

The final steady state solution is the primary concern in the present work. The mathematical formulation of the model leads to a set of coupled partial differential equations with the following assumptions.
(1) Glass is Newtonian and incompressible fluid. (2) Flow is laminar. (3) Boussinesq approximation is applied to buoyancy in momentum balance. (4) The temperature dependence of resistivity is not taken into account in electric potential calculation, but in the the calculation of heat generation rate.

Assuming the above, the equations for the conservation of electric charge, mass, energy, and momentum are formulated in three-dimentional vector notation by the following.

Electric charge:

$$\nabla^2 \phi = 0 \qquad \text{—— (1)}$$

Mass:

$$\nabla \cdot u = 0 \qquad \text{—— (2)}$$

Momentum:

$$\frac{Du}{Dt} + \frac{1}{\rho}\nabla p + (u \cdot \nabla)u - \nabla \cdot \tau - g\beta(T - T_0)z = 0 \qquad \text{—— (3)}$$

Energy:

For molten glass,

$$\rho c_p \frac{DT}{Dt} + \rho c_p u(\nabla T) - \nabla \cdot (\lambda \nabla T) - Q = 0 \qquad \text{—— (4)}$$

For refractory structure,

$$\nabla \cdot (\lambda \nabla T) + Q = 0 \qquad \text{—— (5)}$$

Q is the heat generated by Joule heating in the glass and expressed by the following equations, respectively whether the electric heating control is based on constant power or constant current.

For constant power control;

$$Q = f_r Q' \qquad \text{—— (6)}$$

$$Q' = \frac{1}{R}\left\{\left(\frac{\partial \phi}{\partial x}\right)^2 + \left(\frac{\partial \phi}{\partial y}\right)^2 + \left(\frac{\partial \phi}{\partial z}\right)^2\right\} \qquad \text{—— (7)}$$

Q' is the calculated heat generation, but it is not always kept at constant value Q at which power is to be controlled in operation.

For this reason, the calibration factor f_r is introduced into energy equation.

$$f_r = \int_v Q\,dV \Big/ \int_v \frac{1}{R}\left\{\left(\frac{\partial \phi}{\partial x}\right)^2 + \left(\frac{\partial \phi}{\partial y}\right)^2 + \left(\frac{\partial \phi}{\partial z}\right)^2\right\} dV \qquad \text{—— (8)}$$

For constant current control ;
The calculated current I' is given by the followings.

$$I = \frac{1}{|\phi_1 - \phi_2|}\int_v \frac{1}{R}\left\{\left(\frac{\partial \phi}{\partial x}\right)^2 + \left(\frac{\partial \phi}{\partial y}\right)^2 + \left(\frac{\partial \phi}{\partial z}\right)^2\right\} dV \qquad \text{—— (9)}$$

$$f_I = \frac{I^2}{I'^2} \qquad \text{——(10)}$$

$$Q = f_I Q' \qquad \text{——(11)}$$

The glass properties used in the computation are shown in Table 1. The reference temperature was set to be 1050℃ in eq(3).

Table 1 Glass properties used in computation

properties	unit	symbol	P0730
・density	Kg/m³	ρ	2.509×10^3 (at 1050 ℃)
・thermal coefficient of volumetric expansion	1/K	β	1.674×10^{-4} (at 1050 ℃)
・specific heat	J/kgK	Cp	1.494×10^3 (at 1050 ℃)
・thermal conductivity $\lambda = a+bT+cT^2+dT^3$	W/mK (T:K)	λ	a=-10.05 $b=3.790 \times 10^{-2}$ $c=-4.208 \times 10^{-5}$ $d=1.635 \times 10^{-8}$
・electrical resistivity $\exp\left(a+\frac{b}{T-c}\right)$	Ωm (T:K)	R	a=3.429 b=2028 c=101.6
・viscosity $\exp\left(a+\frac{b}{T-c}\right)$	Ps (T:K)	μ	a=-2.302 b=2128 c=270.0

BOUNDARY CONDITIONS

Boundary conditions for electric charge equation

The boundary condition for elecrical field is $\phi = \phi_0$ at one electrode and $\phi = -\phi_0$ at the other electrode. Since the refractory is not electrically conductive, $\partial \phi / \partial N = 0$ at the inner surface of refractoy. The assumption of symmetrical electric field provides with $\partial^2 \phi / \partial N^2 = 0$ and $\phi = 0$ at the center plane between electrodes.

Boundary conditions for momentum equation

Since velocities at the solid surfaces are zero, the non-slip boundary condition are given at the surface of refractories and the interface with crust layer for the feed operation.

Boundary conditions for energy equations

Boundary conditions for energy equations are modelled as shown in Fig.2. The heat flux determined by heat transfer coefficient and plenum or ambient temperature is given for boundary condition K. For the boundary with overflow section, thermal conductivities of the refractories are taken into account in K_{s1} and K K_{s2}.

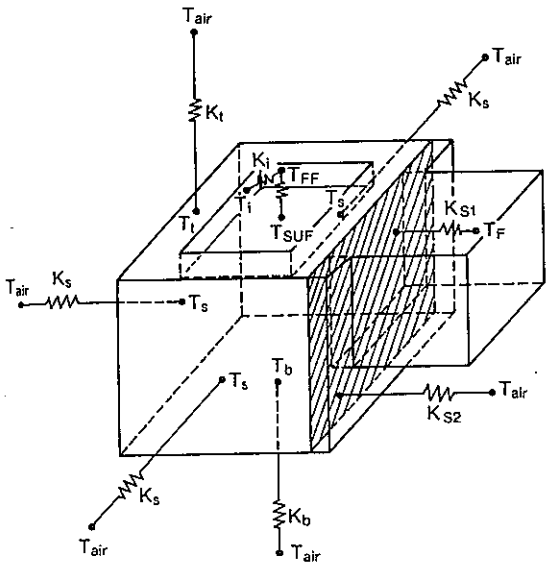

Fig.2 Boundary condition model for energy equation

Heat transfer coefficient for the top surface of glass was assumed to be the sum of the specific heat of glass additives and solid waste contents, and the change in the enthalpy of water in HLLW for vaporization. These boundary conditions are summarized in Table 2.

The boundary conditions for glass drain nozzle and its surrounding port surface are given as the surface temperature from 50℃ at the lower end to 500℃ at the upper. Since main electrodes are air-cooled, 7.15 kW of heat flux determined from the operation is given as heat sink inside of each electrode.

Table 2 Boundary conditions for energy equation

boundary	plenum temp. (℃)	heat transfer (W/m²K)
molten glass interface	148	31.6
plenum space sidewall	148	18.2
top wall surface	20	4.39
bottom floor surface	20	1.92
side wall surface	20	4.36
boundary with overflow section	1083 (overflow section)	3.00
	20 (ambient temp.)	0.925

METHOD OF SOLUTION

Numerical computation was executed by the finite difference method. The total meshes of 32 x38x35 were divided into the two domains which are the internal domain and the external domain outside of the internal to reduce the computation time by limiting the computaion of momentum and mass equations within the internal domain. The internal domain corresponds to the molten glass and a part of the floor refractoy, and the external corresponds to the refractory structure. The mesh size of the internal domain is 14x20x13. The triangle mesh was introduced into the sloped floor boundaries with the glass. The only energy equation was solved in the external domain and in the refractory of internal domain. The computation was done for the energy equation in the internal and external domains alternately until the temperature difference was diminished between the two domains to satisfy the energy equation in the both domains.

The equations are discretized and numerically solved. The solution procedure has

been explained in details in the literature [4].

The computer used in computation was M780-10S of Fujitsu. It took 100 cycles to obtain the stable solution with the time step of 1.000 seconds per cycle.

RESULTS AND DISCUSSIONS

Electrical and power distribution

The contours for the main electrodes and the subsidiary are separately shown for the equipotential and current density in Figs. 3 and 4. The sum for both pairs of electrodes are shown for power intensity in Fig. 5.

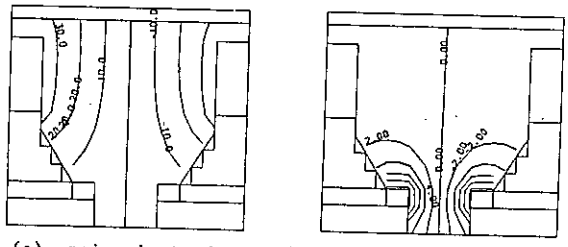

(a) main electrodes (b) subsidiary electrodes

Fig. 3 Equi-potential of electrical field in x-plane (b-b setion) for Advanced B-melter , V

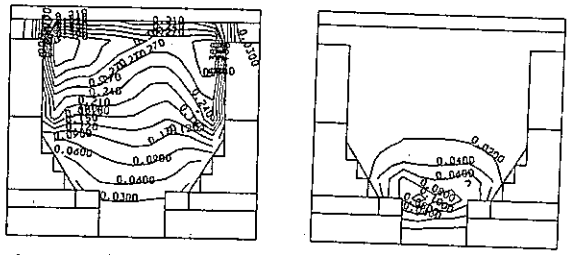

(a) main electrodes (b) subsidiary electrodes

Fig. 4 Current density in x-plane (b-b section) of Advanced B-melter , x 10^4 A/m²

The symmetric boundary conditions produce a central plane which divides into two equal sections for equipotential contour.

Although the equipotential line was symmetric, the contour of the electric current density and power intensity are not symmetric any more and quite different from the electrical potential contour due to the varied electrical resistivity depending on the glass temperature. This means the temperature dependence of resisitivity is predominant to the current or power distribution rather than electrical potential field. For this reason, it is acceptable from the practical viewpoint that resistivity was assumed to be constant in the electrical potential equation.

The current density at the main electrode surface is 2.4×10^3 A/m². The current density at the level of the subsidiary electrode is one tenth of the maximum. The electrical conduction between subsidiary electrode is limited in the lower part area under the main electrode level.

The power intensity profile shown in Fig. 5 is similar to the current density. The maximum power intensity is 1.3×10^5 W/m³ at the same location as for the maximum current density. The value beneath the crust layer is 6×10^4 W/m³.

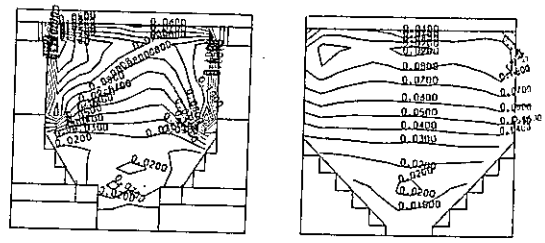

(a) x-plane(b-b section) (b) y-plane(a-a section)

Fig. 5 Power intensity in x-plane (b-b section) of Advanced B-melter, x 10^6 W/m³

Glass flow profile

The velocity profiles of molten glass in the y- z and x- z plane are shown in Fig. 6.

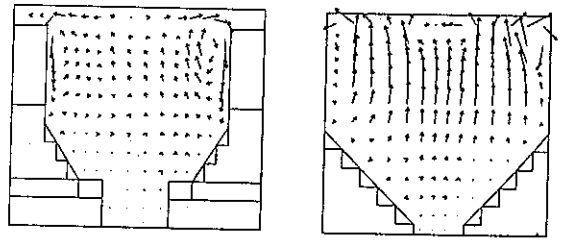

(a) x-plane(b-b section) (b) y-plane(a-a section)

Fig. 6 Velocity vector profile of molten glass for Advanced B-melter

The molten glass flows upward at the center and downward along the front surface of main electrodes, despite the maximum power intensity is observed not in the center of the cavity but in front of the electrode. The downward flow was also observed in the fluid convection adjacent to the cooled electrode as reported in physical modelling by Quigley et al. [5] and two dimensional mathematical modelling by Hielm et al. [6]. This convection profile indicates that the downward flow was caused predominantly by the air cooling in the electrode, rather than by the power intensity profile. The smaller

circulations are also observed near the sidewalls between electrodes beneath the crust layer. The locations of the centers for two circulations are consistent with those of the maximum power intensity. The glass flow was observed in the upper part of the cavity to the extent that the satisfactory mixing can be expected. Little flow is caused in the lower part of the cavity.

Temperature profile

The temperature distributions in the molten glass and refractory structure are shown in Fig. 7. The maximum temperature is located near the main electrode as well as the maximums of power intensity and current density are. The surface temperature of electrode and refractory is important in operation and design of the melter to minimize the corrosion of the glass contact materials. The results indicate electrode surface temperaure ranges at 900 to 1100° C and sidewall surface temperature is also in similar temperature range when the maximum temperature of the molten glass is 1200 ° C.

The isothermal line of 600 ° C which is the softening point of the glass is located in the back-up refractory (mullite) or insulation refractory (alumina castable). It means that the molten glass is contained enough inside of the refractory structure and that the containment of the radioactive materials is provided with by the temperatue gradient in the refractory.

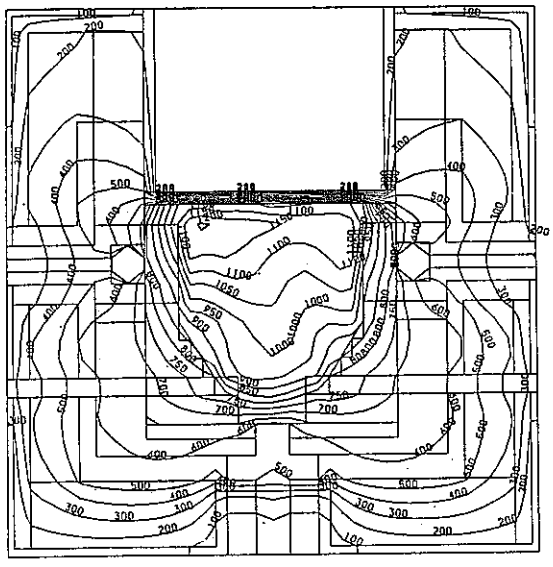

Fig.7 Temperature distribution in x-plane (b-b section) of Advanced B-melter , ℃

Comparison between simulation and operation

The temperature profile in depth from the simulation is compared with the operational data in Fig.8. The electrical data are shown in Table 3.

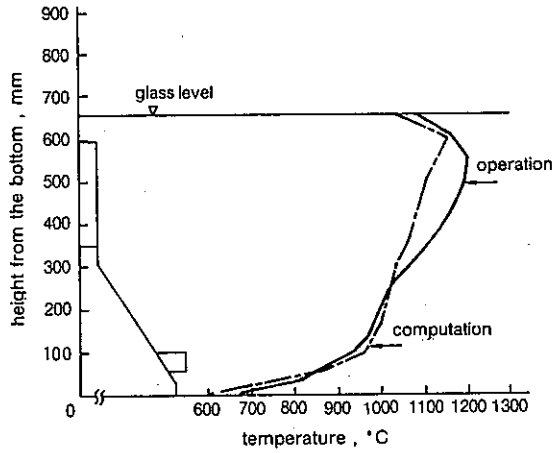

Fig.8 Comparison of molten glass temperature profile between computation and operation

Table 3 Comparison of computational results with operation for electrical data

Electrode	unit	operation	computation
Main electrodes	V	79	73
	A	588	613
	Ω	0.135	0.119
	kW	45*	45*
Subsidiary electrodes	V	54	
	A	28*	28*
	Ω	1.93	0.75
	kW	1.51	0.59

note : * means set value for control in the operation and computation.

The computational profile agreed with the operational except that the maximum temperature of computaion was 100 ℃ lower than operational value. The electrical data of main electrode heating in the power control operation well agreed within 13 % for resistance. The heating of subsidiary electrode in current control operation was different in power input between computation and operation. The simulation agreed well with the operation from the practical viewpoint although the mathematical model was

solved for both molten glass and complex refractory structure to execute the thermal analysis consistent over the whole melter structure. These agreements in the simulation indicate the the mathematical model and computation algorithm are adequate to simulate the glass melter operation.

CONCLUSION

The results of the simulation well explained the transfer phenomena in the melter and agreed with the temperature profile in depth of molten glass for feed operation. And the validity of this model was demonstrated in terms of the design and operational control of the melter.

NOMENCLATURE

Roman

c_p	Specific heat
ϕ	Electric potential
ϕ_1, ϕ_2	Electrode voltage
f_I	Current calibration factor for constant current control
f_P	Power calibration factor for constant power control
g	Gravitational constant
I	Calibrated current for constant current control
I'	Calculated current
K	Heat transfer coefficient
N	Normal component to the concerned plane
P	Electric power
Q	Calibrated heat generation for constant power or constant current control
Q'	Calculated heat generation
R	Electrical resistivity
t	Time
T	Temperature
u (u, v, w)	velocity vector
u	x-velocity component
v	y-velocity component
V	Volume
w	z-velocity component
z	unit vector of vertical coordinate
x, y, z	Axial, lateral and vertical Cartesian coordinates

Greek

β	Thermal coefficient of volumetric expansion
λ	Thermal conductivity
μ	Coefficient of viscosity
ν	Kinematic viscosity
ρ	Density
τ	viscous stress tensor

Subscripts

t	Top outer surface
s	Sidewall outer surface
b	Bottom outer surface
i	Inner surface of upper refractory
FP	Plenum
SUF	Top surface of glass or batch layer
air	Atmospheric air
f	Overflow section
S1	Boundary with overflow section
S2	Boundary with outer side wall around overflow section

ACKNOWLEDGEMENT

The authors acknowledge Mr. Yoshikawa. H and Mr. Iwai, M., of Kohzo Keikaku Engineering Inc. for the good work of programming.

REFERENCES

[1] Tsuboya, T., Masuda, S., Saito, S., and Asakura, Y., 'Overview of High-Level Radioactive Waste Management in Japan', Proceedings of the 1989 Joint International Waste Management Conference, Vol. 2 'High Level Radioactive Waste and Spent Fuel Management', presented at Kyoto JAPAN, Oct. 22-28, 1989, pp105-110.

[2] Yoshioka, M., Igarashi, H., Torata, S., and Horie, M., 'Glass Melter and Process Development for the PNC Tokai Vitrification Facility', ibid. pp13-19.

[3] Sasaki, N., Torata, S., Igarashi, H., Kashihara, H., Yamamoto, M., 'Advances in vitrification technologies in Japan', Proceedings of the American Nuclear Society, International Topical Meeting Waste Management and Decontamination and Decomissioning, Sept. 14-18, 1986, Niagara Falls, New York, USA, pp737-744.

[4] Patankar, S.V., Numerical Heat Transfer and Fluid Flow, McGraw-Hill, New York, 1980.

[5] Quigley, M.S. and Kreid, 'Physical Modelling of Joule Heated Ceramic Melters for High-Level Waste Immobilization,' PNL-2809, UC-70, March 1979.

[6] Hjelm, R.L., and Donovan, T.B., 'Numerical Investigation of Electric Field Effects on Unsteady Bouyant Molten Glass Flows', Joint ASME /AIChE 18th National Heat Transfer Conference, San Diego, Calf., August 6-8, 1979.

題　　名	Dissolution of Mixed Oxide Spent Fuel from FBR		
発表先	RECOD'91		
発表地	仙　　台	発　表 年月日	平成3年　4月14日 ～ 4月18日
発表者 (○印口頭発表者)	所　属　名	再開部　CMS室	
	○根本　慎一，林　正太郎，河田東海夫，富樫　昭夫，岡本　文敏， 山本　隆一，豊田　　修，仁科　　博，算用子裕孝		

(要　旨)

ＣＰＦでは，1982年からＦＢＲ使用済燃料の再処理技術開発に係るホット試験を実施してきている。これらのうち，今回ＦＢＲ燃料の溶解特性について評価を加えたので以下に基づき報告する。

－Ｐｕ富化度30％のＭＯＸの溶解速度は，硝酸濃度の1.7乗に比例する。

－また，溶解速度は温度の上昇に伴い増加し，アレンニウスプロットから評価した活性化エネルギーは6～11ｋｃａｌ／ｍｏｌであった。このエネルギーは溶解槽の形状に依存する。

－これらの結果より，ＭＯＸの溶解速度の実験式を導出した。

－燃焼度の上昇に伴い，溶解速度の低下が観察されるが，この傾向は硝酸濃度に依存する。

－これらの試験中回収した不溶解性残渣は，これまでの報告と同じＭｏ，Ｐｄ，Ｔｃ，Ｒｈ及びＲｕが主であり，54,000ＭＷｄ／ｔ「常陽」ＭＫⅡ－Ｃ型特殊燃料の場合，回収量は1.7ｇであった。

資　料　番　号
ＴＮ８１００　９１－０１０ （８０－０２－２３５）

資料番号 TN8100 91-010

DISSOLUTION OF MIXED OXIDE SPENT FUEL FROM FBR

H. Sanyoshi, H. Nishina, O. Toyota
R. Yamamoto, S. Nemoto, F. Okamoto
A. Togashi, T. Kawata, S. Hayashi

Reprocessing Technology Development Division
Tokai Works
Power Reactor and Nuclear Fuel Development Corporation

ABSTRACT

At the Tokai Works of the Power Reactor and Nuclear Fuel Development Corporation(PNC), the Chemical Processing Facility(CPF) has been continuing operation since 1982 for laboratory scale hot experiments on reprocessing of FBR mixed oxide fuel.
As a part of these experiments, dissolution experiments have been performed to define the key parameters affecting dissolution rates such as concentration of nitric acid, temperature and burnup and also to confirm the amount of insoluble residue. The dissolution rate of the irradiated fuel was determined to be in proportion to the 1.7 power of the nitric acid concentration.
The activation energy ditermined from the experiments varied from 6 to 11kcal/mol depending on the method of dissolution. The dissolution rate decreased as the fuel burnup increased in low nitric acid media below 5 mol/ℓ. However, it was found that the effect of the burnup became negligible in a high concentration of nitric acid media.
The amoumt of insoluble residue and its constituents were evaluated by changing the dissolution condition.

1. INTRODUCTION

It is known that the dissolution rate of mixed oxide fuel depends on temperatures, acid concentrations, plutonium concentrations, methods of fuel preparation and irradiation levels. A rotary-type continuous dissolver is being developed for application to FBR fuel reprocessing in a collaborative effort with the Oak Ridge Natioal Laboratory (ORNL). In this dissolver the internal of the dissolver drum is separated into 8 stages by a spiral separator. The fuel enters the dissolver at one end and the heated nitric acid solution from the other end to form a countercurrent flow. The acid concentration changes from about 8 molar at the feed point to 3 to 3.5 molar at the solution exit[1]. In order to evaluate the perfomance of such dissolution, it is necessary to collect the data on fuel dissolution rate in a wide range of dissolution conditions.
In this study, the effect of nitric acid concentration, temperature and fuel burnup was mainly investigated.
Dissolution of the fuel leaves some undissolved material (insoluble residue) which consists of such elements as ruthenium, palladium, molybdenum and zirconium, and a trace amount of plutonium[2].
The amount of insoluble residue was also evaluated here.
The dissolution experiment was carried out using fuel pins which have about 30% of plutonium content irradiated in the experimental fast reactor JOYO and French reactor Phenix.

2. EXPERIMENTAL

2.1 Dissolution Experiment

One series of dissolution experiments was conducted using a bench scale batch dissolver installed in the CPF hot cell (Fig.1a). Two to four irradiated fuel pins, each containing about 100 grams of mixed oxide, were sheared into small pieces. They were collected in a stainless steel basket and introduced into the dissolver for dissolution.
About 3000 mℓ of nitric acid solution adjusted to meet the experimental conditions was introduced

then the solution was purged with air at the rate of about 500 ℓ/hr, and heated to the required temperatures.

Another series of beaker-scale dissolution experiments were conducted in a round bottomed Pyrex flask with a fitted reflux condenser as shown in Fig. 1b. This apparatus was also placed in the CPF cell.

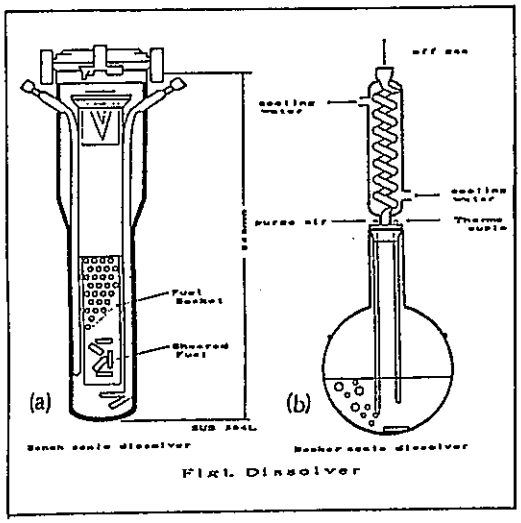

This series of experiments was planned to collect the dissolution data under better defined conditions with a wider range of parameters than in the other series of experiments. All experiments were carried out as follows: 500 mℓ of nitric acid solution adjusted to meet the experimental conditions were placed in the flask and then the solution was purged with air at rate of 200 mℓ/hr, and heated to the required temperature.
A section of a sheared fuel pin with approximately 6g of irradiated mixed oxide fuel was charged into the flask to start dissolution of the fuel for determination of the dissolution rate. For both series of experiments, sample solutions were taken periodically to measure the time variation of uranium, plutonium and FP contents. The radioactivity of Kr^{85} in the off-gas passing though the condenser was also monitored continuously with a NaI(Tl) detector.

2.2 Materials

The irradiated mixed oxide fuels used in the experiments were taken from the irradiated driver fuel of JOYO MK-II core and experimental fuel pins irradiated in Phenix and JOYO as shown in Table 1.

Table 1. Irradiated mixed oxide fuel

Experimental fuel pin	Plutonium content (w/o)	Pellet density (%TD)	Average Burnup (MWd/t)
Irradiated in JOYO	28	93	13,800～54,700
Irradiated in JOYO	30	85	54,100
Irradiated in PHENIX	30	85	94,000

The plutonium content, relative pellet density and average burnup were about 30%, 85% and 13,800～100,000 MWD/t respectively.
The outer diameter of fuel pins was 5.1 to 6.5mm. All the fuels were manufactured by mechanical blending of UO_2 and PuO_2 powders in plutonium fule fabrication facilities in PNC.

3. RESULTS AND DISCUSSION

3.1 Dissolution Rate Experiment

Effect of Nitric Acid Concentration

The effect of nitric acid concentration on the dissolution of the irradiated mixed oxide fuel was investigated in the series(b) experiment. The temperature of the dissolver solution was kept constant at 100℃.
The nitric acid concentration was changed from 2.5 to 8.7mol/ ℓ as a key experimental parameter. In each experment, a 3cm long fuel section was used which was cut from JOYO MK- II test fuel pins irradiated to 54,000MWD/T and contained mixed oxide with 30% plutonium. A molar ratio of HNO_3 to heavy metal larger than 20 was chosen to give a large excess of solvent, so that the HNO_3 concentration was kept relatively constant during the experiments. The results indicated that the dissolution rate increased as the concentration of nitric acid increased as shown in Fig 2.

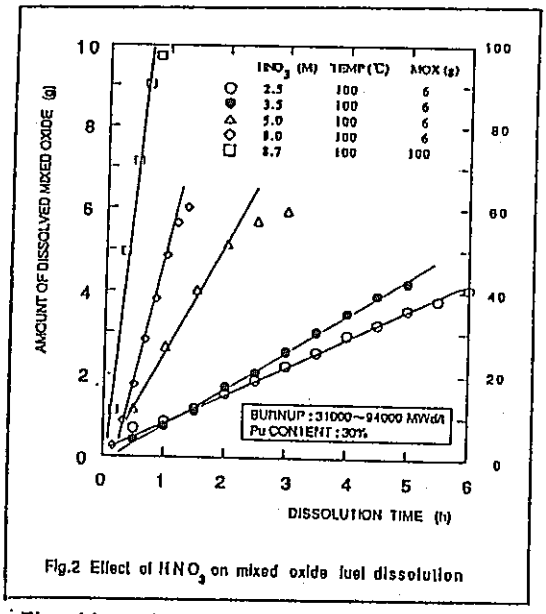

Fig.2 Effect of HNO_3 on mixed oxide fuel dissolution

The time dependence was observed to be almost linear for most of the experiments until about 80% of the fuel was dissolved. The apparent surface area for dissolution seems to be relatively constant up to 80% dissolution when the fuel is wrapped in the cladding which limits the direct exposure of the fuel meat to fresh acid solution.

From these results, apparent dissolution rates were obtained and plotted against HNO_3 concentration in Fig 3. The dissolution rate was found to be proportional to the 1.7 power of the HNO_3 concentration.

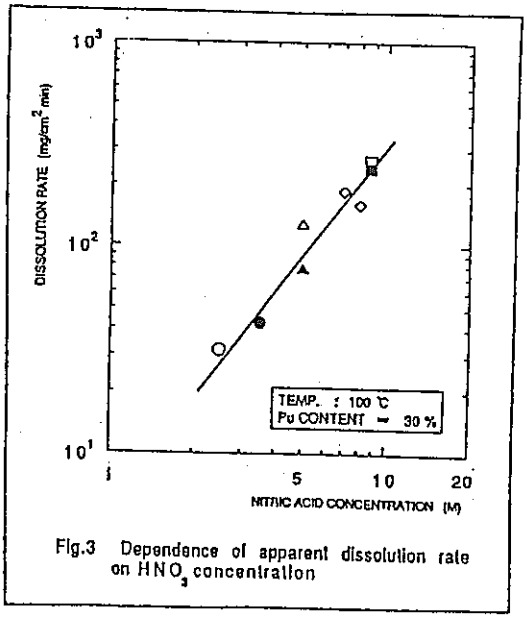

Fig.3 Dependence of apparent dissolution rate on HNO_3 concentration

A typical equation for the dissolution rate was proposed for uranium by J.L. Swanson [3] as follows ;

Dissolution rate =

$K \cdot (\text{surface area}) \cdot ([HNO_3]+2[U])^{2.6}$

This rate is proportional to the total nitrate concentration raised to the 2.6 power. Our experimental results, however, indicate that the dissolution rate for irradiated mixed oxide fuel is proportional to the concentration of nitric acid raised to the 1.7 power as shown in the following equation ;

Dissolution rate =

$K \cdot (\text{surface area}) \cdot (HNO_3)^{1.7}$

Effect of Temperature

Two experiments using different scale dissolution systems were carried out. In both series, fuel dissolution rates were measured in 3.5mol/ℓ and 8mol/ℓ HNO_3 solutions at temperatures ranging from 70 ℃ to 100 ℃. The logarithms of the measured dissolution rate are plotted against the inverse temperatures in Fig 4. The slope of the fitted line yielded an experimental activation energy of 11kcal/mol for the dissolution with 8mol/ℓ nitric acid in the beaker-scale experiments which contained 6g of fuel. On the other hand, the results from the bench-scale dissolver experiments which contained 200-400g of fuel in a stainless steel basket showed an activation energy of 6kcal/mol with 3.5mol/ℓ nitric acid.

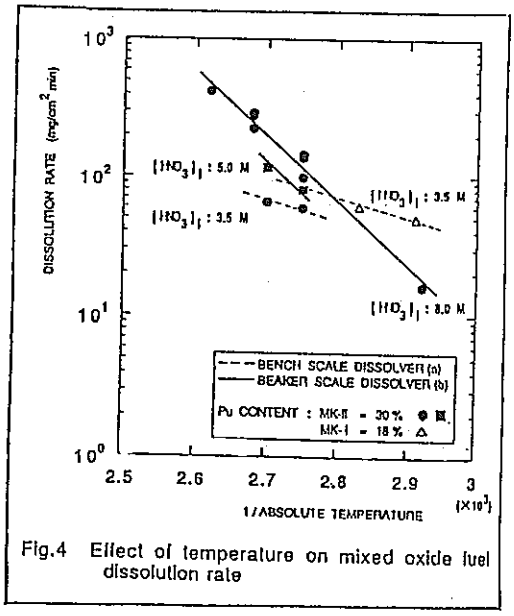

Fig.4 Effect of temperature on mixed oxide fuel dissolution rate

This fact suggests that the rate of dissolution in the bench-scale dissolver is largely controled by diffusion, probably because of the use of the basket which impedes good solution mixing whereas the rate is likely to be controled by chemical reaction in the beaker-scale experiments.
Considering the effects of nitric acid and temperature, the dissolution rate of the fuel can be expressed as follows;
Dissolution rate =
$K \cdot (\text{surface area}) \cdot (HNO_3)^{1.7} \exp.(-E/RT)$
E = activation energy
In a system with high agitation as in a continuous rotary dissolver, the activation energy would be close to 11kcal/mol whereas it would be recommended to use 6kcal/mol for the system with limited agitation as in the batch dissolver with a basket.

Influence of Fuel Irradiation level

The dissolution rate of irradiated fuel decreased as the burnup of the fuel increasesing the range of about 10,000~100,000MWD/t in the relativery low concentration of nitric acid system below 5mol/ℓ. However, in a high nitric acid concentration system(HNO_3;8mol/ℓ), there is little or no effect of irradiation on the dissolution rate as shown in Fig.5.

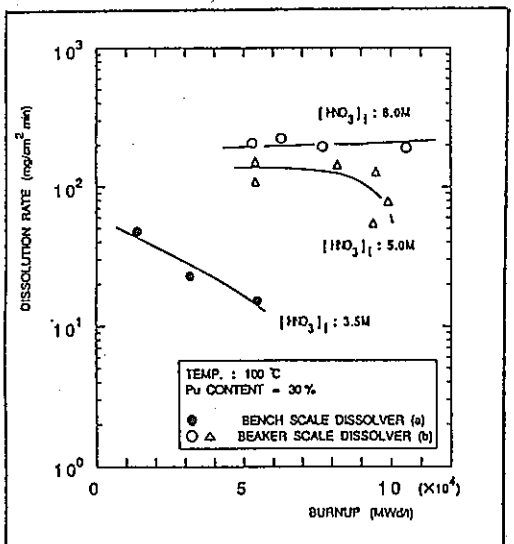

Fig.5 Effect of fuel burnup on dissolution rate

3.2 Insoluble Residue

Four dissolution experiments were conducted to determine the amount of the insoluble residue using 100g of the JOYO MK-II test fuels for each. In this series of experiments, the HNO_3 concentration was changed as a main parameter. The composition of the materials, including plutonium were analyzed by Direct Current Plasma (DCP) method and α, γ spectrometoies. The recovered residual material from the dissolution flask was rinsed 5 times with 3N nitric acid to eliminate any plutonium contamination and then dried for weighing. The weight of the residul material was approximately 1.7g for all cases. The plutonium content in the residual material varied depending on the nitric acid concentration in the dissolver. Analysis of the undissolved material showed that the major constituents were Mo, Pd, Tc, Rh and Ru which are all highly insoluble noble metal fission products. Similar compositions have been observed and reported by others[4].

4. CONCLUSION

The effect on the dissolution rate of irradiated mixed oxide fuels were investigated with various HNO_3 concentrations, temperatures and irradiation levels. The amount of insoluble residue was also measured in this series of experiments. The conclusions drawn from these experiments can be summarized as follow ;
- The dissolution rate for irradiated mixed oxide fuel is proportional to 1.7 power of the HNO_3 concentration.
- The apparent surface area for dissolution seems to be relatively constant until 80% dissolution when the fuel meat is wrapped in the cladding.
- The experimental activation enegy of about 11Kcal/mol was obtained from beaker-scale experiments.
The bench-scale dissolver with fuel basket showed an activation energy of 6Kcal/mol.
- The dissolution equation of the fuel could be obtained from these experiments.

REFERENCE

(1) T.Kawata, et al.
Development of FBR fuel reprocessing technology at PNC, Proc. RECOD '91, April 1991, Sendai Japan.
(2) Nuclear Chemical Engineering, Second Edition.
(3) J.L.Swanson et al.
Laboratory Studies of Shear/Leach Processing of Zircaloy Clad Metallic Uranium Reactor Fuel.
(4) P.De Regge et al.
Dissolution of Mechanically Mixed UO_2-PuO_2 and Insoluble Residue Characteristics, London : Society of Chemical Industry 1980.

題　　名	Maintenance and Calibration of Radiation Monitoring Instruments at TOKAI Reprocessing Plant		
発表先	RECOD '91		
発表地	仙　　台	発　表 年月日	平成3年　4月14日 ～ 4月18日
発表者 (○印口頭発表者)	所　属　名	安管部　放管一課	
	○小嶋　　昇，宮部賢次郎，都所　昭雄		

(要　旨)

東海事業所の計測機器校正施設における放射線測定機器の点検，校正および保守の経験に基づき，施設の概要，放射線測定機器の保全の考え方や方法および代表的な機器についての故障データの解析結果について，再処理施設で使用されている機器を中心に紹介する。

資　料　番　号
TN8100　91－011 (80－02－237)

資料番号 TN8100 91-011

MAINTENANCE AND CALIBRATION OF RADIATION MONITORING INSTRUMENTS AT TOKAI REPROCESSING PLANT

N.KOJIMA , K.MIYABE , A.TODOKORO

Power Reactor and Nuclear Fuel Development Corporation
4-33, Muramatsu, Tokai-mura, Naka-gun, Ibaraki-ken,
Japan 319-11
phone : 0292-82-1111

INTRODUCTION

The spent fuel reprocessing plant has been operated for more than ten years at Power Reactor and Nuclear Fuel Development Corporation (PNC), Tokai Works. Many kinds of radionuclides such as ^{54}Mn, ^{60}Co (corrosion products), ^{90}Sr-Y, ^{106}Ru-Rh (fission products), uranium and plutonium are treated at the reprocessing plant, so that various radiation monitoring instruments have been used to meet the need of the radiation protection program. As the data measured by radiation monitoring instruments are directly reflected to the radiation safety of the reprocessing plant, all of the instruments have to be assured on their reliability. In such point of view, the radiation monitoring instruments have been periodically inspected and calibrated.

This presentation explains the outline of the maintenance and calibration of the radiation monitoring instruments and the results of the failure analysis at the Tokai reprocessing plant.

CLASSIFICATION OF RADIATION MONITORING INSTRUMENTS

Due to handling of a large quantity of the spent fuel in the Tokai reprocessing plant, various types of radiation monitoring instruments are used for the radiation control.

It is necessary to measure the γ-ray and β-ray from ^{54}Mn, ^{60}Co (corrosion products) and ^{90}Sr-Y, ^{106}Ru-Rh (fission products) etc., the same is true for the gaseous radioactive waste such as ^{3}H and ^{85}Kr that released to the ambient environment through a stack. For their purposes, many kinds of radiation monitoring instruments such as survey meters, area monitors, dust monitors and stack monitors have been installed. Approximately 80 types of the instruments are used (excluding personal dosimeters).

The radiation monitoring instruments are used for the radiation control of the radiation field at the plant. They consist of area monitors, survey meters, radioactivity measuring instruments and entrance/exit contamination monitors. The area monitors are used for continuous monitoring of external radiation dose equivalents or airborne radioactivity in workplaces. The survey meters are used for the measurement of external radiation dose equivalents or surface contamination. The radioactivity measuring instruments are used for the measurement of radioactive material concentrations in air of workplaces and various samples of surface contamination control including radionuclide analysis. And the entrance/exit contamination monitors are used for checking surface contamination of human bodies at the entrance/exit of controlled area.

The environmental monitoring instruments are used to measure both the absorbed dose rate

Classification	Instrument	Number of instruments
Radiation Monitoring Instrument		
area monitor	γ-ray area monitor, neutron area monitor α-ray dust monitor, β-ray dust monitor stack monitor, etc.	295
	criticality accident alarm system	12
entrance/exit contamination monitor	gate monitor, hand/foot/clothes monitor, etc.	147
survey meter	ionization chamber type survey meter GM tube type survey meter α-ray scintillation type survey meter, etc.	733
radioactivity analyzer	α/β-ray radioactivity measuring instrument multichannel pulse height analyzer, etc.	34
environmental monitor	monitoring station, monitoring post, etc.	20

Figure 1. The list of radiation monitoring instruments provided at the Tokai reprocessing plant

and the radioactive material concentration in ambient air of the surrounding environment.

Because a large quantity of uranium and plutonium are handled in the reprocessing plant, a criticality accident alarm system is installed to evacuate the workers to safe places in the case of a criticality accident.

The radiation monitoring instruments are classified into five groups, ① area monitors, ② entrance/exit contamination monitors, ③ survey meters, ④ radioactivity analyzers and ⑤ environmental monitors as shown in Figure 1.

CALIBRATION FACILITY FOR RADIATION MONITORING INSTRUMENTS

Outline of the calibration facility

The calibration facility for radiation monitoring instruments consists of two buildings as shown in Figure 2. One is the maintenance building for the radiation monitoring instruments in which the instruments are inspected and repaired, and the other one is the calibration building in which irradiation are carried out by using radioactive sources. In the calibration building, three irradiation rooms, Room (A), Room (B) and Low-level Room are available, in which these rooms can be used in accordance with the types and dose (rate) of the radiation to be handled, and various irradiations can be carried out. The outer walls of the calibration building were built with steel-frames and light-weight concrete to decrease scattered radiation. Furthermore, the calibration rooms are

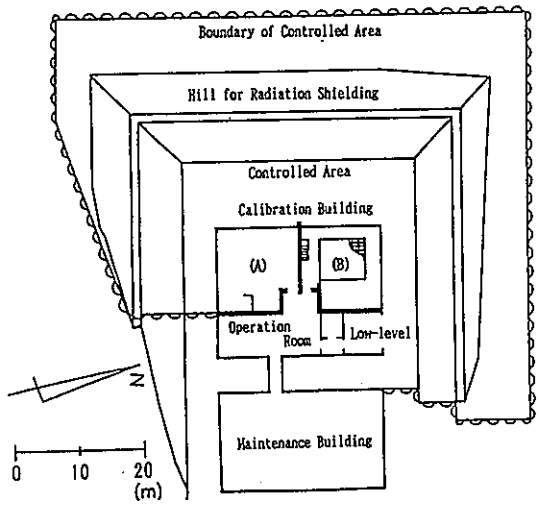

Figure 2. Calibration facility for radiation monitoring instruments

surrounded by the inclined plane of a hill on three sides for radiation shielding.

Irradiator

In the irradiation room (A), calibration of ionization-chamber-type survey meters, γ-ray area monitors etc. are carried out by using a ^{137}Cs γ-ray irradiator and a X-ray generator. Furthermore, the automatic calibration apparatus are provided in this room, because the routine calibrating works were intended to reduce man power and to improve calibration accuracy. This automatic calibration apparatus consists of the ^{137}Cs γ-ray irradiator, the automatic calibration cart and the operating panel.

In the irradiation room (B), calibration of neutron survey meters and neutron area monitors are mainly carried out by using the neutron irradiator. Moreover, the γ-ray irradiator and the low-energy γ-ray irradiator are provided for characteristic tests of the radiation monitoring instruments in this room.

In the low-level irradiation room, calibration of gas monitor is carried out by using a special type gas loop system.

Main sources used for calibration of the instruments are shown in Table 1.

Table 1. Main sources used for calibration

IRRADIATION ROOM	IRRADIATOR	SOURCES
IRRADIATION ROOM (A)	X-ray generator	420kVp / 30mA
	^{137}Cs γ-ray irradiator	1.11 TBq 74 GBq 7.4 GBq 0.555 GBq
IRRADIATION ROOM (B)	Neutron irradiator	^{241}Am-Be 37 GBq ^{239}Pu-Be 370 GBq ^{252}Cf 0.999 GBq
	γ-ray irradiator	^{60}Co 3.7 GBq ^{137}Cs 3.7 GBq ^{226}Ra 1.85 GBq
	Low-energy γ-ray irradiator	^{241}Am 296 GBq ^{57}Co 7.4 GBq

Traceability system

The standard gamma sources and the standard measuring instruments which have the direct traceability with the national standard are used for calibration of the radiation monitoring instruments.

With regard to the calibration for measurements of gamma or X-ray exposure (rate), Japan Industrial Standard (JIS) has estabilished the traceability system from the national standard (The Electrotechnical Laboratory) to the primary, secondary and the practical exposure standard fields. The calibrations are classified into the standard calibration and the practical calibration depending on its objectives.

The standard calibration includes the calibration of the secondary standard measuring instruments based on the primary standard exposure (rate) and the calibration of the practical standard measuring instruments using the primary or secondary standard exposure (rate). The calibration of the radiation monitoring instruments is carried out using the practical standard exposure (rate), the primary or secondary standard exposure (rate). The primary and secondary standard gamma ray sources should be calibrated by the national standard and the primary standard exposure (rate) respectively.

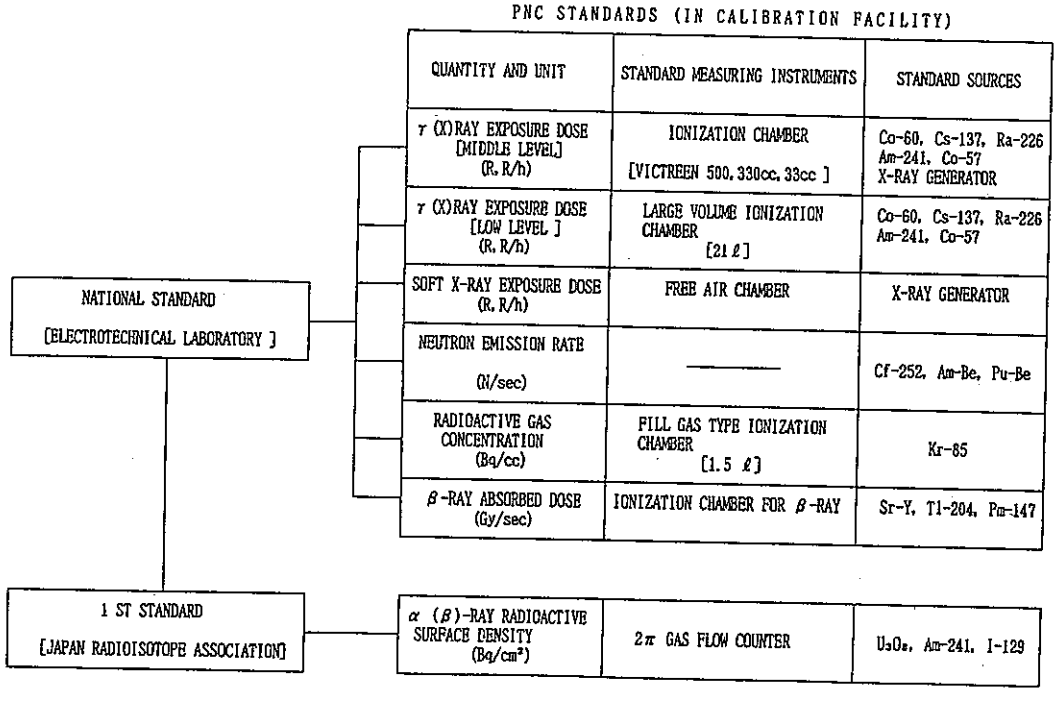

Figure 3. Traceability system of PNC standard

The traceability system for radiation measurements in PNC Tokai Works are shown in Figure 3. These standard measuring instruments have been calibrated by using a national standard periodically (every 3 years) to assure their traceability.

MAINTENANCE OF RADIATION MONITORING INSTRUMENTS

Purpose of maintenance

In general, the maintenance is classified into a preventive maintenance and a corrective maintenance. The preventive maintenance is done according to a routine procedure of examination, adjustment and inspection on a scheduled basis in order to prevent a malfunction before they occur. Education and training of persons operating instruments are involved the preventive maintenance in the broad sense. The corrective maintenance is performed after the failures of systems, instruments or parts. These two types of maintenance have different purposes and therefore must be considered separately.

The preventive maintenance is divided into the time-scheduled maintenance, such as periodic examination, inspection and replacement of parts, and state-watching maintenance which is performed by observing the condition of important portions of instruments by recorder, etc.. Furthermore, the education and training provided for the persons in charge of the maintenance are also the preventive maintenance in the broad sense.

The corrective maintenance of radiation monitoring instruments requires prompt and suitable judgement. From the standpoint of plant operation, the corrective maintenance of the some radiation monitoring instruments (criticality accident alarm systems, area monitors, etc.) is carried out by replacement of parts in order to ensure the quick recovery as soon as possible. Therefore, the instrument consists of some individual units interlinked with connectors.

Method of maintenance

As the maintenance for the reliability of the function and performance of the radiation monitoring instruments, initial examinations upon purchase and receipt, as well as daily and periodic inspections, are performed. When the instruments get failure, they are promptly repaired. In addition, area monitors and stack monitors are inspected before their use and also periodically inspected by governmental officers.

From the standpoint of the preventive maintenance, the most important thing is a periodic inspection, which consists of legal-inspection according to related laws or maintenance regulations and the self-inspection for the purpose of the life-time confirmation of the ability or the detection of malfunctions. The preventive inspection and calibration of radiation monitoring instruments have been made at the period as given in Table 2. As for the basic makeup of the periodic inspections, entire systems including the detectors and electric circuits, are examined twice a year in order to confirm their normal operation and to inspect and calibrate their functions. Furthermore, the performance checks of area monitor, etc., (the confirmation of the normal operation of detector and alarm systems, etc.,) are done periodicaly (e.g., every month or three months) with precise checks of electric circuits once a year.

The inspection procedure is necessary to inspect each type of radiation monitoring instruments periodically.

The main items of the inspection of the

Table 2. The period of inspection for radiation monitoring instruments

CLASSIFICATION	LEGAL INSPECTION		SELF INSPECTION	
	whole system	parts	whole system	parts
	・cleaning ・calibration ・alarm level check ・alarm test	・electric circuit test	・sensitivity check ・alarm test	・probe test ・electric circuit test
Criticality accident alarm system	2 times/year	1 time/month	*	1 time/year
Area monitor	2 times/year	—	1 time/3months	—
Entrance/exit contamination monitor	2 times/year	—	*	—
Survey meter	2 times/year	—	*	—
Radioactivity analyzer	2 times/year	—	*	—
Environmental monitor	2 times/year	—	*	—

* These monitors are inspected everytime at used of them.

radiation monitoring instruments are shown as follows:

- Outer appearance check
- Electronic inspection
- Radiation inspection
- Overall performance check

On the other hand, the maintenance for the failed radiation monitoring instruments is carried out according to the following considerations : ① the repairing time of important instruments is kept as small as possible and ② the maintenance is performed effectively in order to prevent failures.

In case of important instruments such as area monitors fail to function, professional staff members in charge of maintenance find promptly the failed portion and replace the blocked module, detector portion and spare parts in order to recover the functions of the system. In this manner, the non-operating time of instruments due to its failure will be shortened. However, in this case, it is important that the spare parts should be secured corresponding to the knowledge of failure portions and their frequency.

Some results obtained from maintenance

The radiation monitoring instruments used in Tokai reprocessing plant were maintained by the repairments in case they are out of order. The annual failure rates of the main radiation monitoring instruments during the period 1986-1988 were obtained by dividing the number of annual failures by total numbers of each instruments. They are shown in Figure 4 and Figure 5. In the figures, the failure rates of each instrument is given in the respective form as every year or every each failure portion.

As for area monitors, the annual failure rate were 0.3-0.8 for dust monitors and 0.1 for γ-ray area monitors. In this case, main cause of the failure are belong to detectors, such as GM-tube for β-ray dust monitors and solid state detector for α-ray dust monitors.

The annual failure rates of α-ray meters (ZnS(Ag)scintillation counter) and α-ray hand/foot/clothes monitor (air proportinal detector) were about 1-2 per an instrument. On the other hand, the failure rates of the radiation monitoring instruments of ionization chamber type survey meter and GM-tube type survey meter were about 0.4 per an instrument and almost constant during these 3 years.

From the results of the analysis for the failure portion of the radiation monitoring instruments, it was found that there were considerable number of failures at the detector portion of all instruments. In another words, the failure rates of the detector portions were approximately 80-90% for ionization chamber type survey meters, approximately 60-80% for

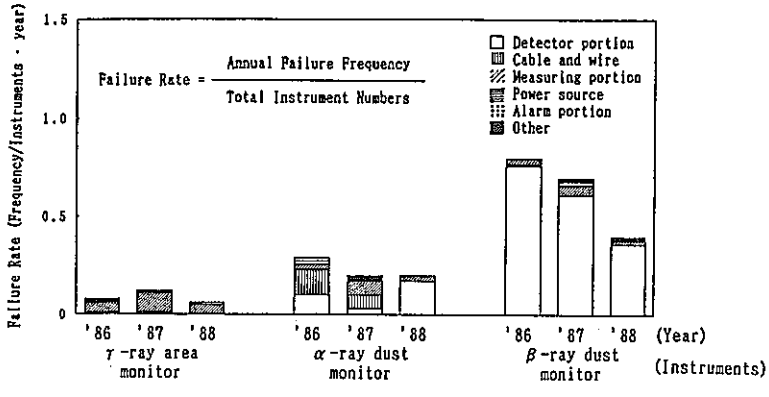

Figure 4. Failure rate of main radiation monitoring instruments at the Tokai reprocessing plant (I)

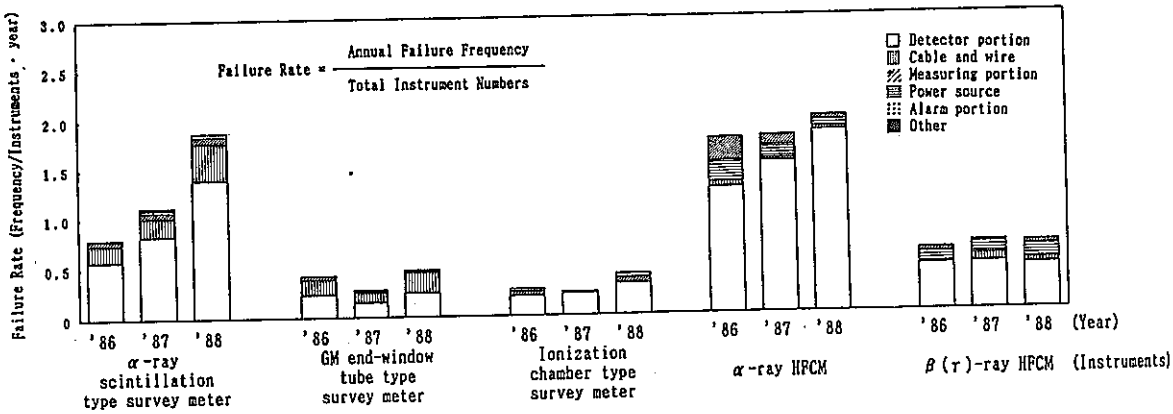

Figure 5. Failure rate of main radiation monitoring instruments at the Tokai reprocessing plant (II)

other survey meters and hand/foot/clothes monitors.

The α-ray survey meter has a thin shielding film (aluminium-vaporized mylar with a thickness of 0.5mg/cm^2) at the entrance window and the α-ray hand/foot/clothes monitor also has a thin window film (gold-vaporized mylar with a thickness of 0.5mg/cm^2). These films are easily broken by mechanical shock and the failure rate increases in proportion with the frequency of their use.

As mentioned above, the failures of radiation monitoring instruments had variety in their portions and causes, but in most of these cases failures were found in detector portions. From the standpoint of maintenance, it is especially important to pay our careful make all attention to the detector portions.

Furthermore, the analysis of failure data is effective in determining the most suitable method and frequency of the inspection and in determining the amount of spare parts and maintenance parts to be stocked.

CONCLUSION

In the use of various kinds of radiation monitoring instruments at the Tokai reprocessing plant, the points for effectual maintenance of radiation monitoring instruments are shown as follows:

① The inspection procedure is necessary to inspect each type of radiation monitoring instruments periodically.
② The maintenance and calibration of radiation monitoring instruments should be executed by technical expert staffs.
③ The spare parts is required to recover the functions of radiation monitoring instruments promptly.
④ The results from the failure analysis of radiation monitoring instruments have been effectively applied to the improvements of maintenance and calibration methods.

REFERENCE

1. Momose, T., Noda, K. and Seki, A., "Control of Radiation Monitoring Instruments" Donen-Giho (PNC Technical Review) No.60, 83 (1986)
2. Miyabe, K. and Kojima, N., "Experience of the Maintenance for Radiation Monitoring Instruments at the Nuclear Facilities" Hoken-Butsuri (Journal of Japan Health Physics Society) No.24, 345(1989)

題　　名	Safeguards for Nuclear Fuel Cycle Facilities in PNC Tokai Works		
発表先	RECOD'91		
発表地	仙　　台	発　表 年月日	平成3年　4月14日 ～ 4月18日
発表者 (○印口頭発表者)	所　属　名	技推部　核管室	
	○平井　健一，岸本洋一郎，鹿島　貞光，内田　孝行		

(要　旨)

東海事業所の保障措置について，その実施及び開発の現状を紹介する。事業所保障措置対象施設に対して，1989年においては，ＩＡＥＡの査察業務量は 1,100人／日であった。地方事業所において保障措置に要した業務量は，約13,000人／日であった（計量管理，査察対応，技術開発など）。再処理工場は，運転中は24時間連続査察を受けており，Ｐｕ製造施設やＰｕ転換施設では，月々中間査察が実施されている。Ｐｕ製造施設では，新しい保障措置システムの導入により，査察のマンパワーを削減出来た。技術開発については，ＴＡＳＴＥＸ，ＪＡＳＰＡＳ及びＰＮＣ／ＤＯＥ協力について紹介する。今後のよりいっそうの効果的・効率的保障措置のためには，核燃料サイクルを指向した保障措置アプローチなどの検討が必要である。

資　料　番　号
ＴＮ８１００　９１－０１４ （８０－０２－２４１）

資料番号 TN8100 91-014

Safeguards for Nuclear Fuel Cycle Facilities in PNC Tokai Works

Y.Kishimoto, S.Kashima, K.Hirai and T.Uchida
Power Reactor and Nuclear Fuel Development Corporation (PNC)
Muramatsu 4-33, Tokai-mura, Naka-gun, Ibaraki-ken,
Japan 319-11
phone: 0292-82-1111

ABSTRACT

This paper describes the present status of safeguards implementation and development activities for nuclear fuel cycle facilities in the Tokai Works of Power Reactor and Nuclear Fuel Development Corporation (PNC Tokai Works). The PNC Tokai Works has five facilities determined by the facility attachments of Japan-IAEA Safeguards Agreement, which are Tokai Reprocessing Plant (TRP), Plutonium Conversion Development Facility (PCDF), PNC Plutonium Fuel Facility (PPFF), Plutonium Fuel Production Facility (PFPF) and Research and Develoment Facility (PNC Tokai R&D Facility).

TRP is subject to both flow and inventory verification, the former is conducted during plant operation by 24 hours continuous inspection, and the latter is conducted by monthly inventory verification activity. PCDF, PPFF and PFPF are mainly subject to monthly inventory verification activity. In particular PFPF fully automated MOX fuel fabrication facility, which started its operation in 1988, adopted an advanced nuclear material accountancy and safeguards measures for saving considerably safeguards manpower of both operator and inspectorate. PNC Tokai R&D Facility is subject to an annual physical inventory verification.

On aspects of safeguards technology development, the PNC Tokai Works has been performing an important role for more than twenty years. The Tokai Advanced Safeguards Technology Exercise (TASTEX) , Japan Support Programme for Agency Safeguards (JASPAS) and PNC/US-DOE Safeguards Cooperation are our main activities in developing and demonstrating safeguards technology.

The inspection work loads by IAEA in 1989 for these five facilities in the PNC Tokai Works was estimated to be about 1,100 person-days. On the other hand operator's manpower to cope with these safeguards business reached about 13,000 person-days.

Activities of MOX fuel cycle development and waste management are expanding in the Tokai Works. However, to further increase safeguards manpower and cost becomes more difficult for both operator and inspectorate because of the zero-growth of the finance. Therefore, developing a new approach is required for more effective and efficient safeguards. Since the PNC Tokai Works composes itself of an active part of MOX fuel cycle in Japan, the study developing a nuclear fuel cycle oriented safeguards approach is necessary.

INTRODUCTION

The Power Reactor and Nuclear Fuel Development Corporation (PNC) has been engaged in a wide range of research and development projects aimed at promoting the peaceful use of atomic energy in Japan. The Tokai Works of PNC has been playing an important role of promoting a number of nuclear energy development programs such as the developments of uranium enrichment technology, reprocessing technology for spent fuels from light water reactors, conversion technology, high-level liquid waste vitrification technology, reprocessing technology for fast breeder reactor fuel, and plutonium fuel production technology. Through these development activities a large amount of nuclear fuel materials such as plutonium and uranium are handled and stored in the facilities in the Tokai Works. Hence, accountancy and safeguards activities for these nuclear materials are essential to pormote the projects. At the PNC Tokai Works large efforts have been made for the establishment of nuclar materials accountancy system and the development of safeguards technology since the first receipt of the nuclear materials in 1957. After the introduction of the Non-Proliferation Treaty regime in 1977, the efforts on safeguards related works have been increasing more and more, and this tendency is continuing at present.

SAFEGUARDED FACILITIES IN TOKAI WORKS

The PNC Tokai Works has five facilities determined by the facility attachments of Japan-IAEA Safeguards Agreement. Main features of these facilities are introduced below from the viewpoint of safeguards implementation. Figure 1 shows the main nuclear material flow and material balance areas in the Works.

Tokai Reprocessing Plant

The Tokai Reprocessing Plant (TRP) went into hot operation in September 1977. This facility was designed to have a capacity of 0.7 tons U/day. The Purex process is employed to produce plutonium nitrate and uranium trioxide as final products. The amount reprocessed reached 500 tons since the start

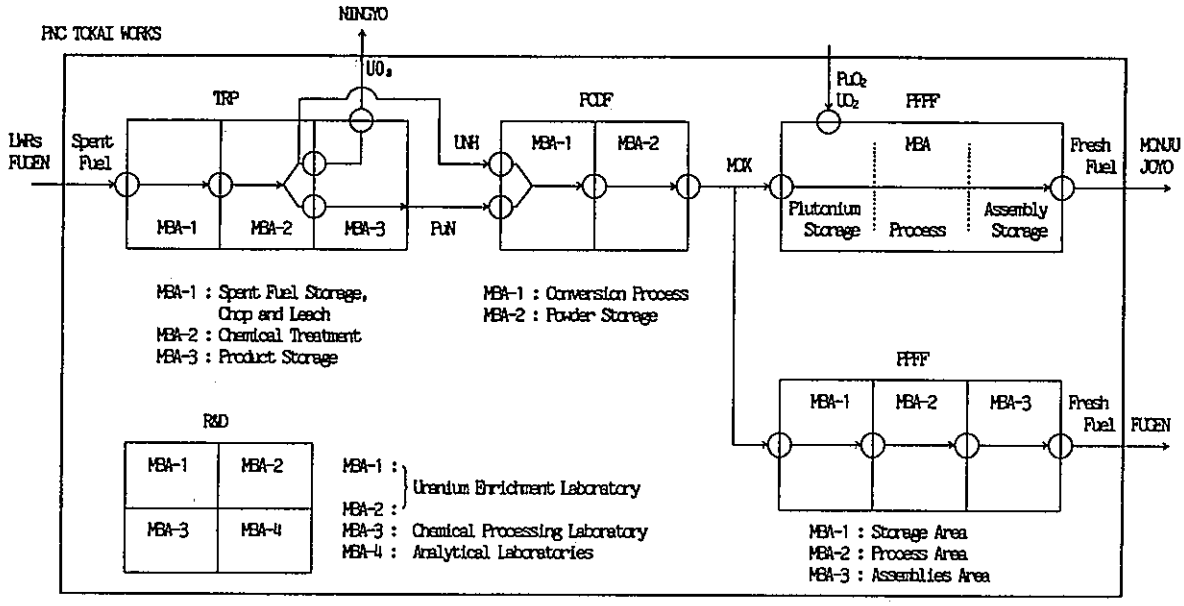

Fig. 1 Main Nuclear Material Flow and Material Balance Areas in PNC Tokai Works

of the operation. TRP has three material balance areas (MBAs); a spent fuel storage, chopping and leaching area, a chemical processing area, and a product storage area. It has also nine flow key measurement points (FKMPs) for flow determination, seven inventory key measurement points (IKMPs) for physical inventory determination, and other strategic points. Normally two operational campaigns per year are scheduled, and physical inventory takings are carried out at the end of each campaign.

During the plant operation, 24 hours continuous flow verification is conducted both by the government and IAEA inspectors. At the time of the receipt of spent fuel assemblies from nuclear power reactors, each subassembly is verified by using a Cerenkov viewing device, and stored in the storage pond under the continuous camera surveillance condition. Before chopping a fuel subassembly the identification number is checked by a periscope. After dissolution solution volume is measured by dip-tube manometers at the input accountancy tank and samples are taken to determine nuclear material contents for both the operator and inspectorate. For determination of plutonium cotents isotope dilution mass spectrometry methods are used for both the operator and inspectorate. Samples for inspectorate are shipped to the government and the IAEA safeguards analytical laboratories after necessary preparations. The solution volume of purified plutonium is measured by dip-tube manometers at the plutonium product accountancy tank, and samples are taken to determine plutonium contents and shipped to the analytical laboratory. Onsite K-edge densitometer measurement is used as plutonium verification technique for timeliness improvements. For the purpuse of timely detection monthly inventory verification for plutonium product solution is carried out. Samples are taken from the selected product tanks, then the plutonium contents are measured by a K-edge densitometer. To improve timeliness for the chemical process area the development and demonstration of near-real-time materials accountancy (NRTA) are conducted by collecting field test data.

During the physical inventory verification, all the nuclear materials are gathered to each IKMP, and item counting, level measurement, sample taking and measurement by K-edge densitometry are performed to determine "material unaccounted for (MUF)".

Recalibrations of main vessels such as the input accountancy tank and the plutonium product accountancy tank are carried out once a year. Inspectorate verify also the operator's recalibration work. Other main verification activities are the obsevation of sample treatment for shipping to the safeguards laboratories and monthly book audit.

Plutonium Conversion Development Facility

The Plutonium Conversion Development Facility (PCDF) has been in operation since April 1983, employing a plutonium-uranium co-conversion process. This process features a unique "microwave heating direct denitration process" developed by PNC. In this process plutonium nitrate and uranium nitrate transferred from TRP through the pipelines are mixed together in a mixing vessel and finally converted into a mixed plutonium and uranium oxide (MOX) powder.

This mixed process was introduced because of its possible contribution to the effectiveness for nonproliferation of nuclear weapons at the time of the plant start-up.

PCDF has two MBAs ; a conversion area and a MOX storage area, and also has seven FKMPs and three IKMPs.

Monthly inspection is conducted for verification of flow and inventory by the government and IAEA inspectors, and physical inventory verification (PIV) is conducted once a year simultaneously with TRP. Activities such as book audit, level measurement of tanks, nondestructive assay (NDA) of solution samples, monitoring of the conversion process, NDA of MOX powder canister, seal applying to the canisters and sample taking of powders are conducted during monthly verification by inspectors. Nearly same verification activities are done during PIV except the increase in the number of samples taken. An unattended NDA verification technique for the product storage area will soon be applied to reduce manpower for both operator and inspectorate.

PNC Plutonium Fuel Facility

The PNC Plutonium Fuel Facility (PPFF) comprises two facilities, the Plutomium Fuel Development Facility (PFDF) and the Plutonium Fuel Fabrication Facility (PFFF). Since its start-up in 1965, PFDF has carried out various tests and studies on the utilization of MOX fuel. PFFF was constructed in 1972 for the fabrication of fuel for use in the experimental fast breeder rector (FBR) "JOYO" and the prototype advanced thermal reactor (ATR) "Fugen". The annual fabrication capacity is one ton of MOX for the FBR line and ten tons of MOX for the ATR line. PPFF has three MBAs; a feed materials storage area, a nuclear materials handling area, and a fuel assembly storage area. It also has six FKMPs and fourteen IKMPs.

For both monthly and physical inventory verification rather conventional verification methods such as direct access of inspectors to the process area and nuclear materials are applied. To further improve efficiency of safeguards for this facility, advanced NDA and containment and surveillance (C/S) measures are expected to be introduced.

Plutonium Fuel Production Facility

The fast breeder reactor fuel line of Plutonium Fuel Production Facility (PFPF FBR line) was constructed to supply fuel for both the experimental fast reactor "JOYO" and the prototype fast breeder reactor "MONJU". Its operation started in November 1988 with a capacity of five tons of MOX fuel per year. To reduce personal radiation exposure, PFPF introduced a fully automated MOX fabrication technique based on a computer controlled nuclear material control system combined with automated process equipments. To design and install the facility material accountancy system and safeguards measure, fully automated systems were considerd to save considerably safeguards manpower of both operator and inspectorate.

The PFPF FBR line consists of one MBA, and has six FKMPs and eight IKMPs. MOX feed materials which came from PCDF are blended with UO_2 powder, and pelletized. Then, the fuel pin is fabricated and finaly assembled to the subassembly. Through these operations almost all nuclear materials are handlled in an itemized form. This implies that safeguards approach to be applied to this facility could not be that of a bulk facility but that of an item facility.

NDA techniques based on neutron coincidence methods are applied to each process material including holdups for verification purpose. For both feed (MOX powder canister) and product (fuel asssembly) materials, unattended mode NDA techniques are adopted, which contributes remarkable reduction of safeguards manpower. Moreover, computer controlled advanced containment and surveillance systems based on CCTVs and radiation monitors are installed in both feed and product areas to assure continuity of knowledge on safeguards integrity. Introduction of NRTA verification techniques is the next step to improve efficiency and effectiveness of this facility. Field trial of NRTA is undergoing.

During monthly verification and PIV, NDA measurements and destructive analyses of each process material are conducted based on a sampling plan. Data reviews of unattended NDA systems, C/S systems, NRTA trials and book audit are also carried out.

PNC Tokai Research and Development Facilily

Beside four facilities above, the Tokai Works has several laboratories to handle a small amount of nuclear materials to develop uranium enrichment technology, nuclear fuel reprocessing technology for FBRs and so on. The PNC Tokai Research and Developpment Facility (PNC Tokai R&D Facility) is composed of these laboratories. PNC Tokai R&D Facility has four MBAs, ten FKMPs and eleven IKMPs. An annual physical inventory verification is conducted to this facility. UF_6 cylinders in the uranium enrichment laboratory are measured by NDA method.

EFFORTS ON SAFEGUARDS TECHNOLOGY DEVELOPMENT

Safeguards works began with the start of the Plutonium Fuel Development Facility (PFDF) operation in 1966. Since then, the efforts have been enlarged in both quality and quantity with the expansion of the plutonium handling facilities such as PFFF, TRP, PCDF and PFPF in the Tokai Works.

With the first receipt of 260 g plutonium from the USA in 1966 to PFDF, construtions of their material accountancy system started. A computerized system was introduced with the increase of plutoninm handling quantity. At PFFF which started operation in 1972, a newer system enabled real time material accountancy was adopted.

The development of NDA technique to measure plutonium quantity in a drum, a carton, a fuel subassembly and other container has been conducted since 1970.

Tokai Advanced Safeguards Technology Exercise (TASTEX)

TASTEX program was started in 1978 to demonstrate various safequards techniques for a reprocessing facility with the cooperation of four participants (Japan, USA, France and IAEA). Thirteen tasks were proposed by participants, which covered almost all areas of reprocessing safeguards. TASTEX terminated in May 1981, and some of the promising tasks were transferred to Japan Support Programme for Agency Safeguards (JASPAS). TASTEX gave TRP the basis for its succeeding safeguards activities. Table 1 shows the list of TASTEX programs.

Participation in Japan Support Programme for Agency Safeguards (JASPAS)

JASPAS was started in November 1981 by the Japanese Government. PNC participated in the program by transferring four tasks from TASTEX. By now, PNC Tokai Works has been engaged in fifteen tasks (as shown in Table 2), of which four, including tasks mainly related to TRP, have already been put into routine safeguards use. Two of these tasks have been applied to the advanced C/S systems for PFPF.

PNC/US-DOE Safeguards Cooperation

To establish safeguards system for a fully remote and antomnated new MOX facility, PFPF, PNC started the development of a system applicable to facility in 1983 with the cooperation of US-DOE. The whole system PNC developed has the following subsystems.

- A fully computerized material accountancy system
- Advanced C/S systems for the feed and product storage areas including authentication subsystems
- Remote-controlled NDA systems for the feed and product storage areas
- Remote-controlled NDA systems for the process areas
- An accountancy verification system to which NRTA is applied

Based on the above cooperation program, PFPF safeguards system was developed, which was envisioned as a solution to the safeguards for an automated MOX fuel fabrication facility.

Besides the program for PFPF, three tasks related to TRP were involved in the PNC/US-DOE cooperation. These tasks are expected to improve the efficiency of the reprocessing safeguards. Table 3 shows the list of PNC/DOE safeguards cooperation program.

INSPECTION WORK LOADS

Each of the facilities is basically subject to government inspections and IAEA inspections to ensure that nuclear materials placed under safeguards are appropriately contorolled in conformity with the relevant government regulations and the safeguards agreement.

Figure 2 shows the actual inspection work loads of IAEA estimated by PNC for the five facilities in PNC Tokai Works during 1981-1989. In 1989 about 1,100 person-days by IAEA were spent to our site, which implies about four IAEA inspectors stay in PNC Tokai Works every day (assuming that working days were 250 days per year). In 1989 inspection work loads to TRP were 290 person-days, this figure was not larger than in previous years because the amount of reprocessed fuel were about 18 tons U. But in 1990 TRP reprocessed about 99 tons U, then inspection work loads are estimated to increase considerlably to about 780 person-days. In case of PFPF, inspection work loads in 1989 counted for about 300 person-days but this figure includes the participation of IAEA staff to various test activities of newly introduced safeguards equipments. After completion of the systems, the number will be decreased.

As shown in Figure 2, inspection activities to PNC Tokai Works are extensive. In 1989, for example, the inspection work loaks (1,100 person-days/year) made by IAEA counted for about 11% of IAEA inspections (10,132 person-days/year) conducted over the world.

MANPOWER SPENT ON SAFEGUARDS IN PNC TOKAI WORKS

For effective and efficient safeguards of the facilities in Tokai Works, wide range safeguards relevant works such as material accountancy, operator's responsive work to inspection and advanced technical development described before are required. In 1989 about 13,000 person-days were spent to all these safeguards activities as shown in Fig.3. This means about 50 persons a day are working for safeguards in the Tokai Works. However it should be noted that this nimder does not include the manpower necessary to carry out physical inventory takings (PITs). In PITs almost all the staff of the facilities under inspection are involved.

Table 1 TASTEX Program

TASK A : Evaluation of performance and application of surveillance devices in the spent fuel receiving areas.
TASK B : Collection and analysis of gamma spectra of irradiated fuel assemblies at the storage pool.
TASK C : Demonstration of hull monitoring systems.
TASK D : Demonstration of the load cell technique for measurement of solution weight in accountability vessels.
TASK E : Demonstration of electromanometer for measurement of solution volume in accountability vessels.
TASK F : Study of the application of the basic concepts of near-real-time materials accountancy to safeguarding spent fuel reprocessing plants.
TASK G : K-edge densitometer for measuring plutonium product concentrations.
TASK H : Measurement of plutonium isotopic abundance by gamma-ray spectrometry.
TASK I : Product area monitoring system.
TASK J : Resin bead sampling and analytical technique.
TASK K : Isotopic safeguards techniques.
TASK L : Gravimetric method (PU/U ratio) for input measurements.
TASK M : Tracer methods for input measurements.

Table 2 JASPAS Program of PNC Tokai Works

Title of Tasks	Facility	Period
JA. SAFEGUARDS SYSTEM DESIGNS AND SAFEGUARDS APPROACHES		
JA- 3 Plutonium Product Area Monitoring System.	TRP	1982-1988
JA- 5 Field Test of Near-Real-Time Material Accountancy at the Tokai Reprocessing Plant.	TRP/JAERI	1985-1989
JB. SAFEGUARDS DATA COLLECTION,TREATMENT AND EVALUATION.		
JB- 2 Isotopic Correlation Technique for Safeguards Data Evaluation.	TRP	1982-
JB- 3 Real Time Item Accounting System (RIAS) of Spent Fuel at the Receiving and Storage Areas.	TRP	1983-1990
JC. MEASUREMENT METHODS AND TECHNIQUES.		
JC- 1 Electoromanometer (for Measurement for Solution Volume in Accountability Vessels)	TRP	1981-1982
JC- 2 K-edge Densitometer for Measuring Plutonium Product Concentrations.	TRP	1981-1982
JC- 3 High Resolution Gamma Spectrometer for Plutonium Product Concentrations.	TRP	1981-1990
JC- 4 Resin Bead Sampling and Analytical Technique.	TRP/NMCC	1982-1990
JC- 7 Automated Gravimetric Sampling System (AGSS) for Safeguards Analysis.	TRP	1985-
JC-11 Rich Man's Densitometer (Non-Destructive Assay System for Uranium and Plutonum in Input Dissolver Solution).	TRP	To be established
JD. CONTAINMENT AND SURVEILLANCE TECHNIQUES.		
JD- 2 Surveillance System in the Spent Fuel Receiving Area.	TRP	1981-1982
JD- 8 Surveillance System Using the CCTV at the Transfer Pond RO108.	TRP	1983-1990
JD- 9 Integrated Containment and Surveillance System for Automated Plutonium Storage.	PFPF	1983-1986
JD-12 Remote Surveillance System for a New MOX Plant.	PFPF	1985-1990
JE. TRAINING AND COST FREE EXPERTS.		
JE- 2 Cost Free Expert.	TRP/PFPF	1984-

Table 3 Program of PNC/DOE Safeguards Cooperation

Project	Site
1. Remote-controlled NDA system for Fast Breeder Reactor (FBR) assemblies (FAAS)	PFPF/LANL
2. Remote-controlled NDA system for MOX canisters (PCAS)	PFPF/LANL
3. Remote-controlled NDA system for FBR fuel pins (FPAS)	PFPF/LANL
4. Remote-controlled NDA system for MOX transfer containers (MACB)	PFPF/LANL
5. Measurement techniques for plutonium holdup in MOX process equipment (GBAS)	PFPF/LANL
6. Remote-controlled NDA system for a small amount of nuclear material with a large volume	PFPF/LANL
7. Remote-controlled NDA system for PuO_2 canisters	PFPF/LANL
8. Remote-controlled NDA system for process holdup in PCDF	PCDF/LANL
9. Authentication system for the Advanced Containment/Surveillance system in Feed storage of PFPF	PFPF/SNL
10. Authentication system for the Advanced Containment/Surveillance system in Product storage of PFPF	PFPF/SNL
11. Authentication system for the FPAS and MACB	PFPF/SNL
12. Authenticated item identification system for PuO_2 canisters	PFPF/SNL
13. System analysis studies of NRTA for PFPF	PFPF/LANL
14. Fissile inventory verification of reprocessing holding tanks using isotope dilution techniques	TRP/ORNL
15. Plutonium isotopic and concentration measurement for chemical processing plant input accountability tank solutions by gamma measurement of resin bead samples	TRP/LANL
16. Plutonium concentration and isotopic composition measurement for plutonium product storage by passive γ-spectroscopy	TRP/LANL

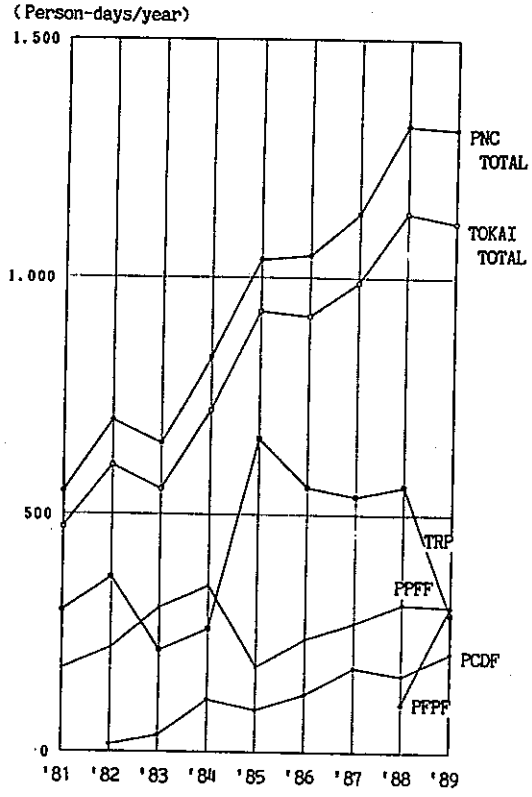

Fig.2 Inspection Work Loads of IAEA (Person-days/year)

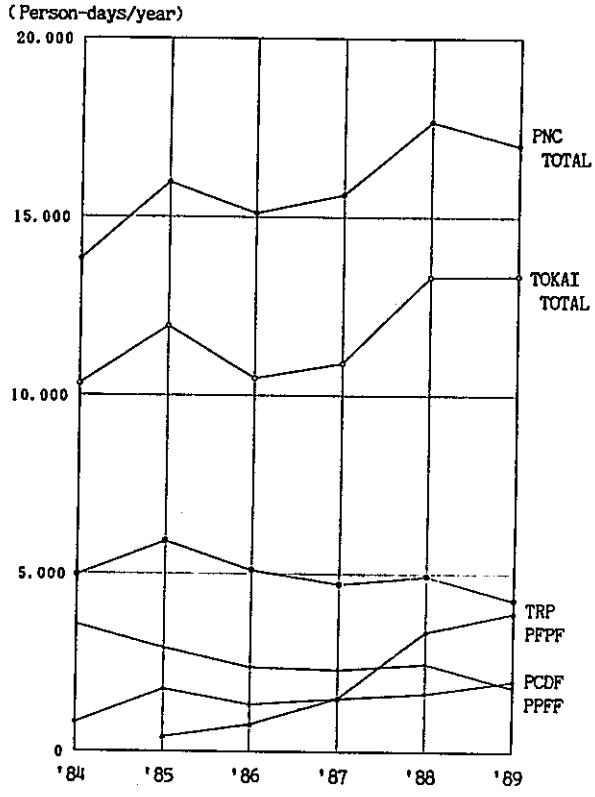

Fig.3 Safeguards Work Loads by PNC (Person-days/year)

FUTURE IMPROVEMENTS AND CONCLUSION

The manpower required for safeguards related activities in PNC Tokai Works will increase in the future because of the expansion of the activities of MOX fuel cycle development and waste management. To increase, however, safeguards manpower and cost further becomes more difficult for the operator because of the nearly zero-growth of the finance. The situation might be similar for the inspectorate. Therefore, to make futher efforts toward the establishment of more efficient and effective safeguards will be inevitable for the operator and the inspectorate. Since the PNC Tokai Works composes itself of an active part of MOX fuel cycle in Japan (as ahown in Fig.1), the study of a new approach such as a nuclear fuel cycle oriented safeguards approach, which recently attracted attention, is necessary. We have just started the survey of its new concepts appropriate to the PNC Tokai Works.

題　　名	The Operational Experience at TOKAI Reprocessing Plant		
発表先	RECOD'91		
発表地	仙　　台	発　表 年月日	平成3年　4月14日 ～ 4月18日
発表者 (○印口頭発表者)	所属名　再処理		
	○高橋　啓三，宮原　顕治，山村　　修		

(要旨)

1. 序　論　東海再処理工場の概説
2. 東海再処理工場の歴史
   - 2.1　建設経緯
   - 2.2　再処理量（５０９ﾄﾝ）
   - 2.3　主要な保守補修作業（酸回収蒸発缶交換，溶解槽補修）
3. 現　状　（計画停止について述べる。またその評価についてもふれる）
4. 再処理技術開発　（過去のＲ＆Ｄ実績と将来のＲ＆Ｄ計画について述べる）
5. まとめ　（結　編）

資料番号
TN8100　91－017 （80－02－245）

資料番号 TN8100 91-017

THE OPERATIONAL EXPERIENCE AT TOKAI REPROCESSING PLANT

K.MIYAHARA, O.YAMAMURA, K.TAKAHASHI

Tokai Reprocessing Plant, Tokai Works

Power Reactor and Nuclear Fuel Development Corporation

Tokai-mura, Ibaraki-ken, Japan 319-11

Tel: 0292-82-1111, Telefax: 0292-82-2321

ABSTRACT

Since the start of construction of the Tokai Reprocessing Plant(TRP) in 1971, large efforts were taken by the Power Reactor and Nuclear Fuel Development Corporation(PNC) and various organizations to root the LWR fuel reprocessing technology in Japan. These efforts produced many achievements around the TRP, and now the future plan for the TRP is being studied.

1. Introduction

The PNC has been operating the TRP since Sept. 1977 when the plant became active status using the spent fuel from the Japan Power Demonstration Reactor(JPDR), and the total amount of reprocessed fuels is exceeded over 500 tons. This amount is next to French achievement in the field of oxide spent fuel reprocessing.

Through these experiences of plant operation, we demonstrated, improved and established the mechanical head-end process and Purex process in Japan.

From the beginning of plant operation, the project to reduce the activities released to environment was started, and the number of facilities were add to the TRP. The actual values of radioactive release to environment have been quite low. During this period, a lot of corrosion problems of important equipments were occurred, which had not been exactly foreseen. On each occasion, the phenomena of corrosion were investigated, new corrosion resistant material was developed, and the procedure for fabrication and welding has been modified and improved step by step.

Recently, the scheduled long period of shut-down of plant operation was set to replace and modify the plant equipments for prevention of sudden equipment failure and for increase of reprocessed amount. The result of major maintenances improved the plant performance satisfactory.

Above mentioned activities were carried out with the participation of domestic industries using the own developed technique, therefore,the reprocessing technique was rooted in Japan and infra-structure of it was established. As for the development of fast breeder reactor(FBR) fuel reprocessing, which has been started from the beginning of 1970, the experiences of TRP operation become the one of design data-base for this project.

Concerning the cooperation with Japan Nuclear Fuel Services(JNFS), the "Basic Agreement between PNC and JNFS for the Technical Cooperation" was signed between both organizations in 1982, and various cooperations are being carried out such as consultation of design, dispatching of engineers, joint R&D activities, contracted projects, etc..

As a summary, the TRP has a key position for the development of technology of LWR fuel reprocessing, FBR fuel reprocessing,waste treatment, and for the realization of commercial reprocessing in Japan.

2.History of TRP

2.1 Construction and Test Campaigns

The reprocessing project of the PNC was started in September 1956 when the Atomic Energy Commission(AEC) of Japan decided that reprocessing of spent fuel and treatment of radioactive waste should mainly be done by the Atomic Fuel Corporation(AFC), the predecessor of PNC. In 1959, an Advisory Committee for reprocessing was formed within the AEC to formulate a guideline for development of the reprocessing technology. In conjunction with the recommendations put forward by a survey team which visited overseas reprocessing plants, a decision was made to construct a pilot reprocessing plant using the advanced technology developed by other countries.

In 1963, the AFC entered into a contract with the Nuclear Chemical Plant(NCP) of UK for a preliminary design of the plant, and in 1966 a detailed design was started by the Société Générale pour les Techniques Nouvelles(SGN) of France. Since 1968 and in parallel with the ongoing detailed design, the governmental licensing procedure had been followed and permission for plant construction was granted by the Japanese Government in 1970.

Plant construction was started in 1971 as a joint venture of SGN-JGC of Japan. The Plant was completed in 1974 and hot testing started in September 1977 after completing the U testing using unirradiated uranium. Up to the end of 1990 the total amount of reprocessed fuel from LWRs and the ATR Fugen(Advanced thermal reactor using heavy water as the moderator) was about 500 tons.

2.2 Reprocessed Fuel

The total reprocessed fuels from the start of hot operation on 22nd of September 1977 to the end of 1990 is about 509 ton of oxide spent fuel. The number of spent fuel assembly and amount of spent fuel is as follows, BWR:1815 and 321.1 tons, PWR:500 and 183.1 tons, and ATR Fugen Mixed Oxide Fuel:34 assemblies of 5 tons, which gave us valuable experiences for MOX fuel reprocessing.

The amount of plutonium nitrate recovered as a final product was about 3.4 tons, and most of Pu has already been sent to Pu conversion plant for use at the ATR Fugen, the experimental FBR Joyo, and proto-type FBR Monju.

2.3 Major Maintenance Activities

(1) Remote Repair of Dissolver R10 and R11

In April 1982, a small amount of radioactivity was found in the steam condensate from a dissolver. After confirming that one of the two dissolvers R11 had small defects which consist of pin holes in the welded part on the barrel of dissolver , operation was resumed using R10 dissolver until February 1983 when dissolver R10 had same kind of defects. The remote repair technology had been developed, and from September to November 1983 the in-situ repair of two dissolvers was carried out successfully first time in the world.

(2) Installation of New Dissolver R12

Leakages in the two dissolvers occurred rather unexpectedly and subsequently the third dissolver was installed in a spare dissolver cell.

Table 1. Total Reprocessed Fuel at TRP

	Number of Assembly	*Reprocessed Uranium (MTU)*	*Maximum Burnup (MWD/T)*	*Average Burnup (MWD/T)*	*Cooling Time (Years)*
BWR	*1,815*	*321.1*	*29,800*	*18,300*	*0.9-21.2*
PWR	*500*	*183.1*	*34,500*	*22,200*	*0.9-17.1*
Fugen(ATR)	*34*	*5.2*	*13,500*	*9,800*	*3.3-6.0*
Total	*2,349*	*509.4*	*34,500*	*19,600*	*0.9-21.2*

A new dissolver R12 was fabricated with improved material and welded lines were eliminated from the inside steam jacket as for the design. A fabrication of dissolver was finished in April 1984, and was installed by the end of November 1984.

(3)Repair of Acid Recovery Evaporator

During the final stage of hot testing in August of 1977, a minor leak was detected which was caused by pin holes of welded part of heating tube in the acid recovery evaporator, and an exchange of whole part of evaporator was done after decontamination and dismantling of leaked evaporator by the end of December 1979. However, the new one leaked again in February 1983 caused by corrosion of heating tube, and at that occasion only boiler part of evaporator was replaced with domestic produced materials. The repairing period was seven months which was shorter compared with former one.

3. Present Status

3.1 Scheduled Shut-down of Plant Operation

The operation of TRP became steady and stable since 1985 after many modifications and improvements, however, the requirement of increasing the reprocessed amount at the TRP is stronger than before because of demand for more plutonium of the ATR and FBR fuel cycle development.

The design capacity of TRP is 0.7 tons per day, and operational license permits the TRP to reprocess up to 210 tons per year. Although it was difficult to reach this maximum, because of yearly regulatory inspection, the physical inventory takings(PIT) of nuclear material and periodical maintenance works. The operational total days of TRP per year had been calculated as about 170 days, and assuming the average plant efficiency factor of 60% the derived yearly production of TRP had been about 70 tons.

For the improvement of the production rate, one is augmentation of operation days and another is to ameliorate the plant performance factor. The operational yearly days were increased by shortening of maintenance and regulatory inspection period, and for the plant efficiency factor, it became clear to improve and modify the fuel assembly shearing process and clarification process for dissolved fuel solution. In the long range, it was also obvious to prevent the sudden stop of plant operation, which will be caused by failure of major equipment due to corrosion. Therefore the scheduled shut-down of plant operation was set to replace the acid recovery evaporator, and to make modification of fuel assembly shearing process, clarification process etc..

3.2 The Major Maintenance Works During the Scheduled Shut-down Period

(1)The Replacement of the Acid Recovery Evaporator

The first acid recovery evaporator leaked in 6000 hours of use, and the leak of second one was occurred in 13,000 hours use. The material of evaporator was 25%-chromium and 20%-nickel alloy of stainless steel, and the conservative estimation was that the third evaporator would leak again in 13,000 hours of use, which was expected around the half of 1988. On the other hand, the development of corrosion resistant material was done continuously since the day of leak of first evaporator, and it became evident that the titanium and 5%-tantalum alloy material shows a good corrosion resistance behavior in this corrosive environment.

The decision was taken to replace the third evaporator with the new one made of Ti-5%Ta alloy. This work was started in June 1988 and was performed smoothly within scheduled 11 months period, based on the old experiences of two times replacement so far.

(2)The Replacement of Plutonium Solution Evaporator

The design of original plutonium evaporator was to connect the washing column to boiler part with the flange, and the material of former one was stainless steel and latter one was corrosion resistant titanium. For the column part a pin hole defect appeared in year 1982 after 10,000 hours of operation and in-situ repair was done. In year 1984 the replacement of whole evaporator was done after 12,000 hours of operation.

The decision was made to replace this evaporator because of 9,000 hours of operation, and the material of column part was chosen as Ti-5%Ta alloy to prolong the operational life. The improvement was made to remove the flange connection by welding the titanium and Ti-5%Ta alloy. The replacement was done in the cell within three months.

(3)Modification of Boiler part of Acid Recovery Distillator

The acid recovery distillator was fabricated from the stainless steel, and in February 1981 the corrosion leakage was occurred on the part of heating coil after 13,000 hours of use, and repair work was done within 1.5 months. In 1984 the boiler part of distillator was replaced within 4 months.

The new distillator was installed to replace the old one which operation time was about 13,000 hours of use. The new distillator has separable heating tubes from boiler part of distillator for easy maintenance.

(4)Modification of Fuel Assembly Shearing Machine

Many modification works for internal parts of shearing machine were done to improve the operability and maintenance ability.

(5)The Addition of Second Pulsed Filter

The clarification method of the TRP was to use pulsed filter. The filtration of dissolver solution clogs the sintered stainless filter gradually and finally it will necessitate the replacement of filter cartridge affecting the plant.

To improve the plant efficiency factor, the second pulsed filter was added in the clarification process. The new type of valve for changing use of both filters was developed to install inside cell for easy maintenance and high fidelity. The modification works inside cell was done after tedious decontamination of equipments and piping, and working time was limited because of still rather high radiation dose. The time of total installation work was more than one year after delay of four months for final modifications.

3.3 Evaluation of Major Modifications on Plant Performance

The scheduled shut-down of plant operation continued 15 months, and the PNC person who is involved in this work were around 500 and the number of contracted workers of constructor and engineering firms were about 1,600(about 100,000 man-day). The accumulated radiation dose of person was 5 man•Sv(500 man•rem), which is higher than average 1-2 man•Sv/year of record of the TRP operational staff exposure rate.

The original intention of improving the plant was to increase the yearly processing amount from 70 tons to 90 tons. The start of operation from the major modification works was in the end of September 1989 and after one year in September 1990 the reprocessed amount was 83 tons of spent fuel and during the year 1990 from January to end of November 99 tons of fuel was reprocessed.

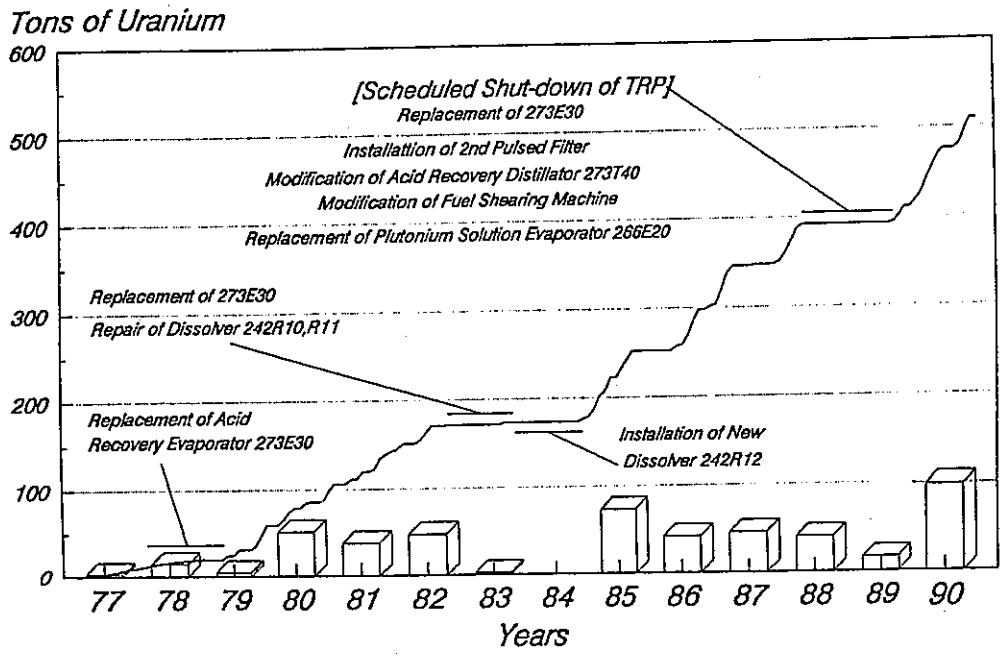

Figure 1. Operational History of TRP

4. Developments of Reprocessing Technology

4.1 The Achievements of R&D Activity

The main process of TRP was designed by SGN in the latter part of 1960s, when the experiences of LWR fuel reprocessing were very limited in the world, and the TRP had to encounter many difficulties from the start of construction, hot test and regular operation.
These difficulties were solved one by one at the TRP with cooperations of many people and organizations, and through theses efforts the many successful results of R&D were obtained such as:

(1)Fluidized denitration technique of uranyl nitrate solution to uranium tri-oxide powder

(2)Waste evaporation treatment technique for reducing the activity release to sea and de-oiling technique from the discharge liquid by charcoal filtration.

(3)Solidification for concentrated waste and used solvent by bitumen and plastic

(4)Development of new corrosion resistant materials and fabrication technique for the use in the corrosive environment

(5)Remote maintenance and repair technique in the high radiation area

(6)Preventive and removal technique for the clogging of piping caused by sludge

(7)Advanced operation support systems using computers

Furthermore, the one of most important achievement at the TRP is in the area of Safeguards(SG) of nuclear material. The plant start-up schedule was somewhat influenced by the negotiations between the governmment of United States of America and Japan. After both governments had agreed on the terms and conditions of plant operation, the first hot campaign was started. The TRP was regularly inspected by IAEA as well as Science Technology Agency(STA),and international SG project was done as the Tokai Advanced Safeguards Technology Exercise(TASTEX) from year 1978 to 1981 which have been followed by the Japan Support Program for Agency Safeguards(JASPAS).
In last July 1990 PNC received the Industrial Award of Institute of Nuclear Material Management(INMM) for the peaceful use of plutonium and efforts for development of SG technique.

4.2 Future Plan for R&D

The R&D activities at the TRP until now are primarily aiming at keeping steady operation, and the before mentioned schedule shut-down of plant operation was for the concentrated measures to expect the stable and improved operation.

From now the purpose of R&D activity of TRP shall be toward more advanced and sophisticated areas compared before. The main items of interest are as follows:

(1)Advanced Technique for Reprocessing of High Burn-up Fuel

The burn-up specification of spent fuel reprocessed at the TRP is average 28,000 MWD/T per day of processing and Maximum 35,000 MWD/T per fuel assembly. Recently the project to increase the burn-up of LWR fuel is going on in Japan above 50,000 MWD/T, and also the demonstration program for plutonium(MOX) fuel recycling in LWR core is proceeding smoothly. The study is being done to reprocess these special fuel at the TRP by current purex method.

(2)Development of Remote Handling Technique

(i)The Development of Advanced Repair Machine for the Dissolvers
The improvement of remote repair machine is continued to widen the area of access inside the dissolver and to make a machine as a multi-function.

(ii)The Development of In Service Inspection(ISI) Equipment
The remote ISI equipment is needed to verify the soundness of high active liquid waste evaporator which is very difficult to access, also under developing equipment to check the drip trays in the cell.

(iii)The Remote Dismantling Technique of Dissolver
The operational life of dissolver will be limited for corrosion of material, and in case of failure not possible to repair by remote device, it will be necessary to remove the dissolver itself from the cell. The remote machine to do this work requires high standards of technique because of the complicated work to dismantle and remove the large, high active dissolver from a rather small cell.

(3)The Strengthening of Engineering Data-base

Concerning the various technical data which were acquired during the construction, operation and maintenance works, the data-base with computers is being developed for the use of operation and R&D activity. One of data-base is the Tokai Reprocessing Plant Maintenance and Management Support System(TORMASS) to store the specification of various equipments and the maintenance data, analyze the data and retrieve the data easily for maintenance schedule.

(4)Operational Support System for Main Process

The instruction system for operation of extraction process is under development to support operators. The process simulator of extraction process is also being developed to support instruction system. These activities will help the analysis of mal-operation and safety evaluation of reprocessing operation.

(5)Development of Head-end Facility

The head-end process which is composed of shearing, dissolution and clarification of spent fuel is one of critical part of reprocessing, and some new reprocessing plants have parallel lines on this part. Also at TRP, the head-end process is main area to lower the performance of plant and caused a frequent shut-down of operation. In other words, there remains many areas of improvements and developments for the head-end process, and the study to add a new head-end facility to the TRP is started to demonstrate the advanced equipments in hot environment.

As for the operation of Recycling Equipment Test Facility(RETF) which will be used for development of FBR fuel reprocessing technology, the active products and wastes produced from the experiment will be treated in the TRP connecting the both facilities with piping.

5. Conclusion

The design of main process of the TRP was made in abroad and the improvements and developments were done from the start of construction to today to accommodate the various situations in Japan. Around the TRP plutonium and uranium conversion facility, krypton recovery facility, bituminization facility and vitrification facility etc. were constructed and operated, and the development activities for back-end fuel cycle were concentrated at PNC Tokai site.

The initial aim of strengthening and stabilizing the operation of the TRP is now almost obtained, and the future plan for the TRP is to toward the R&D oriented areas.

REFERENCE

(1)NAKAJIMA,K.,NAKAMURA,Y.,"Results and experience of nuclear fuel cycle technology development by PNC: Operating experience with the Tokai Reprocessing Plant", Nuclear Power Experience(Proc.Int.Conf.Vienna,1982), Vol.3, IAEA, Vienna(1983)825-829

(2)TSUJI,T.,YAMANOUCHI,T.,TAKAHASHI,K., FURUKAWA,H.,"Development and Improvement of Reprocessing Technology at the TOKAI Reprocessing Plant", Proceedings of an International Symposium on the Back End of the Nuclear Fuel Cycle:Strategies and Options, IAEA, Vienna,1983

(3)OMACHI,S.,YAMANOUCHI,T.,MATSUMOTO,K., "Decadal Operational Experience of the Tokai Reprocessing Plant", International Conference on Nuclear Fuel Reprocessing and Waste Management "RECOD 87", Proceedings Vol.1, Paris(1987)195-202

題　　名	The Operational Experience at TOKAI Reprocessing Plant		
発表先	RECOD'91		
発表地	仙　　台	発　表 年月日	平成3年　4月14日 ～ 4月18日
発表者 (○印口頭発表者)	所属名	再処理	
	○高橋　啓三，宮原　顕治，山村　　修		

(要旨)

1. 序　論　東海再処理工場の概説
2. 東海再処理工場の歴史
   - 2.1　建設経緯
   - 2.2　再処理量（５０９ﾄﾝ）
   - 2.3　主要な保守補修作業（酸回収蒸発缶交換，溶解槽補修）
3. 現　状　（計画停止について述べる。またその評価についてもふれる）
4. 再処理技術開発　（過去のＲ＆Ｄ実績と将来のＲ＆Ｄ計画について述べる）
5. まとめ　（結　編）

資料番号
TN8100　91－017 （80－02－245）

資料番号 TN8100 91-018

DECONTAMINATION CHARACTERISTICS OF HLLW EVAPORATOR IN TOKAI REPROCESSING PLANT

T.KASHIMURA , A.MAKI , M.OTSU , K.ISHIKAWA

Power Reactor and Nuclear Fuel Development Corporation
4-33 , Muramatsu , Tokai-mura , Ibaraki-ken
Japan 319-11
Phone: 0292-82-1111

A B S T R A C T

The decontamination factors (DFs) of the high level liquid waste (HLLW) evaporator in Tokai Reprocessing Plant (TRP) were investigated regarding such dominant nuclides as Zr-95, Ru-106, Cs-137, Ce-144 by measuring those radioactivity concentrations of concentrate in evaporator and vapor condensate. The measured DFs for Ce, Cs and Zr, known as non-volatile elements, showed good consistency each other and comparable to the values reported so far. On the other hand Ru shows volatile characteristics, however, its release fraction is sufficiently small and the DF for Ru, as well as for non-volatile nuclides, is satisfactory. Based on the measured DFs, the entrainment generated in the HLLW evaporator was also evaluated by using entrainment model calculation.

INTRODUCTION

Decontamination characteristics of the evaporator are primarily determined by the entrainment. The mist entrained into gas is scrubbed with bubble cap trays. However, volatile radioactive elements are not captured effectively by the trays which causes the decrease of decontamination factor for those elements.

This paper surmarizes the release mechanizm of radioactive elements and decontamination characteristics of HLLW evaporator based on the data collected in TRP.

OUTLINE OF HLLW CONCENTRATION PROCESS

Fig.-1 shows the outline of HLLW concentration process in TRP. The HLLW evaporator in this process concentrates

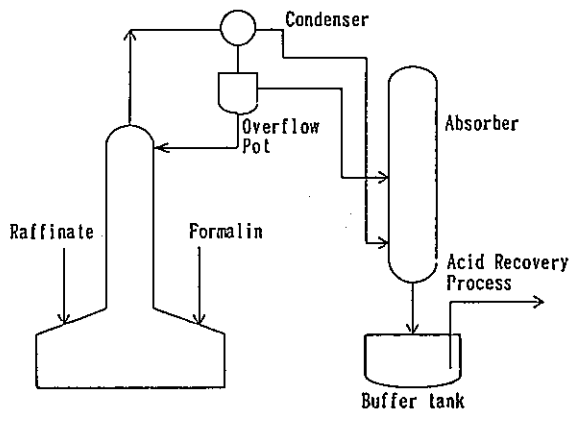

Fig.-1 The outline of HLLW concentration process

the raffinate solution from the 1st extraction (co-decontamination)cycle and the concentrated solution from the acid recovery evaporator. This evaporator is operated batchwisely and the concentrated solution is sent to HLLW vessels.

In operation, nitric acid is decomposed by formalin in order to keep solution acidity in the evaporator around 2N. The vapor which occurs in the HLLW evaporator is distilled in a condenser, and the distilled solution is transferred to acid recovery process through a overflow pot. For non-condensable gases nitric acid component is recovered in the absorber.

OUTLINE OF HLLW EVAPORATOR

Fig.-2 illustrates the HLLW epaporator. The lower half of the evaporator is a boiler portion with coil pipes and jackets for heating, and the upper half functions as the washing column which contains five stages of bubble cap tray and a cyclone at its lowest part in order to separate mist from vapor gas. The vapor is scrubbed with the trays, where the entrained mist is captured.

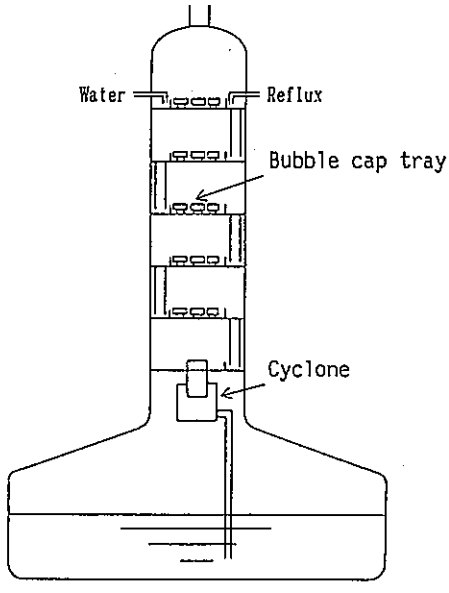

Fig.-2 The outline of the HLLW evaporator

The bubble cap trays are 70cm of diameter, and placed at the interval of 40cm.

BEHAVIOR OF RADIOACTIVE ELEMENTS IN HLLW EVAPORATOR

Fig.-3 shows the vapor mass velocity versus decontamination factors for dominants nuclides, such as Zr-95, Ru-106, Cs-137, Ce-144 in the evaporator. The decontamination factors were caluculated as ratios of activity concentrations in the boiler solution to in distillate. The distillated solution is sampled at the overflow pot.

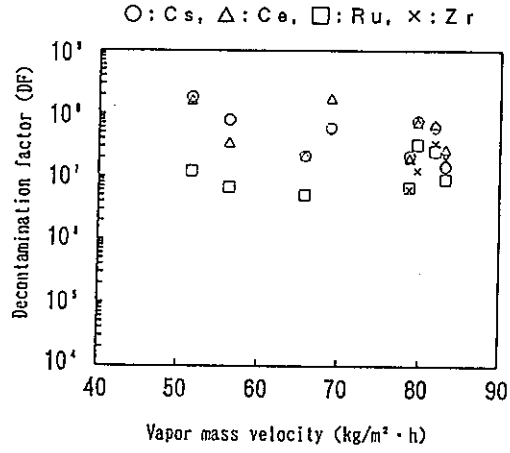

Fig.3 DF of HLLW evaporator

As the DFs for non-volatile Ce, Zr and Cs are similar, it is considered that Ce, Zr and Cs move to the condensate by entrainment. Becuse Ru has a little volatility, its DF is slightly smaller than the other elements

when the vapor mass velocity is low. However, the DF of Ru is satisfactory as it gets over the value of 10^6. The DFs of Ce, Cs and Zr are decreaseing according to the increase of the vapor mass velocity, due to increase of the entrainment formed on each trays.

ENTRAINMENT MODEL

Non-volatile elements move to distillate primarily by entrainment. Therefore the decontamination characteristics of HLLW evaporator can be estimated using the model of entrainment. The assumptions adopted in the model are as follows:

(1) The activity moves to distillate only by the entrainment.

(2) The entrainment occuring on each trays is constant.

(3) The probability of entrained fume passing through the trays is constant.

The activity balance expressions are established in each tray using above assumption and activity concentrations of solution on each tray are calculated. The unknown factors of the expression are:

① The amount of entrained fume which is generated at the solution surface in evaporator and reaches the lowest tray through cyclone.

② The amount of entrained fume occuring on each trays.

③ The probability of entrained fume passing through each trays.

The results of parametric survey of above unknown factors are shown in Fig.-4 ~Fig.-6 in order to see activity concentrations

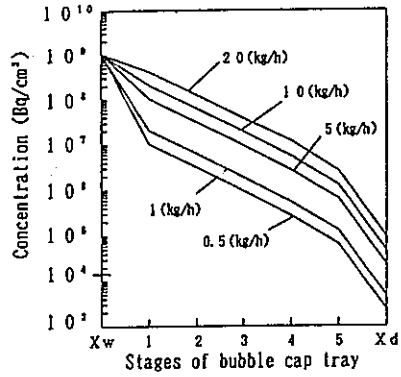

Fig.-4 Effect of entrainment in evaporator

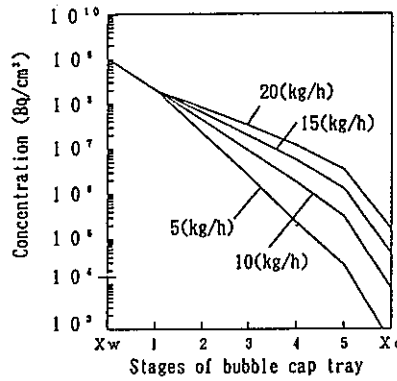

Fig.-5 Effect of entrainment on the tray

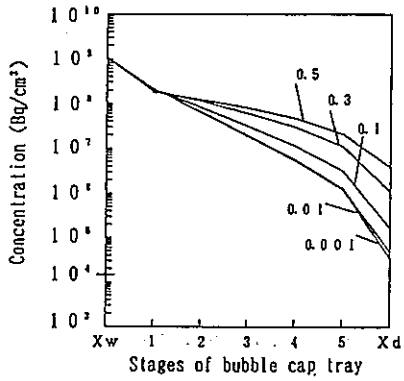

Fig.-6 Effect of mist passing probability

affected by those factors. Xw shown in Fig.-4 ~Fig.-6 corresponds to concentrate and X_D to condensate.

The activity concentration is largely affected by the entrainment in evaporator and on trays, and by the probability passing through tray.

ENTRAINMENT OCCURING IN HLLW EVAPORATOR

The decontamination efficiency of evaporator is determined by the entrainment formed at the surface of concentrated solution and on trays, and probability of entrained fume passing through trays. The probability of entrainment passage is reported about 0.01 [2] ,and the entrainment formed on trays can be calculated by the relation of Fair-Mathews [1] . Therefore the entrainment reached to the lowest tray through cyclone is calculated with the ratio of activity concentrations of the concentrate to the distillate as the DF, by using the entrainment model. The result is shown in Fig.-7. Because the capture efficiency of cyclone for entrained fume is increased depending on increasing vapor velocity, the entrainment decrease according as the the vapor mass velocity increases. However, the entrainment formed on trays is also increased depending on vapor mass velocity. The DF of the evaporator decreases when the vapor mass velocity increases as shown in Fig.-3.

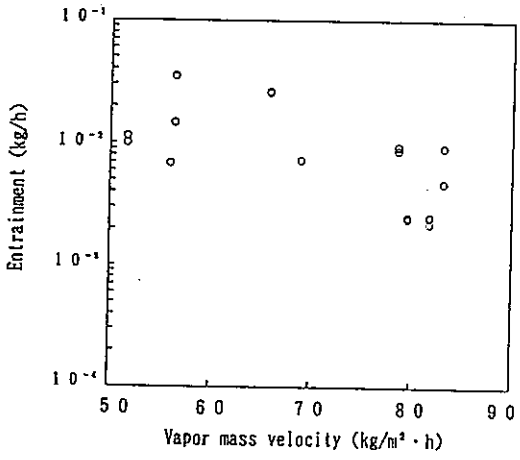

Fig.-7 The entrainment occuring at the surface of the concentrated solution (with cyclone)

The relationship between the vapor mass velocity (G) and the entrainment (M) is expressed as follows, using least squares method, when the vapor mass velocity is ranging from 50 to 90 (kg/m² ・h):

$$M = 0.186 \cdot \exp(-4.52 \times 10^{-2} \cdot G)$$

Similarly, the relationship between the vapor mass velocity (G) and the DF of evaporator (DF) for the same range of vapor mass velocity is expressed:

$$DF = 8.96 \times 10^{0} \cdot \exp(-4.32 \times 10^{-2} \cdot G)$$

The entrainment which is generated at the liquid surface and passed through the cyclone is $10^{-1} \sim 10$ (kg/h) assuming the DF of the cyclone as $10 \sim 10^{2}$. This DF of the cyclone is estimated by comparing with DFs of other evaporators without cyclone in TRP.

CONCLUSION

(1) It is confirmed that the DF of the HLLW evaporator is satisfied with the design value.

(2) Ce,Cs,Zr is not volatile and move to the distillate by entrainment. As for Ru volatilization quantity is relatively larger than entrainment,however, the

DF of Ru is still satisfactory.

(3) The DF of the HLLW evaporator tends to decrease with the increase of the vapor mass velocity, because the entrainment occuring on bubble cap trays increases according to the vapor mass velocity.

(4) The entrainment which is generated at the liquid surface and passed through the cyclone is 10^{-1}～10 (kg/h) assuming the DF of the cyclone as 10 ～10^{2}.

REFERENCE

(1) MITSUISHI,N.,SAKATA,A.,MATSUDA,Y., YAMAMOTO,Y.: J. At. Energy Soc. Japan, Vol.1, No.6 (1959)

(2) MIZUSHIMA,T.,TAKAMATSU,T.,MITSUISHI,N., IJICHI,S.,KAWAI,H.,: J. At. Energy Soc. Japan, Vol.3, No.9 (1961)

(3) MIZUSHIMA,T.,TAKAMATSU,T.,MITSUISHI,N., FUKUMOTO,T.,MORI,T.,: J. At. Energy Soc. Japan, Vol.5, No.9 (1963)

(4) Fair,J.R.,R.L.,Mathews : Petrol Refiner 37,153 (1958)

(5) H.W.Godbee : " USE OF EVAPORATOR FOR THE TREATMENT OF LIQUID IN THE NUCLEAR INDUSTRY", ORNL4790

題　名	Development of Shearing Technology in the TOKAI Reprocessing Plant (TRP)		
発表先	RECOD'91		
発表地	仙　台	発表年月日	平成3年 4月14日 ～ 4月18日
発表者 (○印口頭発表者)	所属名	再処理 前処理課	
	○清水 武範, 龍輪 正彦, 大谷 吉邦, 山内 孝道		

(要旨)

1988年から1989年の計画停止期間中に東海再処理工場のせん断装置に主として以下の様な改良を行った。

(1) 燃料送り不調対策のため，マガジン内につなぎ目，すき間のないU字形スペーサを採用した。

(2) ブレードカートの着脱性向上のため，ピン接続方式を採用した。

このような改良により，マガジンスペーサにはさまることによる燃料送り不調がなくなり，また，ブレードカート着脱作業性が向上した。

資料番号

TN8100 91-019

(80-02-270)

資料番号 TN8100 91-019

Development of Shearing Technology in the Tokai Reprocessing Plant(TRP)

Takenori SHIMIZU, Masahiko TATSUWA, Yoshikuni OTANI, Takamichi YAMANOUCHI
Tokai Reprocessing Plant(TRP)
Power Reactor and Nuclear Fuel Development Corporation (PNC)
4-33, Muramatsu, Tokai-Mura, Ibaraki-ken,
JAPAN , 319-11
Phone 0292-82-1111 Fax 0292-82-2321

Abstract

TRP has reprocessed more than 500tHM of spent fuel. Shearing operation in the TRP was often hampered by fuel debris. The removal of fuel debris from the shearing system required a lot of time. Difficulties in remote maintainability, as well as the fuel debris problem affected reprocessing operations in TRP. Hence, the refurbishment of the shear system was carried out from June 1988 to January 1989 to counteract the fuel debris problem and enhance remote maintainability. The refurbishment has been found very effective in improving the operations and maintenance.

1. Introduction

Construction ,operation and maintenance of Tokai Reprocessing Plant (TRP) have played an important role for establishment of the chop & leach PUREX method in Japan. The experiences obtained from activities in TRP have contributed in forming the foundation of FBR fuel reprocessing and waste management technology.

TRP has reprocessed more than 500tHM of spent fuel, since the hot test started in September 1977 up to the end of 1990. (see table 1)

In that period , several accidents such as leakage from dissolvers and acid recovery evaporator occurred. Measures were taken against every accident while investigating the causes, developing the advanced equipment and techniques for the repairs. Most of the activities mentioned above were achieved by means of in-house technology.

Much equipment has been improved, replaced and added to, in order to operate TRP smoothly and decrease the amount of radioactive discharge into the environment.

Equipment including the shear system were improved or replaced during the long planned shut-down period, from June 1989 to August 1990.

This paper describes improvements to the shear system conducted during this long planned shut-down period.

Table 1 Total reprocessed Spent Fuel in TRP

Fuel Type	BWR	PWR	ATR*1	JPDR *2
Reprocessed heavy Metal(tHM)	312.1	183.1	5.2	8.9

*1 Advanced Thermal Reactor "FUGEN"
*2 Japan Power Demonstration Reactor

2. Outline of the mechanical treatment process and shear system in TRP

(1)Mechnical treatment process(see fig.1)

The fuel assembly is introduced into the Enriched Uranium Mechanical Treatment Cell (EMPC) from the fuel storage pool by the fuel introduction conveyor. The fuel assembly is then transferred by the gantry grab to be placed on the Loading Table.

The Cart of the Loading Table feeds the fuel assembly horizontally into the magazine.

After the magazine is closed, the pusher in the chain magazine feeds the fuel assembly towards the shear.

The pusher head pushes the fuel assembly to the appropriate location in the shear housing for the cutting off of the first end piece, before shearing of the active part of the fuel assembly is carried out.

The movable blade driven by a hydraulic cylinder cuts off the first end piece, which falls into the end piece drawer. The end piece is then lifted out of the shear, and is tipped into a waste can.

The fuel assembly is held tightly by the gag before being sheared by the movable blade.

After cutting, the movable blade and gag move back, the fuel is advanced by one step, and the next cut made.

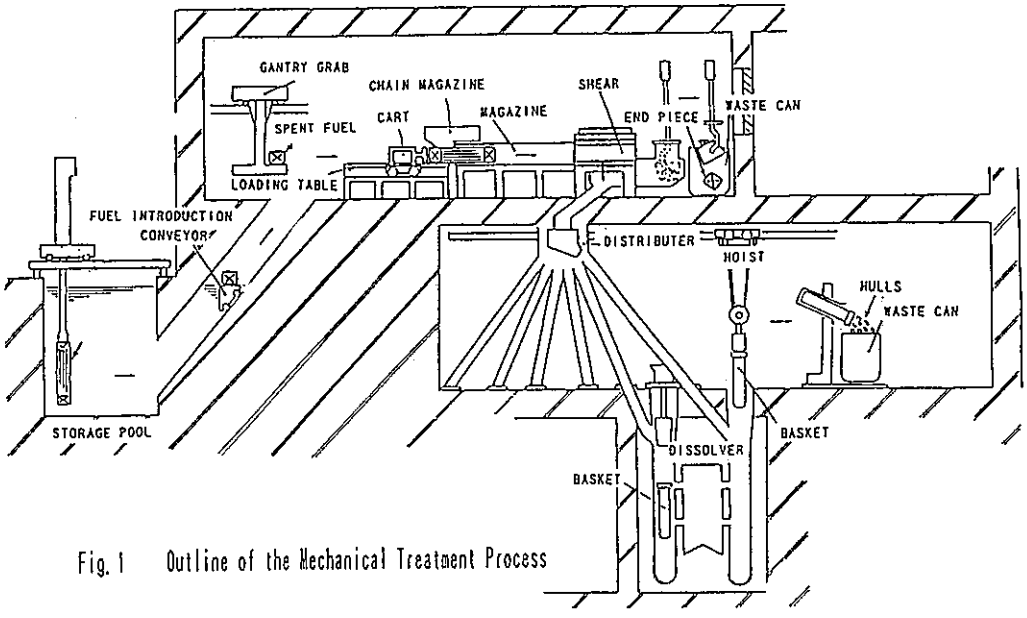

Fig. 1 Outline of the Mechanical Treatment Process

The small pieces of cut fuel fall through a chute into the distributer through which the pieces are loaded into one of the dissolver baskets.

The dissolver is put into the dissolving mode soon after it has been filled with sheared pieces. After dissolution , the in-cell hoist lifts the hulls, inside the basket, out of the dissolver.

Hulls are then put into waste cans.

(2)Shear system (see Fig.2 & 3)

Shear system is composed of the magazine, chain magazine, shear, hydraulic cylinders, end piece drawer and control unit.

The magazine has a hollow rectangular structure, and is connected to the shear. Since the cross section of the magazine is too large to cope with the fuel used in Japan, the magazine had the spacer named narrowing side to reduce the cross section.

The role of the chain magazine is to close the magazine entrance and also to feed the fuel assembly towards the shear. A special pushing chain is used in the chain magazine.

The pusher head is attached and is adjusted for the different fuel configuration used.

The shear is assembled inside the shear housing together with the blade, blade carrier, gag, and beams. The gag and blade carrier move along the plane of beams as guides. The blade carrier which holds the movable blade is driven by a hydraulic cylinder. The gag which clamps the fuel assembly to be sheared is also driven by a hydraulic cylinder.

The lid restrains the internal parts in the shear housing.

The hydraulic cylinders located outside the EMPC drive the blade carrier and the gag by means of extension rods.

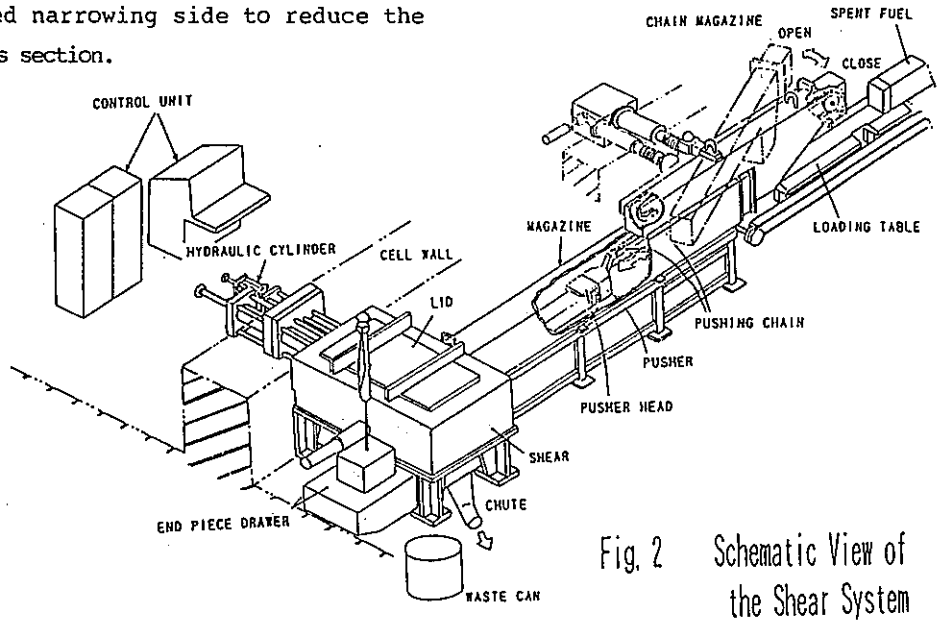

Fig. 2 Schematic View of the Shear System

The end piece drawer which removes the end pieces from the shear is installed underneath the shear housing. The end pieces are put into waste cans .

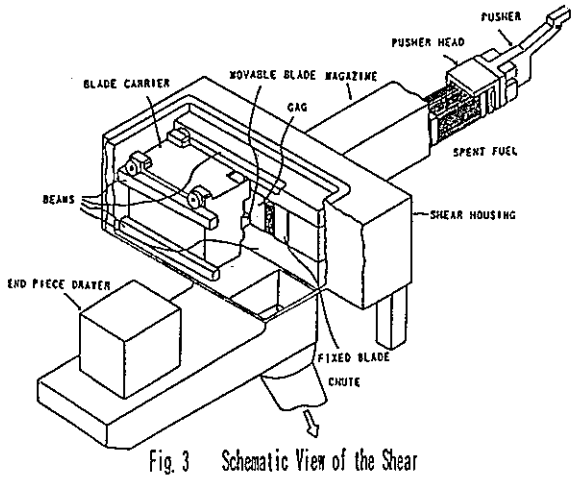

Fig. 3 Schematic View of the Shear

3. Problems of the shear system and their improvement

The original shear system in TRP had two main problems. One was the fuel debris problem and the other was the poor remote maintainability. Hence, improvement of the shear system (refurbishment work) was carried out from June 1988 through January 1989, and components of the shear system were replaced by improved ones, as described below.

(1)Fuel debris problem

The fuel assembly changes into small length of tubing together with large amounts of crushed pellets, and chips (fuel debris) during shearing.

Part of the fuel debris remains in the shear housing and magazine. The operation of the shear system was often hampered by it.

In particular, chips sometimes stopped the assembly feeding towards the shear because chips were jammed in the clearance between the narrowing side and the magazine. Fuel feeding was interrupted due to mechanical contact made between chips, fuel, pusher, and pusher head. Temporary removal of fuel debris required so much time as to affect reprocessing operations in TRP.

So features of improvement are as follows:

① A "U shaped spacer" was installed which eliminates the clearance between spacer and the magazine so as to prevent the fuel debris from jamming in the clearance between them (see Fig.4)

② The pusher head was equipped with a scraper to remove fuel debris automaticaly every time the pusher is moved.

③ The shapes of components were designed to avoid horizontal surfaces and grooves, and to eliminate clearances as much as possible so that fuel debris is not held up.

④ The shear and the end piece drawer were equipped with a water washing device to flush out fuel debris effectively.

(2)Poor maintainability problem

Before the refurbishment, the exchange of pusher head to accomodate a variety of fuel configurations required removal of the chain magazine from the shear system. This exchange accompanied by the removal of the chain magazine took about 48 hours. The blade carrier, which was fastened by a connection

bolt on the end of the extension rod, was often removed and attached during reprocessing campaign for cleaning-up the fuel debris or for exchanging the blade. It took about 12 hours to remove and attach the blade carrier.

This work affected reprocessing operations in TRP, so it was essential to enhance the remote maintenability in order to reduce work time and effort.

Features of improvement are follows:

① A pin connection between the blade carrier and extention rod of hydraulic cylinder was adopted so as to make it easy to remove and attach the blade carrier.(see Fig.5)

② A remotely exchangeable pusher head was designed so that there is no need to remove the chain magazine to exchange the pusher head.

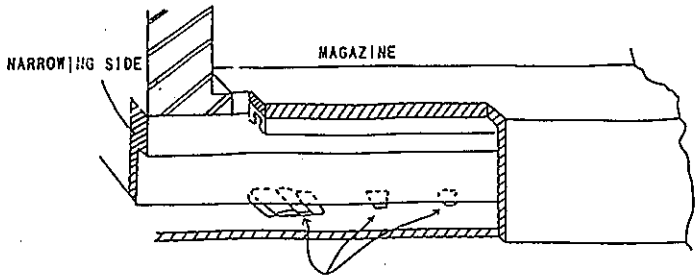

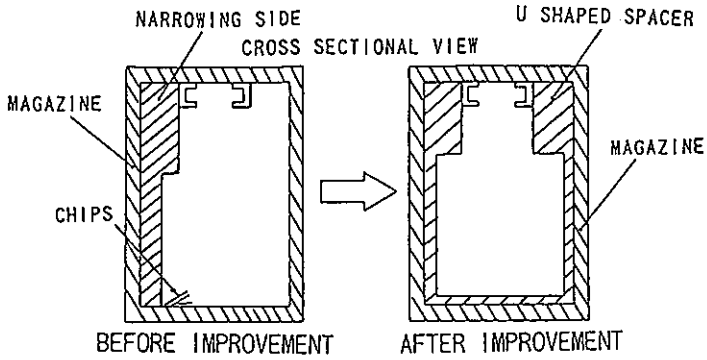

Fig. 4 Improvement of the Spacer to prevent the Chips from holding-up

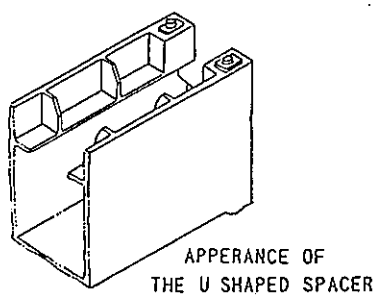

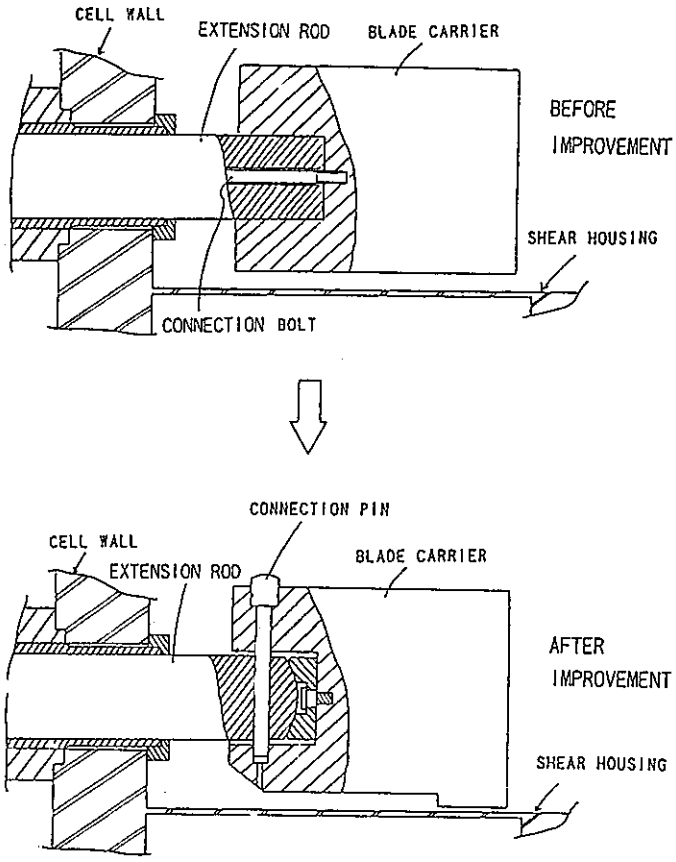

Fig. 5 Improvement of Connection between the Extension Rod and the Blade Carrier

4. Effect of improvement

After finishing the refurbishment, 117tHM of spent fuel were reprocessed between September 1989 and December 1990.

The improvements to the shear system have been found very effective during the operation and maintenance period.

(1)Measures against fuel debris

U shaped spacer and pusher head equipped with the scraper eliminate hampering the fuel feed. Water washing device has not been used yet but will be tested in the near future.

(2)Enhancement of remote maintainability

The refurbishment allows exchanging of the pusher head to take only 2 hours and the removing and attaching the blade carrier to take no more than 2 hours.

5. Conclusion

The improvements have been found to be very effective and have made operation of the shear system much more reliable.

We will further improve and refurbish the equipment to operate and maintain the mechanical treatment process effectively.

題　名	The Development of Computer-Aided Extraction-Status Diagnostic Technique at the TOKAI Reprocessing Plant		
発表先	RECOD'91		
発表地	仙　台	発表年月日	平成3年 4月14日 ～ 4月18日
発表者 (○印口頭発表者)	所属名	再処理 化処一課	
	○巌渕 弘樹，乳井 大介，小山 兼二，山名 元		

(要旨)

東海再処理工場の分配工程を対象にコンピューターを利用した抽出プロセスの異常診断手法について検討を行った。

異常事象の同定は，計装機器の監視によるＣＣＴ（Cause Consequence Tree)診断と，インラインモニタ指示値の変動パターンを利用したテーブル処理の組み合わせにより行われることは，既にＩＳＥＣ'90において示した。異常原因はテーブル処理においてニュートロンモニタの指示パターンの変化により同定される。本研究の重要な課題は，ニュートロンモニタの指示パターンの正確な認識にある。この指示パターンの変動について，東海再処理工場の実信号を用いて評価し，その信号処理方法を検討した。この結果，実信号を用いての原因同定が十分に可能であることを確認した。

資料番号
TN8100 91－020 (80－02－271)

資料番号 TN8100 91-020

The Development of Computer-Aided Extraction-Status Diagnostic Technique at the Tokai Reprocessing Plant

Hiroki IWABUCHI, Daisuke NYUUI, Kenji KOYAMA and Hajimu YAMANA

Tokai Works
Muramatsu 4-33, Tokai-Mura, Ibaraki-Ken,
Japan 319-11
phone : 0292-82-1111

Abstract

The computer aided system that automatically diagnoses the status of the extraction process is under development at the Tokai Reprocessing Plant(TRP), Power Reactor and Nuclear Fuel Development Corporation(PNC). The second extraction cycle of TRP was chosen as the base model of this system. It was shown in ISEC'90 that the combination of the CCT(Cause Consequence Tree) and the determination of the extraction profile-change by the indication pattern of in-line monitors (Table-Treatment) is the best way for the automatic diagnosis and the cause identification of the anomaly.[1]

The cause of the anomaly that changes Pu profile will be identified by the change of the indication pattern of neutron monitors by the Table-treatment. However this method greatly depends on how accurately the indication pattern of neutron monitors can be identified. In this study the fluctuation of the indication of neutron monitors was examined by investigating the actual record of the neutron monitors obtained in the TRP's operation, and the method of signal treatment was proposed. As a result, it was confirmed that the cause of the anomaly can be identified by the indication pattern of neutron monitors, with an appropriate signal treatment.

Introduction

The purpose of this study is to find a suitable method for the treatment of the fluctuation of the indication of neutron monitors and to develop a method to extract information of the significant status change from their back ground fluctuation. The fluctuation of the indication of neutron monitors of the TRP includes a high frequency component (noise) and the low frequency (long period) component (wave). The high frequency fluctuation can be attributed to the statistical error of the counting system and can be reduced simply by averaging the signal. It is assumed that the causes of the low frequency fluctuation are the variation of the liquid interface in the settlers and of the concentration of Pu. The change of the indication pattern caused by the anomaly can be distinguished with its non-periodic feature, from the periodic background fluctuation.

The actual fluctuation of every neutron monitor was incorporated to the calculated

change of extraction profiles (by MIXSET), and the efficiency of Table-treatment was examined.

Location of neutron monitors at the TRP

Fig.1 shows the location of the neutron monitors in the second extraction cycle (partition process) of the TRP. The neutron monitors are installed at some key stages, to detect the change of Pu concentration with real time. Fig.2 shows the schematic of a neutron monitor installation in the mixer-settler. The neutron detector is set to cover neutron emissions from both aqueous and organic phase. The effect of emission from the next stages was not considered in order to simplify the model.

Table-treatment

Examination of the indication of neutron monitors

The change of the Pu concentration in the extraction bank is monitored with

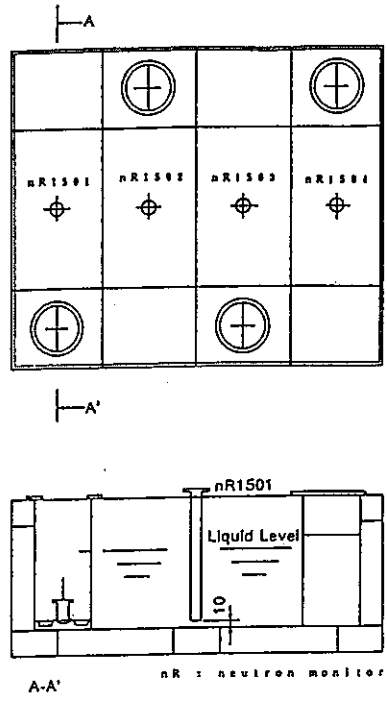

Fig.2 The schematic of a neutron monitor installation in the mixer-settler.

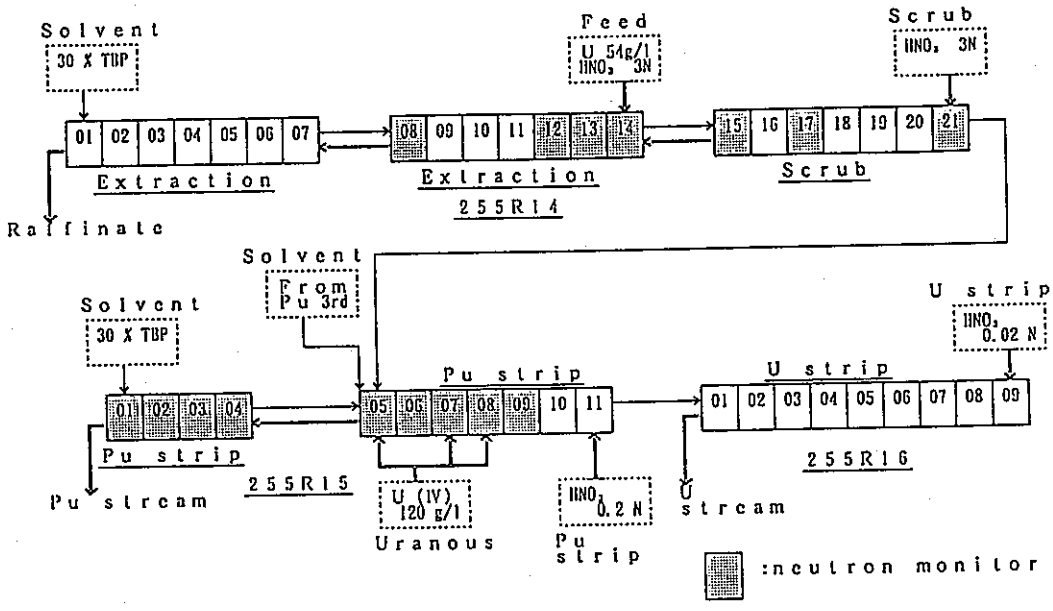

Fig.1 The location of neutron monitor in the second extraction cycle of the TRP.

neutron monitors placed at some stages. Because the neutron monitor counts the neutrons emitted from both phases, a slight change in one phase can not be detected, which means the profile change of Pu may have an obscure appearance on the monitors. We simulated their counts (cpm) by summing the neutron emission rate in both phases using the Pu concentration result obtained by MIXSET.

The U concentration in the aqueous phase is monitored with density meter. However, because the density is defined as the combination with the nitric acid concentration, U concentration change can not singly be detected. The density in the aqueous phase was calculated using the equation for uranyl nitrate solution with the uranium and nitric acid concentration obtained by MIXSET.

Fig.3 shows the typical example of the actual record of neutron monitor under steady operation condition. The fluctuation of the raw data is very large and is likely to hide the slight sign of anomalous events. Therefore, some data treatment is required. In order to decrease the random fluctuation to enhance the detection sensitivity, the data of the latest 30 points (after 30 minutes) were averaged. The fluctuation of the averaged data was reduced to about 1/3 of the raw data's one. This averaging treatment lowers the weight of the latest point even in the case of anomaly, which means that there is a kind of delay lowering the detection timeliness. However this delay doesn't affect the effectiveness of the diagnosis system very much because the change of the extraction profile in the mixer-settler bank is rather slow. The indication of all neutron monitors were averaged with this method. Suitable trigger levels for different neutron monitors under a certain equilibrium condition were given based on the maximun range of the fluctuation of the averaged data. The trigger level is defined as follows.

$$N \pm R \quad \text{(cpm)}$$

N ;Standard value

R ;1/2 of the maximum width of the fluctuation of the 30 point average.

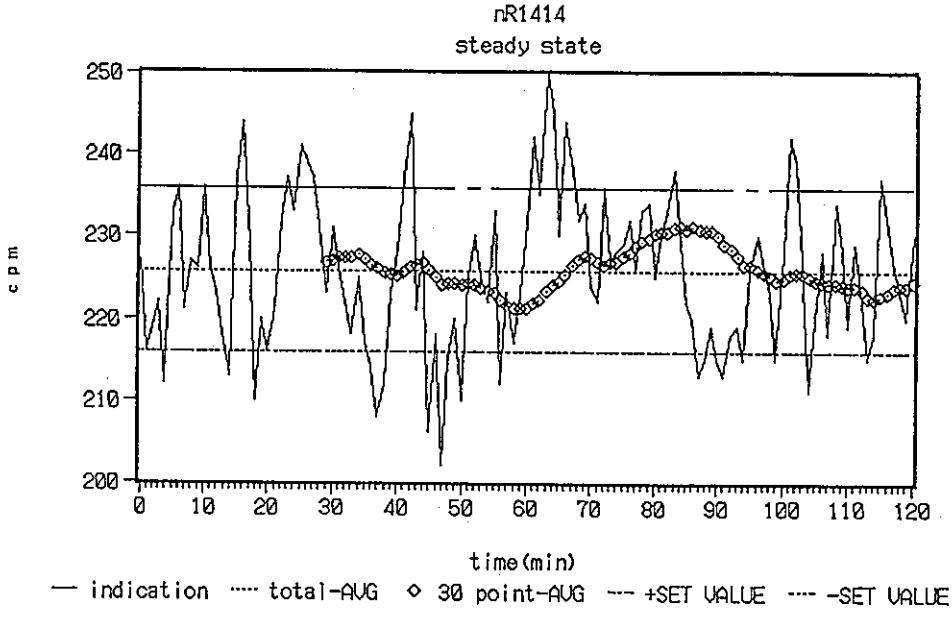

Fig.3 The typical example of the actual record of neutron monitor under steady operation conditon.

The fluctuation of the density meter to indicate U concentration was revealed to be as low as 0.01 (g/cm³) in the actual record, therefor the trigger level was defined as follows.

$M \pm 0.01$ (g/cm³)

M ;Standard value

Principle of the Table-treatment

Fig.4 shows an example of the reference data table of in-line monitor's appearance. This example includes 5 typical anomalous cases. Each in-line monitor is marked when its indication crosses over its own trigger level (mark-on time). And the dynamic change of the extraction profile of Pu, U and nitric acid can be distinguished by the pattern of marking of in-line monitors. Because different anomalous events will cause different characteristics in the pattern of marking both in terms of time and the stages, it is possible to distinguish the cause of the anomaly when a typical marked pattern appears.

The time when the first mark appears is defined as the standard time (00:00). At the early stage after the standard time, there is a case when different causes achieve same pattern, however the pattern will become unique as time proceeds.

Characteristic marking patterns of in-line monitors for the various causes of anomalous conditions were examined by simulation calculation to get a reference data table. A pattern actually appears on in-line monitors is referred to this data table and the cause of the anomaly is identified. 0.5h was chosen as an unit time in this data table. This means, the comparison between actual pattern and data base will be done at every 0.5h after the first appearance of anomaly.

Examination of the detection time

Fig. 4 is usable only for code-calculation result in which the indication change smoothly proceeds without any uncertainty. However, actual in-line monitors indication still have a long-period fluctuation and a noise component even after the averaging treatment. This fluctuation gives some uncertainty to the mark-on time of monitors.

No.	Events	Variation of concentration at each bank																		
		U by density meter				Pu by neutron monitor														
		1412	1414	1415	1505	1408	1412	1414	1415	1417	1421	1501	1502	1503	1504	1505	1506	1507	1508	1509
1	decrease of H+ conc. in scrub									14.0 ↑ 12.0	3.0 ↑ 1.0						2.0 ↓ T	>20 ↓ >18	>20 ↓ >18	17.5 ↓ 15.5
2	increase of feed rate					0.5 ↑ T	0.5 ↑ T	0.5 ↑ T	1.0 ↑ 0.5	2.0 ↑ 1.5	4.0 ↑ 3.5	6.0 ↑ 5.5	5.5 ↑ 5.0	5.0 ↑ 4.5	3.5 ↑ 3.0	5.5 ↑ 5.0	3.5 ↓ 3.0	>20 ↓ >19.	16.0 ↓ 15.5	12.0 ↓ 11.5
3	decrease of U(IV) conc.																1.0 ↑ T	2.5 ↑ 1.5	18.0 ↑ 17.0	18.5 ↑ 17.5
4	decrease of H+ conc. in strip																7.0 ↓ T	>20 ↓ >13	20.0 ↓ 13.0	15.0 ↓ 8.0
5	decrease of solvent feed rate		1.0 ↑ 0.5	2.0 ↑ 1.5	4.5 ↑ 4.0	0.5 ↑ T	0.5 ↑ T	0.5 ↑ T	1.0 ↑ 0.5	2.5 ↑ 2.0	2.0 ↓ 1.5		>20 ↓ >19.	>20 ↓ >19.		0.5 ↓ T	0.5 ↓ T	1.5 ↓ 1.0	0.5 ↓ T	9.0 ↓ 8.5

: can be detected at 1 hour later from the first appearance

↑ , ↓ : Upward and Downward deviation from standard with the time after the occurrence (Top) and the first appearance. (Bottom)

U ; M±0.01 (M=Standard density (g/cm³))

Pu ; N±R (N=Standard count rate (cpm), R=(max.count rate)-(min.count rate))

Fig.4 An example of the reference data table of in-line monitor's appearance.

Fig.5 shows an example of a simulated indication change which was obtained by adding the observed fluctuation onto the transient result by MIXSET. In this figure, the 30 points average crosses the lower detection limit earlier than the mathematical line because of the under-directing fluctuation. This means that

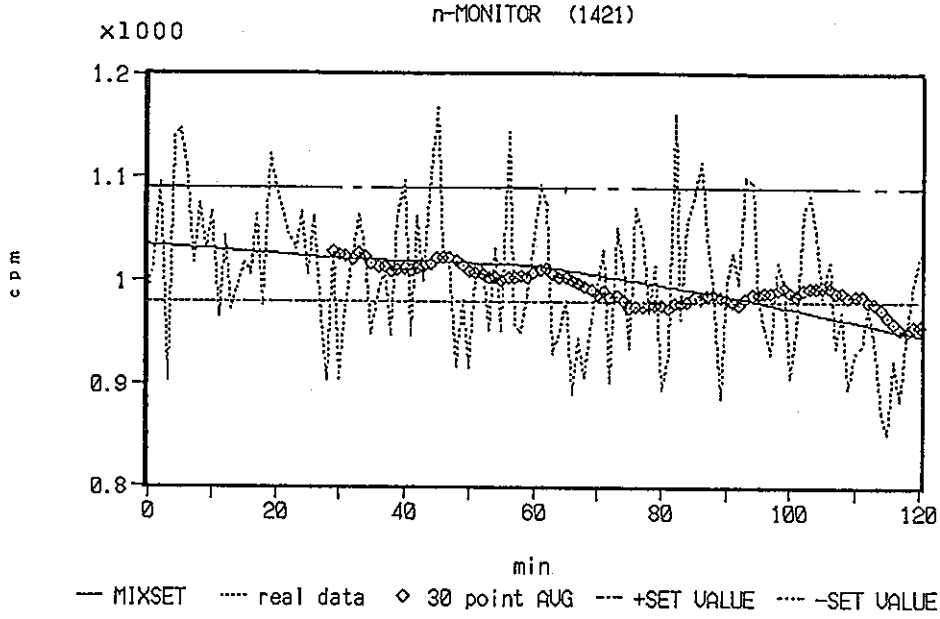

Fig.5 An example of a simulated anomalous case including the actual fluctuation of a neutron monitor.

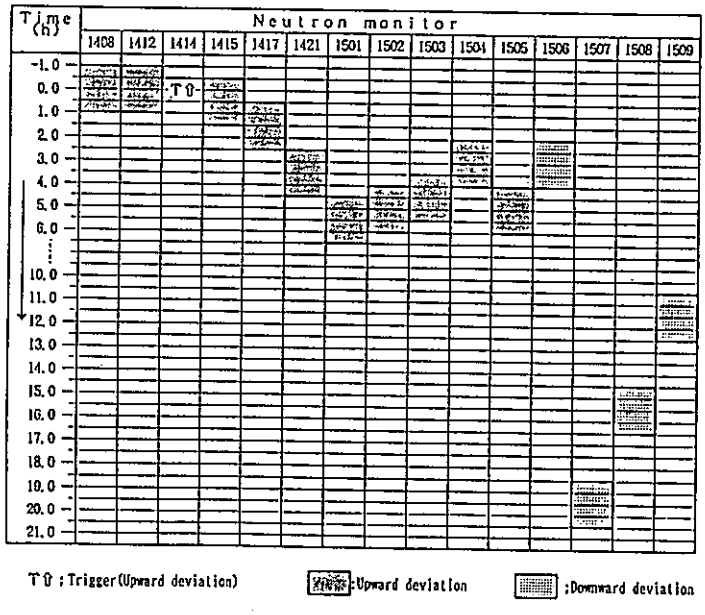

Fig.6 An example of the new reference data table having a range in the mark-on time.

there should be a possible range in the mark-on time for every monitor and case. Therefore, we concluded that the reference data base table as was shown in Fig.4 has to have an time range in the mark-on time. It was revealed that the difference of the time caused by the remaining fluctuation is as long as ±30 minutes in every case. The standard time(zero time) itself may change its time with the same time range making other monitor's time range be± 1h of the mathematical results.

Fig.6 gives an example of the new reference data table having a range in the mark-on time. Under actual operation, computer has to see the marking pattern of the neutron monitors with this time range taken into its consideration. This requires additional time to identify different patterns, however the slow change of the extraction status in the mixer-settler enables the use of this method with good reliability.

Conclusion

The fluctuation of neutron monitor was evaluated with actual process data of the TRP, and a method of signal treatment was examined. As a result, it was confirmed that the cause of the anomaly can be identified well with the actual neutron monitor's signal.

Reference

1) Hiroki IWABUCHI, Kei SASAKI, Kenji KOYAMA and Hajimu YAMANA, "Conceptual study for a computer-aided extraction-status diagnostic system for the Pu-U partition cycle of the Tokai Reprocessing Plant", Proceedings of the International Solvent Extraction Conference 1990 (ISEC'90), Kyoto Japan (1990)

題　　名	Remote Inspection of Repaired Dissolvers and Improvements of the Remote Maintenance Robots		
発表先	RECOD'91		
発表地	仙　　台	発　表 年月日	平成3年　4月14日 ～ 4月18日
発表者 (○印口頭発表者)	所　属　名	再処理　技術課	
	○内藤　誠也，住谷　昭洋，大高甲子男，古川　博章， 立原　富夫，岡本　弘信		

(要　旨)

動燃東海再処理工場の濃縮ウラン溶解槽は，1982年に漏洩を発生したため，加熱部分に存在する溶接部等に対し，遠隔補修を実施した。その後，約2000時間の溶解を行い，各種の遠隔検査を実施した。また，定期的な検査や予防保全に対応させるため遠隔検査・補修装置の高機能化開発を実施した。本報告では，遠隔補修後の遠隔検査の結果及び装置の開発について述べる。

資料番号

TN8410　91－021

(80－02－249)

資料番号 TN8410 91-021

Remote inspection of repaired Dissolvers and Improvements of the remote maintenance robots.

Seiya NAITO, Akihiro SUMIYA, Kashio OHTAKA,
Hiroaki FURUKAWA, Tomio TACHIHARA, Hironobu OKAMOTO
Power Reactor and Nuclear Fuel Development Corporation
4-33 Muramatu , Tokai-mura
Naka-gun , Ibaraki-ken , 319-11 , Japan
Telephone : 0292-82-1111 , Telefax : 0292-82-9382

ABSTRACT
Remote inspections of dissolver welds after 2,000 hrs of actual dissolution of nuclear spent fuels were performed using robots. Accelerated corrosion tests under simulated dissolver conditions were also performed to collect fundamental data on the corrosion behavior of the dissolver. The results of the accelerated corrosion tests were compared with that of the above remote inspections. These tests provided information for improvements in the mechanical structure and maintenance capabilities of the robots.

INTRODUCTION

Two dissolvers of the PNC Tokai Reprocessing Plant leaked in 1982 due to the pinhole corrosion at or near the heated sections of welded part. Remote repair of weld lines of dissolver barrels using remote maintenance robots was attempted. In order to evaluate this remote repair technology, remote inspections such as the surface observation for the repaired weld zone were performed after actual dissolution of the spent fuels. Accelerated corrosion tests were also performed to investigate the corrosion behavior of the dissolver. The remote maintenance robots were prototype models for the remote repair and inspection, and some improvements were identified which included improved handling and performance capabilities and reduction in space required for storage of the robots in a small hot cell made on the robots. That were to simplify the handlings of the robots, to reduce the space for handlings and storage in the small hot cell.

ACCELERATED CORROSION TEST

The test piece is shown in Fig.1. The materials of the all parts of the test piece were the same as that of the repaired dissolvers. The material of the base part of the test piece was URANAS 65. The test piece was made of three base parts that were attached to each other by butt welds using the welding rods of SOUDINOX 65. After the butt welds on the test piece, a ditch was made around each weld line to simulate the corroded weld line of the dissolver. Then a welding overlay using the welding rods of WEL MIG SW310 was performed over the weld lines including the ditch in the same way of welding the actual dissolver. The apparatus of the accelerated corrosion tests is shown in Fig.2. This apparatus is composed of the electric heater, thermocouples, condenser, and water trap. The test pieces were covered with heat insulator and heated by an electric heater. The temperature of the solution

and test pieces were measured by the thermocouples. In order to accelerate the corrosion the solution contained 14 mol/l HNO_3 and 10^{-3} mol/l $(Ru^{3+})_6$. The temperature was kept about 120 ℃ in the solution (boiling point) and about 140 ℃ outside the test piece. The solution was changed every 100 hrs and its heating continued for a total of 1,200 hrs.

ACCELERATED CORROSION TEST RESULTS

The surface appearance of the test piece after the accelerated corrosion test is shown in Photo.1. The base part of the test piece was attacked uniformly. The butt weld was gradually attacked around the dendrites and showed the needleshaped corrosion in which the dendrites dropped off from the surface. The ripple lines of the weld overlay gradually disappeared. The edges and the overlapped parts of the weld overlay were especially attacked. From 100 hrs to 200 hrs, the structure of the dendrite began to be seen and the ripple lines were seen clearly. From 300 hrs to 500 hrs, the structure of the dendrite was seen clearly and the ripple lines disappeared. After 1,200 hrs, the structure of the dendrite was seen like needles and the width of the weld overlay was decreased but sealing of the ditch by the weld overlay was still intact. These observations on the test pieces are shown in Table.1.

REMOTE INSPECTION

The operation mode of the dissolver is shown in Fig.3. The sheared spent fuel was put into the dissolver with 550 l of pure water. Then 1,000 mols of HNO_3 is added. When the temperature reached the boiling point, 5,000 mols of HNO_3 was added. Dissolution ended after several hours when heating was stopped. After this batchwise dissolution was repeated up to a total of 2,000 hrs, remote inspections of the repaired dissolver were performed. The general view of the remote inspection is shown in Fig.4. The surface observation robot has a viewing head and lifting device. The lifting device can move the viewing head inside the dissolver barrel. The viewing head is composed of the mirror, lamp, centering device, and a motor for turning the mirror. The mirror reflects the surface appearance of the dissolver to the periscope installed in the cell wall over the dissolver.

REMOTE INSPECTION RESULTS

One of the surface observation results is shown in Photo.2. It is the weld overlay that was made in 1983. Its outside was covered with the heating jacket. The ground surface did not glitter and has begun to lose its grains. Part of the weld overlay was attacked around the dendrites and the structure of the dendrite was seen slightly. A decrease of the width of the weld overlay was not seen. Comparison of the results of the remote inspection and that of the accelerated corrosion test indicates that the first stage of corrosion has occurred but the seal has been kept intact. These results are shown in Table.2. From other results of the remote inspections such as ultrasonic and leak tests, no special abnormality was recognized.

REMOTE MAINTENANCE FLOW

The remote maintenance flow and the robot functions are shown in Fig.5. The grinding using the grinding robot with the periscope is the surface treatment for the repair part before the weld overlay is made. The ground surface is observed using the surface observation robot and the periscope after grinding. Then the weld overlay using the welding robot is performed on the butt weld line and the electron beam weld line including the points where leakage had occurred. Then the surface observation, dye penetration test, ultrasonic test, and leak test were performed in sequence using each robot. The leak test is to observe the bubbles from the leak points when applying air pressure to the heating jacket of the dissolver filled with the water.

IMPROVEMENTS OF THE ROBOTS

All of the robots have been developed to be prototypes for use inside the small hot cell. The movements of the robots are complicated and the time required for remote maintenance is long. Also the cost of renovation of these robots is enormous. To solve these problems, the multi-use type robot was developed with improvements which expanded the capability of the robots. The general view of the multi-use type robot is shown in Fig.6. The multi-use type robot consists of the multipurpose lifting device and 7 heads. Each head has a function such as grinding, welding, surface observation etc. Each head can be connected remotely to the multipurpose lifting device by the remote connector. The electric connector, water coupler and air coupler are installed into the remote connector. The operation of the remote connector to join or detach the multipurpose lifting device with a head can be done by a manipulator and the in-cell crane. The multipurpose lifting device includes the spiral shaped cable which is for common use to supply all utilities to each head.

EVALUATION TEST OF THE LIFTING DEVICE

Prior to fabrication, the evaluation tests of the lifting device were performed for noise and remote operational functions. If electronic noise is generated in the remote connector, the spiral shaped cable of the lifting device by the electric current of the power source of the welder or the motor, it influences the TV and the ultrasonic testing signals. The experimental multipurpose lifting device including the remote connector and the spiral shaped cable was fabricated and tested. Also the experimental head including the motor and the ultrasonic probe was also fabricated and connected to the TV camera and the welding torch. The general view of the test of the influence of the noise on the ultrasonic testing signals is shown in Fig.7. The TV camera and the welding torch were also connected with the experimental head to determine the effect of the welder on the TV signal. The controllers for these apparatuses were joined with the experimental lifting device by the cables whose length are the same as that of the real robot system. The noise was investigated when the spiral shaped cable was expanded, drawn and half expanded. When the motor was rotating, the influence of the noise on the ultrasonic testing signals was very slight and the influence of welding on the TV was also very slight. The test of the remote operational function of the remote connector was performed using the crane and the manipulator. The results indicated that the experimental head could be joined and detached to the experimental multipurpose lifting device remotely.

ASSEMBLY OF THE ROBOT

The functions of the robots cannot be maintained remotely. And the direct maintenance of the robot results in large difficulties mentioned above and the high cost of the maintaining individual robots for desired function, we developed a single robot with different heads for each function. These heads can be easily changed by a manipulator and the in-cell crane. This system also improves the in-cell storage problem for the robot. Improvements were also made in the operation and replacement procedures for assembly heads including procedures for replacement of parts within each assembly head such as the mirror, lamp, ultrasonic testing probe, strainer, and motor for the lifting device.

EXPANSION OF THE CAPABILITY

The scope of the remote repair and inspection of the robots is restricted to the large diameter(ϕ270 mm) portion of the dissolver barrel. In order to expand the use of the scope into the small diameter (ϕ220 mm) portion of the dissolver barrel, evaluation tests of the experimental miniaturized heads were

performed. These heads were the surface observation head, grinding head, welding head, dye penetration testing head and washing head. The washing head can wash the inside surface of the dissolver barrel with a water jet and then pump the water out to a drain. The functional and operational conditions of these heads were evaluated when used in the small or large diameter portions of the dissolver barrel. From the results of this preliminary evaluation, these heads require some changes for practical use as follows.
(1)The surface observation head;
The installation angle of the lamp and the lamp reflector.
(2)The grinding head;
The stroke of the grindstone.
(3)The welding head;
The stroke of the torch and the heat quantity.
(4)The dye penetration testing head;
The installation angle of the nozzles which spray the dye penetration testing liquids.

CONCLUSION

The corrosion rate of the repaired weld zone of the barrels was negligible even after 2,000 hrs actual dissolution of the spent fuels. The sealing by the weld overlay has been kept intact after 2,000 hrs of actual dissolution of the spent fuels. Improvements such as the provision of modular assembly heads for the robots were expected to improve the remote maintenance, to reduce the personnel exposure in the case of direct maintenance of the robots, and to reduce the overall cost of the system.

REFERENCES

1. K. MATSUMOTO, S. OHMACHI, T. YAMANOUCHI, "Decadal operational experience of the TOKAI reprocessing plant", Proc. of 3rd Int. Conf. on Nuclear Fuel Reprocessing and Waste Management, (RECOD'87), Vol.1, 195 - 202, Paris, (1987).

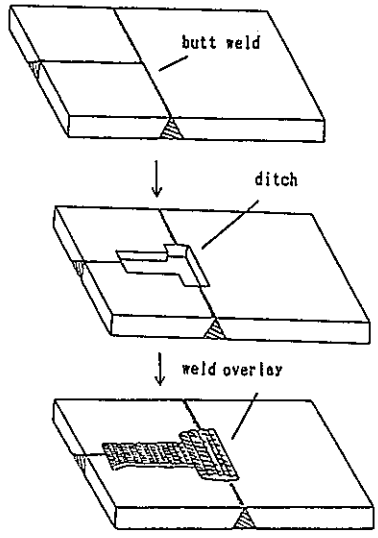

Fig.1 Test piece for accelerated corrosion test

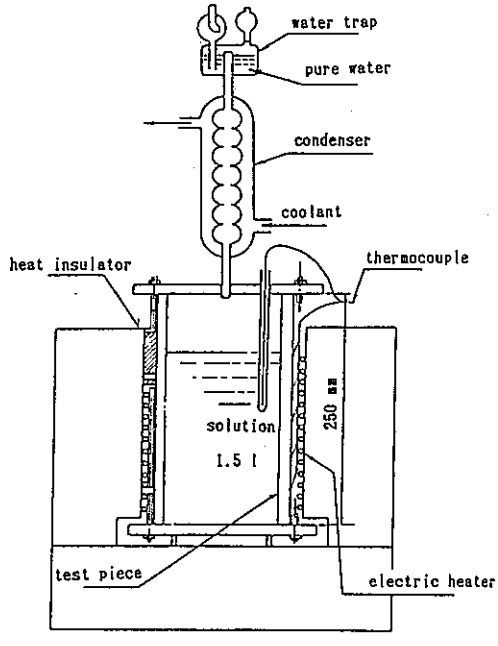

Fig.2 Apparatus for accelerated corrosion test

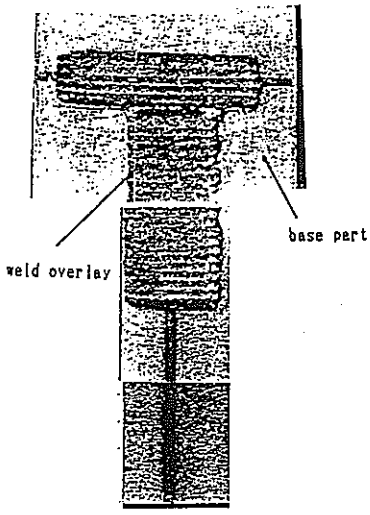

Photo.1 Test piece after accelerated corrosion test

Table 1 Accelerated corrosion flow

	1st step	2nd step	3rd step
appearance peculiarity	dendrites begin to be seen ripple lines are seen (100~200hrs)	dendrites are seen clearly ripple lines disappeared (300~500hrs)	dendrites are seen like needles decrease of the width (1,200hrs)

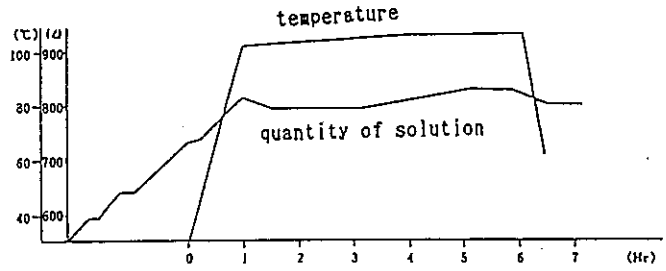

Fig.3 Operation mode of the dissolver

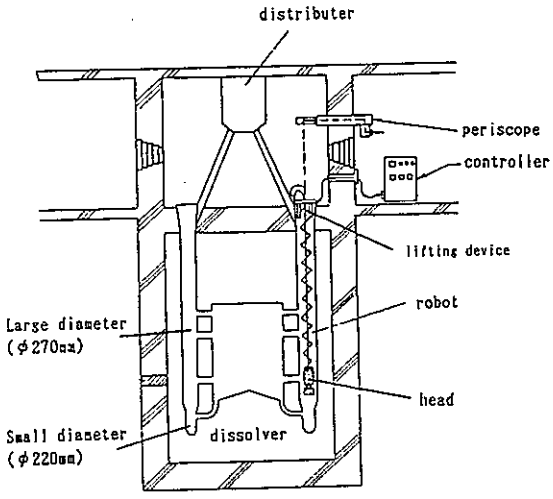

Fig.4 General view of the remote inspection

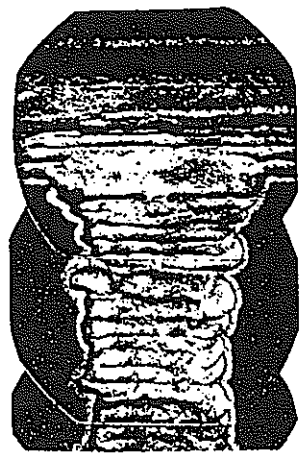

Photo.2 Inner surface appearance of the dissolver

Table 2 Results of the remote inspection and accelerated corrosion test

appearance peculiarity	glittter	obscured	dendrites are seen	ripple lines disappeared	reduction of width
corrosion test (hr)		100	200	500	1,200
actual dissolver operation (hr)		2,000			

grinding	periscope, grinding robot
↓	
surface observation	periscope, surface observation robot
↓	
overlaid weld	welding robot
↓	
surface observation	periscope, surface observation robot
↓	
dye penetration test	periscope, dye penetration testing robot
↓	
leak test	TV robot
↓	
ultrasonic test	ultrasonic testing robot

Fig.5 Remote maintenance flow and functional robots

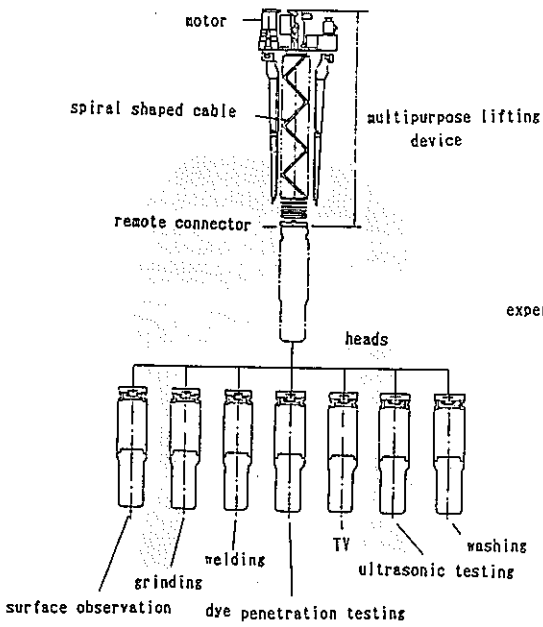

Fig.6 General view of the multi-use type robot

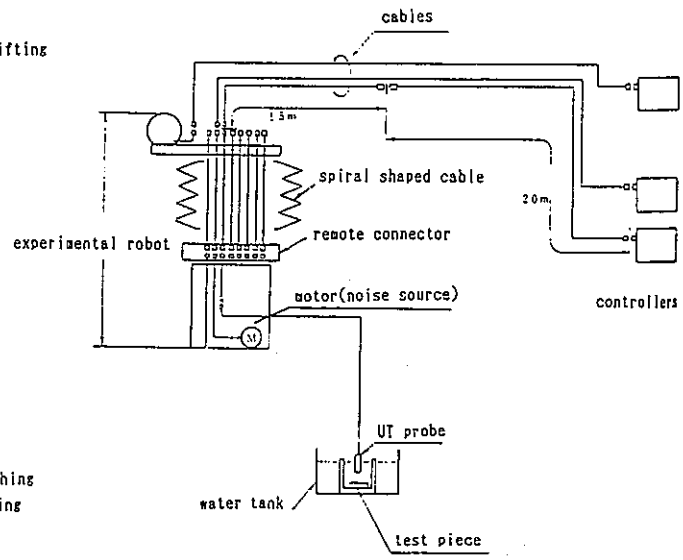

Fig.7 General view of the evaluation test

題　　名	Development of Highly Reliable Air Purge and Declogging System at the TOKAI Reprocessing Plant		
発表先	RECOD'91		
発表地	仙　　台	発　表 年月日	平成3年　4月14日 ～ 4月18日
発表者 (○印口頭発表者)	所　属　名	再処理　技術課	
	○田中　伸幸，福有　義裕，立原　富夫，岡本　弘信		

(要　旨)

再処理工場の放射性流体の物理量は，エアーパージ測定システムによって測定している。本システムは，放射性流体にパージ管を挿入するだけで，検出部には，可動部を全く持たないため，原子力関係施設では，幅広く採用されている。しかしながら，本システムは，パージ管先端に溶液からの塩の析出，蓄積が原因で，頻繁にパージ管から出るパージエアーを詰まらせ，液位・密度といった物理量の測定を異常にする。そのため，詰まり除去のための保全作業は膨大な量になり，詰まりを除去する際，パージ管を開放状態にするため，汚染の恐れもある。以上の問題点を解決するため，導圧管の詰まりを計測系に異常を来す前に検知し，パージ管を開放状態にすることなく除去する装置を開発したので報告する。

資　料　番　号
TN8410　91－022 (80－02－250)

資料番号 TN8410 91-022

DEVELOPMENT OF HIGHLY RELIABLE AIR PURGE AND DECLOGGING SYSTEM AT THE TOKAI REPROCESSING PLANT

N.TANAKA, Y.FUKUARI, T.TACHIHARA, H.OKAMOTO
Power Reactor and Nuclear Fuel Development Corporation(PNC)
Ibaraki, Japan

1.ABSTRACT

In the Tokai Reprocessing Plant the process parameters such as level, density, flow rate and pressure of radioactive fluid are measured mostly by the air purge measurement system. This system is used extensively in the nuclear industry,because only the dip-tube is installed in the radioactive fluid vessel, and the detector itself has no moving part, so that it is maintenance free in the hot cell. Also, this system is very important for the nuclear material control and the process operations.

However, it is well known that the end part of the dip-tube is often clogged by the salt accumulated from the process solution in the Purex-process. The clogging of the dip-tube end makes the process parameters measurement abnormal, so that the process operations may be influenced. Therefore, much maintenance work is routinely required for removing the clog in order to have reliable measurement data.

Furthermore, when the operator remove the clog by blowing air through the dip-tube, there is a possibility of an inverse air flow in case of operational error at the instrumentation maintenance area, resulting in contamination of that area.

We invented a method for detecting the clogging of the dip-tube end before the measurement data are abnormal. We also developed an automatic declogging system without any inverse air flow from the in-vessel atmosphere to the instrumentation maintenance area.

This development provides a reduction in a maintenance manpower,reduces the risk of radioactive contamination and to increase measurement reliability.

2.INTRODUCTION

Clogging of the dip-tube in the air purge measurement system can be monitored by monitoring the number of bubbles purged from the dip-tube in any time period this suggests that monitoring of the bubbling frequency could be used to determine, the degree of clogging and thus provide information to prevent abnormal process parameter measurements.

The present paper deals with the method of detecting the clogging before measurement data are abnormal.

3.CLOGGING OF THE DIP-TUBE

Back pressure in the dip-tube begins to increase when a hole diameter of the clogging salt is about 2mm,after that, the back pressure increase rate becomes larger and larger, and at last it exceeds the full range of the transmitter. The typical clogging of the dip-tube is shown in Photo 1.

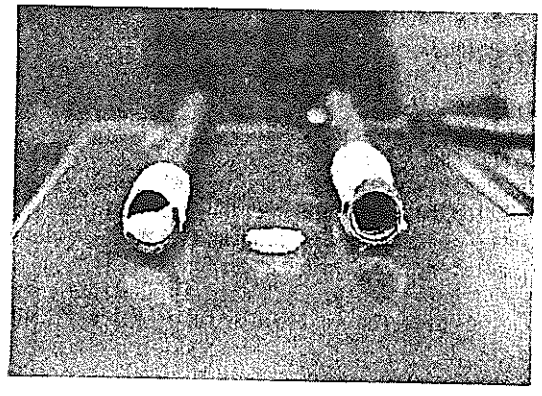

Photo 1 TYPICAL CLOGGING OF THE DIP-TUBE

When the long tube shown in Fig.1 is clogged, the back pressure(P_1) increases. It increases the level data (P_1-P_0/ρ) and the density data($(P_1-P_2)/h$). After this the signals of both transmitters 1 and 2 increase respectively. Thus this clogging makes measurement data abnormal and may interfere with the nuclear material control and the process operations.

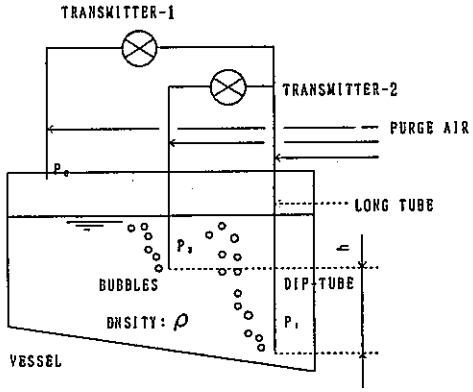

Fig.1 AIR PURGE MEASUREMENT SYSTEM

4.METHOD OF DETECTING THE CLOGGING

The output signal from the pressure sensor is the direct current voltage which corresponds to the liquid level in the vessel. And the signal overlaps the alternating current signal by the bubbles purged from the dip-tube in a certain period. The inner diameter of the dip-tube decreases in case of clogging, the charged bubbles become small and the number of bubbles purged from the dip-tube in a certain period, i.e.bubbling frequency, is changed. The pressure fluctuation due to bubbling and the power spectrum without clogging are shown in Fig.2 and Fig.3. The pressure fluctuation due to bubbling and the power spectrum with clogging are shown in Fig.4 and Fig.5.

The relation between the bubbling frequency H and the inner diameter R at the end part of the dip-tube is shown in Equation 1. The relation between the amplitude ΔL of the wave of the back pressure fluctuation and the inner diameter R is shown in Equation 2.

Also,the measurement data is abnormal when a hole diameter in the dip-tube is less than 2 mm.

Therefore, we can detect the clogging by monitoring the bubbling frequency and the amplitude.

$$H=\frac{F}{\frac{(4/3)\pi(R\cdot\cos45^\circ)^2\cdot(r+(r^2+2\rho g(1.641R\cdot\cos45^\circ)^2/r)^{0.5}}{1.641\rho gR\cdot\cos45^\circ}} \quad \cdots\cdots(1)$$

$$\Delta L=\frac{(r+(r^2+2\rho g(1.641R\cdot\cos45^\circ)^2/r))^{0.5}\cdot1.707}{1.641\rho gR\cdot\cos45^\circ}+\frac{0.20394r}{R\cos45^\circ} \quad \cdots\cdots(2)$$

, where
- H: Bubbling frequency (Hz)
- ΔL: Amplitude (mmH_2O)
- F: Purge air flow rate (m^3/s)
- R: Inner diameter of the dip-tube (m)
- r: Surface tension (N/m)
- ρ: Density (kg/m^3)
- g: Gravity acceleration (m/s^2)

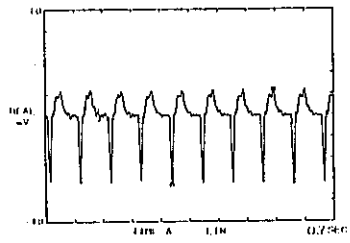

Fig.2 PRESSURE FLUCTUATION DUE TO BUBBLING WITHOUT CLOGGING

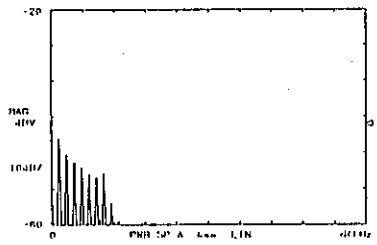

Fig.3 POWER SPECTRUM WITHOUT CLOGGING

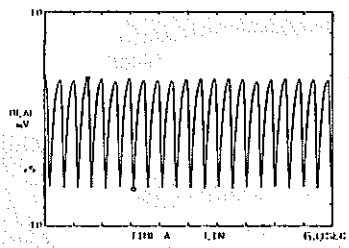

Fig.4 PRESSURE FLUCTUATION DUE TO BUBLLING WITH CLOGGING

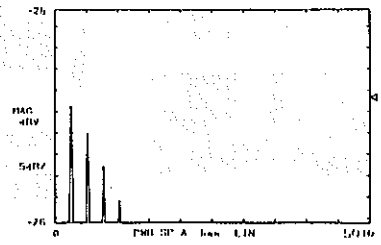

Fig.5 POWER SPECTRUM WITH CLOGGING

6.EXPERIMENT

The diagram of a highly reliable air purge and declogging system is shown in Fig. 6. Such components as differential pressure transmitters, constant-flow-rate regulators, valves, copper tubes and so on are mounted on racks and connected with each other using tube fittings. The experimental vessels are shown in Photo 2 and the computer unit and transmitter rack are shown in Photo 3. The air way diverges from the upper point, goes through the selector device, then to the pressure sensor. The electric signal of the pressure sensor is sent to the computer unit. The declogging system is installed between the dip-tube and the transmitter. This system is controlled with instrumentation pressurized air and the electric signal from the computer unit.

The system works as follows, at first, the selector device selects the measurement loop which detects the bubbling frequency and the amplitude. Next the pressure sensor detects the wave of the bubbling. And the computer unit calculates the bubbling frequency and the amplitude from this wave. The computer unit then judges whether the end part of the dip-tube is clogged by the above-mentioned method. When clogging of the end part of the dip-tube is detected, the computer orders the clog to be blown out by an electric signal without any inverse air flow from the in-vessel atmosphere to the instrumentation maintenance area.

We measured the bubbling frequency and the amplitude when the inner diameter of the dip-tube decreased by clogging from the salt accumulated from the cold test solution.

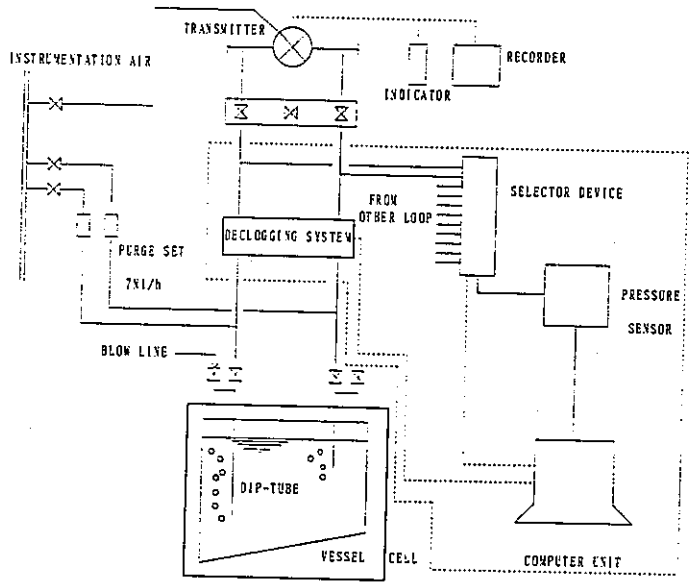

Fig.6 HIGHLY RELIABLE AIR PURGE AND DECLOGGING SYSTEM

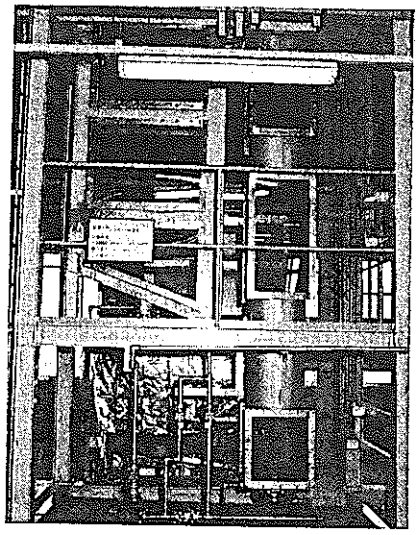

Photo 2 EXPERIMENTAL VESSEL

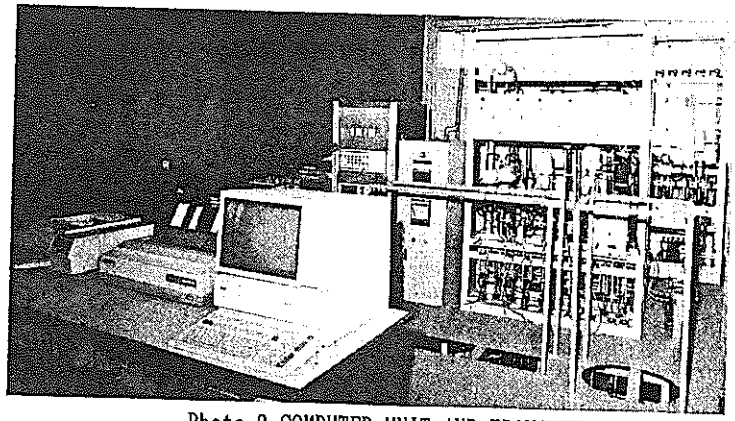

Photo 3 COMPUTER UNIT AND TRANSMITTER RACK

6. RESULTS

The relation between the bubbling frequency and the innner diameter of the end part of the dip-tube is shown in Fig.7 (initial condition, air purge flow rate:7Nl/h, inner diameter: 15mm). The bubbling frequency increases as a hole diameter in the dip-tube decreases from salt clogging. The bubbling frequency is 1.5Hz at the inner diameter of 15mm, after that the bubbling frequency becomes larger and larger, and at last, it gets to 4Hz at the inner diameter of 4.5mm. Then the bubbling frequency decreases, and at last it gets to 2.3 Hz at the inner diameter of 1mm.

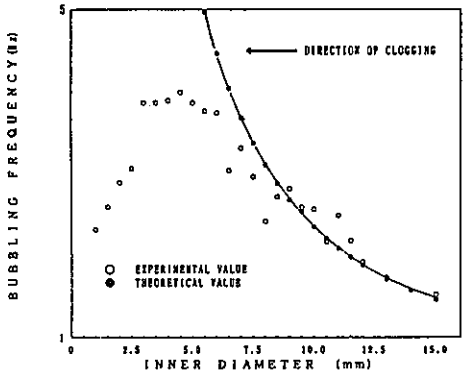

Fig.7 RELATION BETWEEN THE BUBBLING FREQUENCY AND INNER DIAMETER DUE TO CLOGGING

The relation between the amplitude and the inner diameter is shown in Fig.8 (initial condition, air purge flow rate: 7Nl/h, inner diameter: 15mm). The amplitude begins to increase when the hole diameter in the dip-tube about 4 mm, after that the amplitude increase rate becomes larger and larger, and at last, it gets to 4.3mmH_2O at the inner diameter of 2mm (4mmH_2O at 15mm).

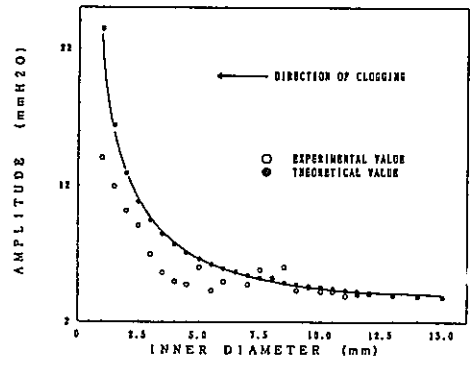

Fig.8 RELATION BETWEEN THE AMPLITUDE AND THE INNER DIAMETER DUE TO CLOGGING

The relation between the back pressure and the decreasing diameter of the end part of the dip-tube is shown in Fig.9. The back pressure in the dip-tube, i.e. measurement data, begins to increase when a hole diameter in the clogging salt is about 2mm.

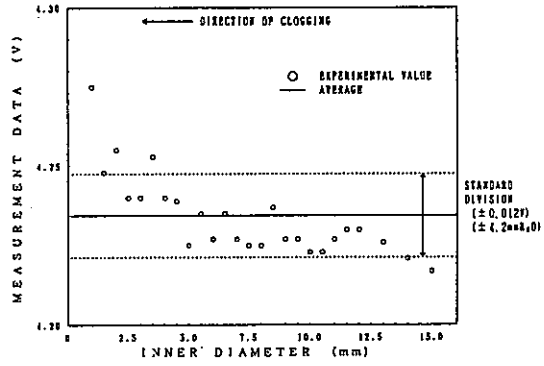

Fig.9 RELATION BETWEEN THE MEASUREMENT DATA AND THE INNER DIAMETER DUE TO CLOGGING

Also, the relation between the magnitude of the power spectrum and the inner diameter of the end part of the dip-tube is shown in Fig.10. The magnitude increases as the hole diameter in the dip-tube decreases. In other words the bubbles purged from the dip-tube are more and more certain as the clogging occurs.

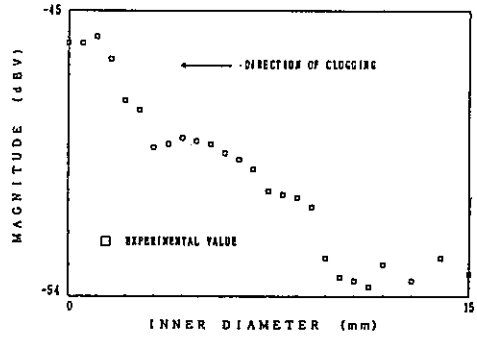

Fig.10 RELATION BETWEEN THE MAGNITUDE AND THE INNER DIAMETER DUE TO CLOGGING

The number of discharged bubbles at regular conditions is shown in Fig.11 and at 1mm of inner diameter is shown in Fig.12. Many bubbles are purged from the dip-tube in a given period at inner diameters greater than 4mm and a lot of little bubbles are purged from the dip-tube in a longer period at less than 4mm of inner

diameter. In other words, the bubbling frequency increases as the inner diameter decreases from 15mm to 4mm, after that, the bubbling frequency decreases. Also, the amplitude is constant when the inner diameter decreases from 15mm to 4mm, after that, the amplitude increases.

This indicates the method of detecting the clogging by monitoring the bubbling frequency and the amplitude is very effective.

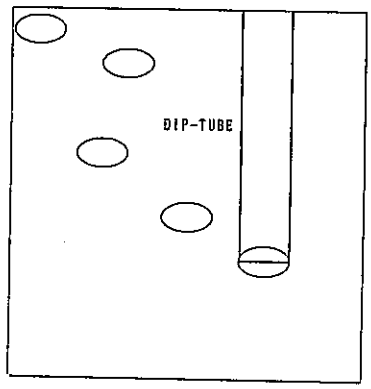

Fig.11 DISCHARGED BUBBLES SITUATION
INNER DIAMETER: 4～15mm

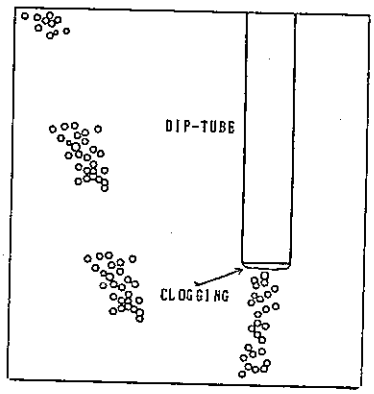

Fig.12 DISCHARGED BUBBLES SITUATION
INNER DIAMETER: ≤4mm

7. CONCLUSION

This system allows us to detect the clogging of the dip-tube before it makes the process parameters measurement abnormal and to do declogging automatically without any inverse air flow from the in-vessel atmosphere to the instrumentation maintenance area. The air purge measurement system is better for nuclear material control and process operations. The air purge measurement system may also have some leakage, the number of bubbles purged from the dip-tube in a certain period, i.e. bubbling frequency, is changed. We can detect the leakage in the air purge measurement system by monitoring the bubbling frequency.

8. REFERENCES

1) Y. TANAKA, T. TARUMI, K. WAKIMOTO:
PC Statistics Analysis Hand Book, Kyouritsu-shuppan, (1984).
2) Y. MIYAI: Water Dynamics, Morikita-shuppan, (1983).
3) T. IMAI, M. HIRAYAMA: "Development of the Method of Preventing the Dip-Tube Clogging" Proc. of 1984 Spring Meeting of Atomic Energy Society of Japan, G13, (1984).
4) Japan Machine Sc.:
Industry Measurement Hand Book, P684, Oomu-Sha, (1984).

9. APPENDIX

Derivation of the Equation of the relation between the bubbling frequency and the inner diameter and the relation between the amplitude and the inner diameter. 1) 2) 3) 4)

1)Bubbling Frequency-Inner Diameter

The bubble's form under the plate is shown in Equation 1

$$r=(1/2)\rho g h^2(1.641R/(1.641R+h)) \cdots\cdots (1)$$

$$\therefore h=(r+(r^2+2\rho g(1.641R)^2 r)^{\frac{1}{2}})/\rho g(1.641R) \cdots\cdots (1')$$

,where r: Surface tension (N/m)
ρ: Density (kg/m^3)
g: Gravity acceleration (m/s^2)
R: Max. radius (m)
h: Hight of the bubble (m)

(Assumption 1)
When the max.radius equal the outer radius of the dip-tube, the bubble discharges from the end part of the dip-tube. But the max. radius is shown in Equation 3 because the outer diameter is much larger than the inner diameter.

$$R=d_{out}/2 \cdots\cdots (2)$$

$$R=d_{in} \cdot \cos 45^\circ \quad (d_{out} >> d_{in}) \cdots\cdots (3)$$

,where d_{out} : Outer diameter (m)
d_{in} : Inner diameter (m)

(Assumption 2) The form of the bubble is oval.

(Assumption 3) The bubble contacts with the inside of the dip-tube.

Cross section of the oval is shown in Equation 4

$$(x/R)^2 + (y/h)^2 = 1 \cdots\cdots (4)$$

$$x=b=d(in)/2 \cdots\cdots (5) \rightarrow \text{Equation 4}$$

$$y(=a)=h(1-(b/R)^2)^{\frac{1}{2}} \cdots\cdots (6)$$

Volume (V(m^3))of the oval is shown in Equation 7

$$V=(4/3)\pi R^2 h \cdots\cdots (7)$$

After all, the bubbling frequency is shown in Equation 8

$$H=F/V \cdots\cdots (8)$$

,where F: Purge air flow rate (m^3/s)

2)Amplitude-Inner Diameter

The distance (c(m))from the end of the dip-tube to the top of the bubble is shown in Equation 9.

$$c=a+h \cdots\cdots (9)$$

The relation between the inside pressure and the surface tension is shown in Equation 10.

$$\Delta p=2r/R \cdots\cdots (10)$$

,where
Δp: (Inside pressure)-(outside pressure) (N/m^2)

After all, the amplitude is shown in Equation 11.

$$\Delta L=c+\Delta p \cdots\cdots (11)$$

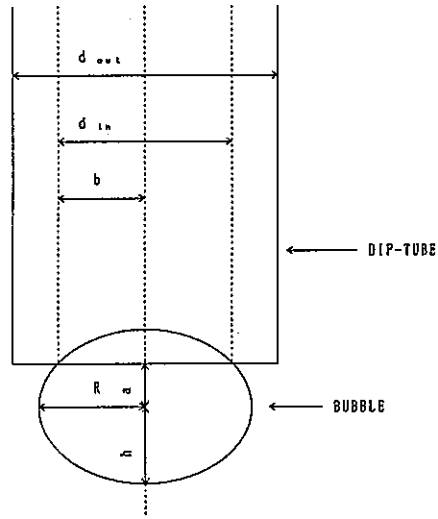

Fig.13 CHARGED BUBBLE FROM THE DIP-TUBE

題　　名	Radiation Control System at TOKAI Reprocessing Plant		
発表先	RECOD'91		
発表地	仙　　台	発　表 年月日	平成3年　4月14日 ～ 4月18日
発表者 (○印口頭発表者)	所　属　名	安管部　放管二課	
	○高崎　浩司，江花　　稔，野村　　保		

(要　旨)

東海再処理施設の作業環境の放射線管理について，管理の考え方と具体的な方法，放射線モニタリングの概要（放射線モニタ，パトロール監視等）およびこれまでの放射線管理の結果を説明する。また，現在実施している放射線監視の集中化についても説明する。

資　料　番　号
TN8410　91－023 (80－02－228)

資料番号 TN8410 91-023

RADIATION CONTROL SYSTEM AT TOKAI REPROCESSING PLANT

K. TAKASAKI , M. EBANA , T. NOMURA

Power Reactor and Nuclear Fuel Development Corporation
4-33 , Muramatu , Tokai-mura
Naka-gun , Ibaraki-ken , 319-11 , Japan
Telephone : 0292-82-1111 , Telefax : 0292-82-9382

ABSTRACT

At Tokai Reprocessing Plant(TRP), radiation control for workers and workplaces has been carried out effectively in consideration of the ALARA principle by the automated monitoring system and area survey. Until now no excessive exposure over the dose equivalent limits has occurred, and annual collective dose equivalent in plant operations was less than 1 man・Sv.

INTRODUCTION

TRP consists of the Main Plant where spent fuels are processed, waste management facilities and product storages. Various kinds and levels of radioactive materials are treated in these facilities, where the monitoring of the workplace is conducted by the automated monitoring system and area survey. Radiological protection for workers has been carried out effectively more than one decade. In this paper, we present the concept and the outline including experiences of radiation control at TRP.

CONCEPT AND METHOD FOR RADIATION CONTROL

Radiation control at TRP is based on the authorized regulations in Japan and the ALARA principle. Occupational exposure is limited in the regulations, i.e. effective dose equivalent limit of 50 mSv in a year, and is also provided the criteria of the controlled area as shown in Table 1. Beside the regulations, we have some standards for minimizing exposure of workers and localizing air and surface contamination.

The controlled area is divided into three types of area, which are called Green Area, Amber Area and Red Area respectively, according to the control level at TRP. Green Area and Amber Area are those for operation and maintenance works, the control levels of which are shown in Table 2. Red area is the cell type rooms containing instruments or vessels with high level of radioactivity, where workers usually prohibited entering except for repairing or replacing the installations. To minimize exposure and avoid excessive exposure of an individual in plant operation, investigation levels for dose equivalent are set over three months, e.g. 3 mSv for effective dose equivalent.

RADIATION MONITORING

Measurements of radiation fields are conducted for the purpose of avoiding excessive exposure of workers and confirming that working environment is satisfactory for operations. Exposure rates and concentrations of airborne radioactive materials are measured continuously by the automated monitoring system. The schematic diagram of the system is shown in Fig. 1. The system includes area monitors for gamma-rays and neutrons, dust monitors for α and β particles, criticality detection systems, etc. High reliability is needed for the criticality detection system, since warning of the system seriously affect safety of workers and the process. "2 out of 3" detection system is applied to judge critical state. The specifications of monitors are shown in Table 3, and the number of monitor channels in Table 4. The safety control rooms were placed separately in facilities, because the auxiliary facilities were installed by degrees. Signals of detectors are centralized to the health physics panels in the safety

control room. The system is also equipped with warning devices for workers. Alarm signals of facilities are centralized to the central safety control room. Detection limits and warning levels are set according to intensity and energy of radiation and the kind of radioactive material treated in the area. For dust monitors, key nuclides are chosen to set these levels, i.e. plutonium-239 for an α-particle dust monitor and strontium-90 for a β-particle dust monitor. Although these dust monitors are influenced by natural radioactive nuclides, the influence is minimized by means of filtering the supplied air into the facilities.

To support the automated monitoring system, area survey of external radiation, airborne radioactive materials and surface contamination is carried out periodically. The frequency and the points of the monitoring are shown in Table 5.

Dose equivalent rates of fixed points in each facility are measured with survey meters daily, weekly or monthly. In low dose-rate area, e.g. the boundary of controlled area, the cumulative doses are measured quarterly by TLD's.

Airborne radioactive materials in workplaces are weekly sampled by the air sampling systems. Filtered samples are measured by the low background proportional counters, and concentration of the workplaces is estimated. Surface contamination at fixed points in the workplaces is estimated by smear sampling daily or weekly.

To detect contamination promptly and to avoid its spread, Hand foot cloth monitors are set up at the gates of Amber Area, controlled area and principal rooms where alpha radioactive material is treated. Workers have a duty to check contamination of their body surface and instruments.

Individual external exposure by gamma rays, beta rays and neutrons is measured with a TLD badge. And the tissue dose equivalent of fingers is measured with a ring type TLD in compliance with the radiation work. Internal exposure of an individual in plant operation is estimated from air contaminations. Since concentrations of airborne radioactive materials in workplace are determined by the methods mentioned above and is kept in low levels, a routine program of bioassay or whole-body counting is provided only for personnel working in plutonium or uranium processing area.

In case of a work in a high radiation area or a contaminated area, e.g. repairing work in Red Area, a special radiation work plan needs to be authorized, including procedures of the work, the radiation monitoring program, the choice of radiation protection apparatus, etc. Advice on radiation protection are given to the plan in consideration of minimization and optimization of exposure of workers.

CONSEQUENCES OF RADIATION CONTROL

At TRP more than 500 tons of spent fuels have been reprocessed since beginning of the hot test in 1977. Auxiliary facilities, e.g. Waste Management Facilities, Plutonium Conversion Facility, were built after the hot test. According to increase of facilities, workers have increased. The number of worker, collective dose equivalents and the reprocessed fuels from 1977 to 1990 are shown in Fig. 2. Higher collective dose equivalents in 1979, 1983, 1984, 1988 and the first half of 1989 were derived from the large maintenance works. From 1980 to 1982 and from 1985 to 1986 TRP was operated for a year. In plant operation the average collective dose equivalent was about 0.7 man・Sv in a year and the average exposure of an individual was about 0.6 mSv. These values resulted from external exposure, and internal exposure was less than the recording levels. This depended upon good house keeping of facilities in respect of radiation control, earlier detection of air and surface contamination and prompt countermeasures for radiological protection, localization and elimination of contamination.

CONCLUSION

The radiation control has been carried out effectively by the automated monitoring system and area survey. Occupational exposure has been minimized enough and until now no excessive exposure over the dose equivalent limits has occurred.

Auxiliary facilities are located around the Main Plant. And each automated monitoring system of these facilities is independent from that of the Main Plant. For the purpose of efficient monitoring works, radiation monitoring data of the auxiliary facilities are being centralized to the central safety control room and processed with a computer system.

REFERENCES

1. NCRP Report No. 57 Washington, D.C. (1978)
2. ICRP Publication 35, Annuals of the ICRP, 9(4) Pergamon Press, Oxford (1982)
3. TAGO I., ISIGURO H.: J. At. Energy Soc. Japan, 29(8), P681 (1987)

Table 1 The criteria of controlled area

Dose Equivalent Rate Outside of Boundary	Surface Contamination α-particles	Surface Contamination β-particles	Air Contamination
300 μSv/week	4×10^{-1}Bq/cm^2	4 Bq/cm^2	DAC × 3/10

Table 2 The levels of controlled area at TRP

Dose Equivalent Rate	Surface Contamination α-particles	Surface Contamination β-particles	Air Contamination
Green Area ≦ 12.5 μSv/h Amber Area ≦ 500 μSv/h*	< 4×10^{-2}Bq/cm^2	< 4×10^{-1}Bq/cm^2	<DAC × 3/10 × 1/5

* ≦ 25 μSv/h in routine operation area

Table 3 The specification of monitors

Monitoring	Monitor	Detector	Range of Detection
External Dose Equivalent Rate	Gamma-ray Area Monitor Neutron Area Monitor	GM Counter BF_3 Proportional Counter	1 μSv/h~ 10 mSv/h 1 μSv/h~ 50 mSv/h
Concentration of Radioactive Materials	β-ray Dust Monitor	GM Counter (Filter Sampling)	~10^{-3}Bq/cm^3
	Plutonium Dust Monitor	Si Solid State Detector (Filter Sampling)	~10^{-3}Bq/cm^3
Critical incident	Criticality Detection System	Plastic Scintillation Counter (Gamma-ray Detection)	—
		Enriched Uranium target type Si Solid State Detector (Neutron Detection)	—

Table 4 The number of monitor channels

Facility	Gamma-ray Area Monitor	Neutron Area Monitor	Beta-ray Dust Monitor	Plutonium Dust Monitor	Criticality Detection System
Main Plant	44	3	25	7	4
Other Auxiliary Processing Facilities	27	-	17	6	-
Plutonium Conversion Facility	18	4	-	17	8
UO_3 Storages	7	-	-	-	-
Waste Management Facilities	96	-	45	-	-

Table 5 The number of survey points

Facility	Gamma-ray (Daily)	Gamma-ray (Weekly)	Gamma-ray (Monthly)	TLD (Quarterly)	Air Sniffer (Weekly)	Smear (Daily)	Smear (Weekly)
Main Plant	11	35	14	58	108	20	55
Other Auxiliary Processing Facilities	10	48	14	64	99	27	52
Plutonium Conversion Facility	4	23	3	3	53	21	40
UO_3 Storages	-	7	-	6	-	-	6
Waste Management Facilities	19	109	23	141	215	66	128

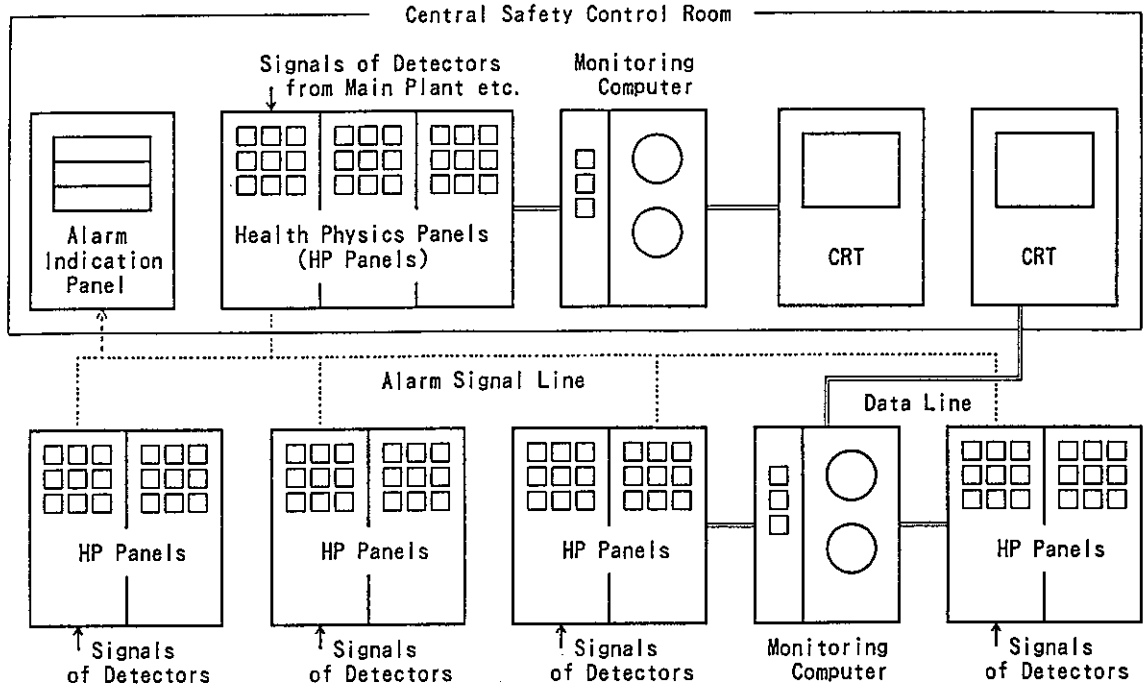

Fig.1 Semantic diagram of automated monitoring system

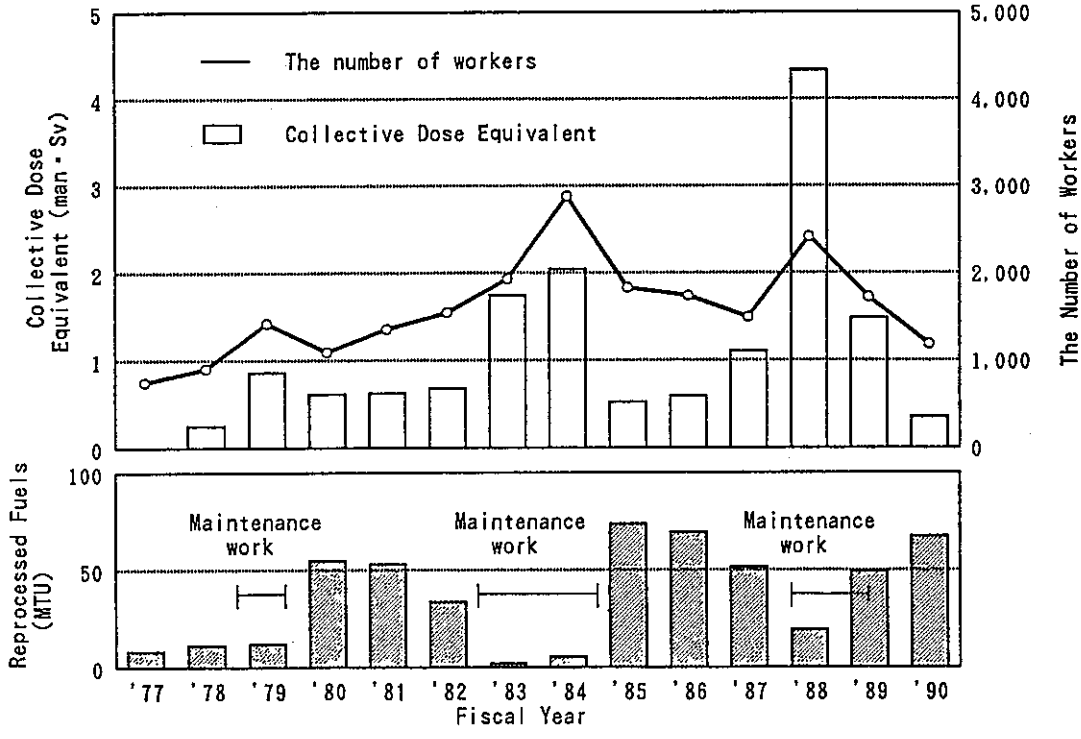

Fig. 2 Trends of Collective Dose Equivalent and The Number of Workers at Tokai Reprocessing Plant

題　　名	Effect of Heat from High-Level Waste on Performance of Deep Geological Repository		
発表先	RECOD'91		
発表地	仙　　台	発　表 年月日	平成3年　4月14日 ～ 4月18日
発表者 （○印口頭発表者）	所　属　名	環開部　GIS室	
	○岡本　二郎，藤田　朝雄，佐々木憲明，原　　啓二		

(要旨)

高レベル放射性廃棄物からの放出熱による処分システム性能への影響を評価するために，ニアフィールド及びファーフィールドの二次元熱解析を実施し，人工バリア及び周辺母岩の温度分布に与える各種パラメータの影響度を評価した。また，同一条件で三次元熱解析を実施し，二次元解析との比較検討を行うとともに，熱－地下水の連成解析を実施して，地下水流動の熱伝導特性に与える影響等を評価した。

本文はこれらの結果を第3回再処理・廃棄物処理処分に関する国際会議に発表するためにとりまとめた論文である。

資料番号
TN8410　91－028 （80－02－257）

資料番号 TN8410 91-028

EFFECT OF HEAT FROM HIGH-LEVEL WASTE ON PERFORMANCE OF DEEP GEOLOGICAL REPOSITORY

J. OKAMOTO, T. FUJITA, K. HARA AND N. SASAKI
Power Reactor and Nuclear Fuel Development Corp.
4-33, Muramatsu, Tokai-mura
Naka-gun, Ibaraki-ken, 319-11, JAPAN

ABSTRACT

The estimation of the increase of the temperature in the vicinity of a repository, is an important issue for the designing and the performance assessment of the repository. The transient heat analyses were carried out in order to evaluate the heat effects on the engineered barriers and the host rock, and the coupled thermo-hydraulic analysis was carried out to evaluate the effects of the groundwater flow on the temperature distribution of the host rock.

The transient heat analyses for near-field and far-field were conducted by two dimensional and three dimensional model. The results from these analyses showed that the increase of the temperature within the engineered barriers was mainly dependent upon the heat release properties of the HLW, the occupied area of the packages and the thermal conductivity of the host rock. The maximum temperature of the engineered barriers and the host rock does not exceed the temperature to change the crystallization of the waste glass or the alteration of their minerals by adjusting the occupied area of the waste package.

As the results of the coupled thermo-hydraulic analysis, the temperature distribution and its temporal change showed a good accordance with the transient heat analysis, so that the effect of the groundwater flow on the temperature distribution is considered to be negligible. Hydraulic gradient of the convective flow in the vicinity of the repository was estimated to be approximately 1/10,000.

INTRODUCTION

The high-level radioactive waste (HLW) will be disposed in a designed underground repository constructed deep in a selected geological environment. The safety of the repository depends on the performance of the overall waste disposal system and the isolation effectiveness of the system depends on a number of natural and emplacement-induced effects (ref. 1). Heat generated from the HLW is included in this effectiveness. The engineered barriers and the surrounding host rock will be affected by the thermal effects from the HLW.

By the heat generated from the HLW, the increase of the temperature of the engineered barriers and the host rock in the vicinity of a repository depends on the heat release properties of the waste, the size, the shape and the thermophysical properties of each engineered barrier, the occupied area of the packages in a repository, as well as the heat transfer properties of the host rock. The increase of the temperature of the engineered barriers and the host rock is an important issue for the designing and the performance assessments of the repository. This paper presents the results of the transient heat transfer analyses to evaluate the heat effects on the engineered barriers and the host rock in the vicinity of a repository.

BASIC ASSUMPTION

The heat transfer analyses were carried out on the basic conditions as shown in Table 1. Vitrified high-level radioactive waste confined within a canister is enclosed in a carbon steel overpack after interim storage for the period of 30 to 50 years and is emplaced within a buffer material at a depth of several hundreds of meters or more below the ground surface (ref. 2). Number of waste packages in a repository is supposed to be approximately 40,000, estimated to be generated until 2,030 in Japan.

The thickness of the carbon steel overpack is set to 30 cm considering not only the mechanical strength to withstand the rock pressure at a repository depth but also the corrosion rate of the carbon steel (ref. 2.).

The thickness of the buffer material around the carbon steel overpack is set to more than 30 cm to have the enough retardation of the migration.

Table 1 Basic conditions

Item	Basic condition
Total number of disposal waste package	40,000pieces
Heat release rate of waste package	670W after interim storage of 30 years
Period of interim storage	30~50years
Vitrified waste	External diameter : φ430mm Height : 1350mm Weight : 492kg
Overpack	External diameter : φ1040mm Thickness : 300mm Height : 1950mm Weight : 11,500kg Material : Carbon steal
Buffer material	Compacted sodium bentonite Minimum thickness : 30cm Allowable maximum temperature : 100℃

THERMAL ANALYSIS

Conditions

Transient heat transfer analyses of near-field and far-field with two and three dimensional models were carried out to identify the sensitivity parameter to suppress the maximum temperature at the buffer material (ref. 3). Influence of the following parameters were studied:

-occupied area per waste package
-interim storage period of the vitrified waste
-number of waste packages within borehole
-thickness of the buffer material
-thermal conductivity of the host rock
-heat capacity of the host rock
-disposal depth

Analytical model

Near-field analysis

Near-field analyses were carried out with the models of an axisymmetric FEM and a three dimensional FEM.

The geometry of the near-field used for the analysis is shown in Figure 1. Figure 2 shows the axisymmetric FEM model for the near-field. The temperature gradient of the host rock is assumed to be 3 ℃/100 m. The repository is located at the depth of 1,000 m below the ground surface, and the initial temperature at the depth is assumed to be 45℃. The upper boundary is located at 200 m above the repository, and the temperature of the ground surface is assumed 15℃. The lower boundary is assumed to be located at 200 m below the repository, and the

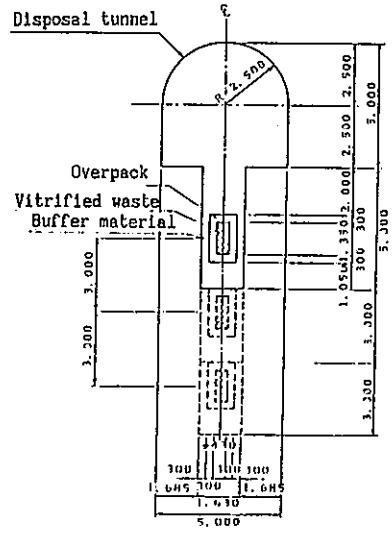

Fig.1 Geometry of near-field used for analysis

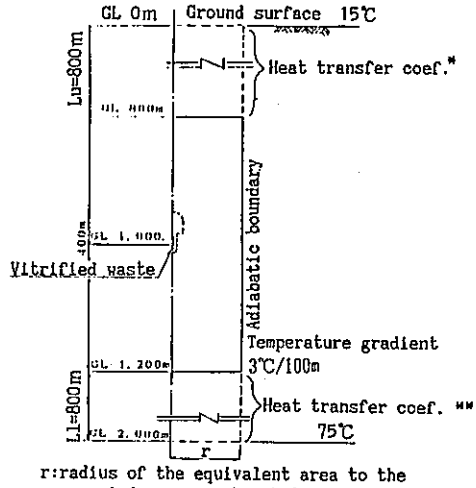

r:radius of the equivalent area to the occupied area per borehole
*:(Thermal conductivity of the host rock)/Lu
**:(Thermal conductivity of the host rock)/Ll

Fig.2 Model for near-field

isothermal condition is located at the depth of 2,000 m below the ground surface (GL-2,000 m). The sides boundaries are assumed to be adiabatic.

Figure 3 shows the three dimensional model for the disposal in a tunnel. The diameter of the tunnel is assumed 3 m and the waste package is located at the center of the tunnel. The boundary condition of the ground surface is assumed to be a heat transfer surface, the lower boundary is located at 200 m below the repository and the boundary condition is isothermal. All sides boundaries are assumed to be adiabatic because of the symmetry of the model.

The three dimensional analysis with the pit disposal model was carried out in order to compare with the results of the axisymmetric model. All boundary conditions are assumed to be the same as those for the disposal in a tunnel.

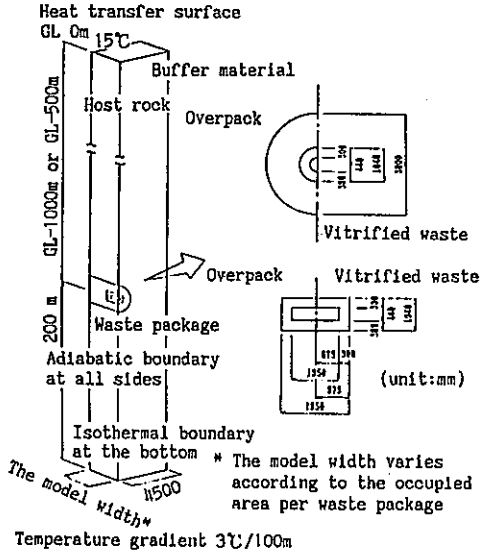

Fig. 3 Model for the disposal in tunnel

Far-field analysis

The far-field analysis was carried out with the axisymmetric FEM model as shown in Figure 4. The shape of the repository is assumed to be a disc with the radius of 1,125 m because of the axisymmetric analysis. Radius of the repository is determined as an equivalent area to the area based on the assumption of a 30 years interim storage period, 40,000 pieces of the waste packages for inventory, the 100m'/package occupied area, and the repository tunnel height of 5 m. The location of the repository considered is two cases, one is 500 m depth below the ground surface, and another is 1,000 m depth. The ground surface is assumed to be a heat transfer surface, the lower boundary is isothermal, and the sides boundaries are adiabatic.

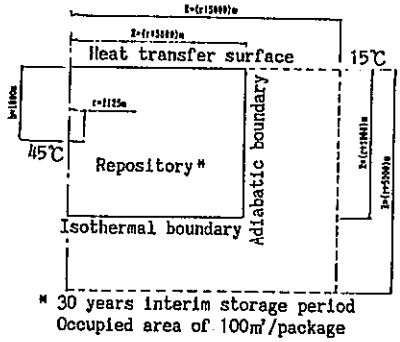

Fig. 4 Model for far-field

Results

Near-field analysis

Figure 5 shows the time dependency of the near-field temperature in the case of a 30 years interim storage period of the HLW and the 100 m'/package occupied area. The thickness of the buffer material is 30 cm, the thermal conductivity of the host rock is 2.5 kcal/mh℃, and the heat capacity of the host rock is 525 kcal/m'℃ in this case. The temperature inside the buffer material comes up to the maximum after 10 to 50 years after disposal and decreases after that.

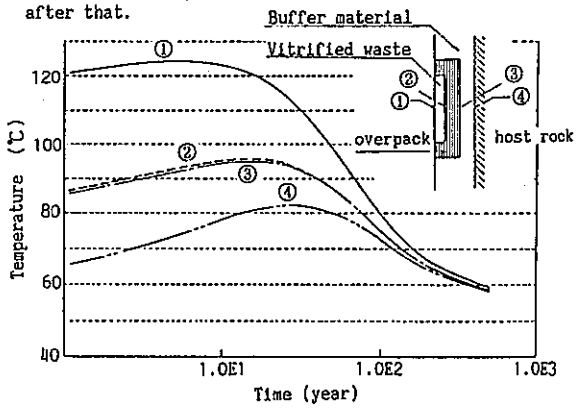

Conditions:
- Occupied area per waste package; A= 100(m'/package)
- Interim storage period;30 (year)
- Number of packages per borehole; N= 1 (package)
- Thermal conductivity;
  - Rock λ = 2.5 kcal/mh℃
  - Buffer material λ = 0.78 kcal/mh℃

Fig. 5 The time dependency of near-field temperature

Figure 6 shows the relationship between the maximum temperature within the buffer material and the occupied area per borehole, with the interim storage period of the HLW and the number of packages per borehole. Assumed 100℃ for the allowable maximum temperature of the buffer material, the occupied area per borehole is increasing with the number of packages per borehole. However, the occupied area per package does not change so much. The occupied area per package mainly depends on the interim storage period. The occupied area per package is 85m' /package in the case of a 30 years interim storage period.

The effect of the occupied area on the maximum temperature of the buffer material for the pit disposal is shown in Figure 7, with the results of the axisymmetric model under the same conditions. From this figure, the results of both analyses are a good agreement although the temperature within the near-field obtained from the axisymmetric model is somewhat lower than that of the 3D model.

Figure 8 shows the effect of the occupied area on the maximum temperature of the buffer material for the tunnel disposal. Assumed 100℃ for the allowable maximum temperature of the buffer material, the occupied area of the package to suppress the maximum temperature, is in need 100 m²/package though that for the pit disposal is 80m²/package. The maximum temperature of the buffer material with a constant occupied area is higher than that in pit disposal, because of the larger thickness of the buffer material. However, if the partial alteration of the buffer material is allowed, the tunnel disposal is not necessarily inferior to the pit disposal in terms of the occupied area.

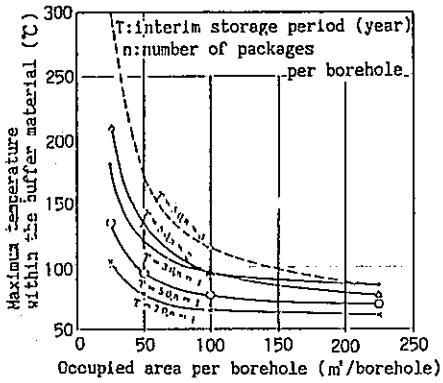

Fig. 6 Max. temperature within the buffer mat. and occupied area per borehole

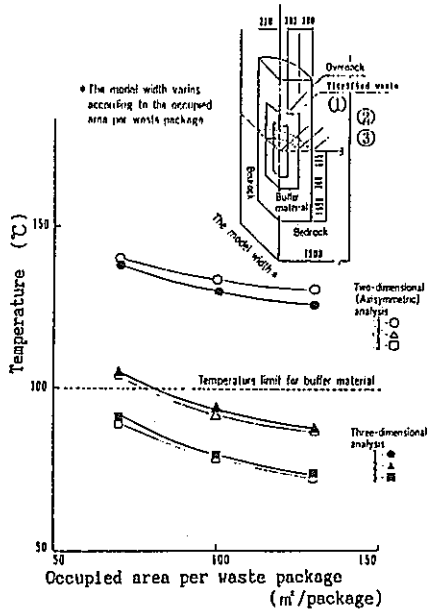

Fig. 7 Relationship between the temperature and the occupied area per waste package (pit disposal)

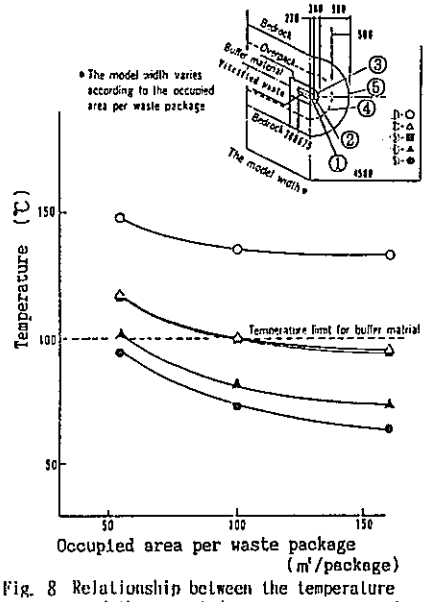

Fig. 8 Relationship between the temperature and the occupied area per waste package (tunnel disposal)

Far-field analysis

Figure 9 shows the temperature distribution of the far-field in the case of the repository at a depth of 1,000 m. The temperature at the depth of the repository becomes the maximum, approximately 75℃, at the time of 50 years after disposal. However, the thermal effects from the HLW is almost negligible after 10,000 years. The temperature after 1,000 years is estimated to be approximately 55℃. This means the increase of 10℃ from the initial temperature. An increase of the temperature at a point 500 m from the repository is estimated to be less than 2℃. The case of the repository depth at 500 m was simulated. The temperature distribution is almost similar as the case of the repository depth at 1000 m, and the thermal effects from the HLW is negligible after 10,000 years, though the maximum temperature at the depth of the repository is approximately 60 ℃ after 50 years.

Figure 10 shows the effect of the thermal conductivity of the host rock on the maximum temperature. Although the temperature of the repository are affected by the value of the thermal conductivity of the host rock, the increase of the temperature at a point where the vertical distance is 100 m from the repository is little affected by the thermal conductivity and it is estimated to be approximately 1 to 3℃.

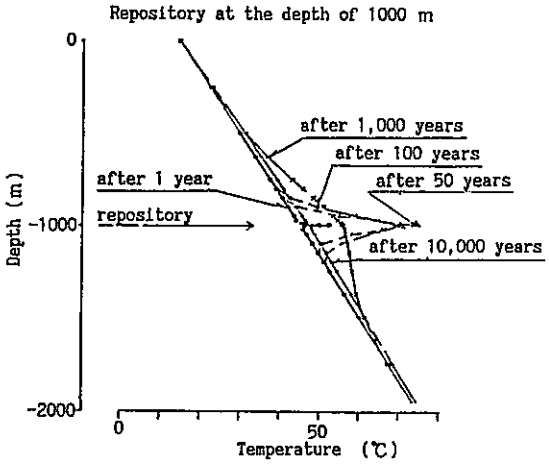

Conditons:

Occupied area per package; 100 m²/package
Interim storage period ; 30 year
Thermal conductivity
rock ; 2.5 kcal/mh℃
buffer mat. ; 0.78 kcal/mh℃

Fig. 9 Time dependency of the far-field temperature

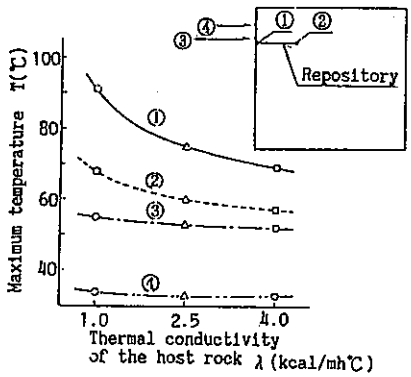

Fig. 10 Effect of the thermal conductivity of the host rock on max. temperature

COUPLED THERMO-HYDRAULIC ANALYSIS

Conditions

Coupled thermo-hydraulic analysis was carried out to evaluate the effect of the groundwater flow on the temperature distribution (ref. 5). The occupied area of the package is assumed to be 100m²/package, and the number of disposed waste packages are 40,000 pieces.

Analytical model

The effect of the heat generated from the HLW was studied with the axisymmetric model on the assumption of a 30 years interim storage period, and instant emplacement and closure. The topographic gradient is assumed to be 0 to observe the groundwater movement induced only by the heat from the repository. The access shaft within the model is assumed to be located at the center of the repository and the diameter of that is assumed to be 15 m, so that the area is equivalent to the total area of 5 access shafts of diameter 6.5 m.

Two kinds of repository models are considered in order to evaluate the effects of the superimposed heat source. One is two layered repository model located at 800 m and 1,000 m, and the other is a single layered model. Also, two kinds of repository depth are considered, one is located at 500 m and the other is located at 1,000 m as shown in Figure 11. The analysis were carried out with these models under the same boundary conditions. The lower boundary is located at 3,000 m below the repository, and the conditions are impervious and isothermal. The right side boundary is located at 3,000 m from the edge of the repository. The conditions of both sides are impervious and adiabatic. The boundaries of the ground surface are the isobaric condition and the heat transfer surface.

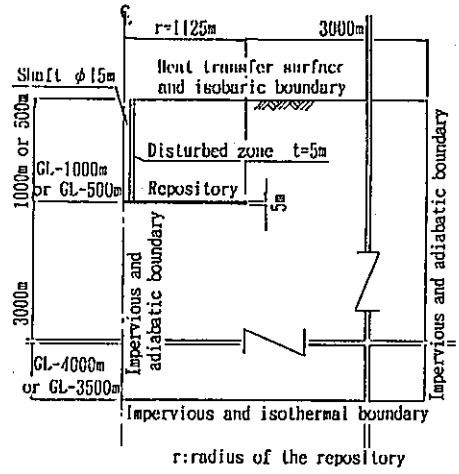

Fig. 11 Model for the coupled analysis

Results

Figure 12 shows the time dependency of the temperature in the case of the repository at a depth of 1,000 m together with the results of the axisymmetric thermal analysis under the same conditions. The thermal conductivity of the host rock is 2.5 kcal/mh ℃, the thermal capacity is 530 kcal/m³℃, and the hydraulic conductivity of the host rock is 1.0E-6 cm/s in this case. The result of the coupled analysis is approximately in agreement with the result of the axisymmetric analysis. The maximum temperature within the far-field based on the coupled analysis is estimated to be 75℃ after 30 to 40 years from disposal.

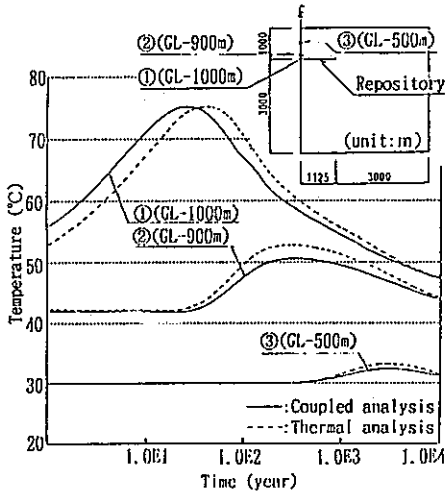

Fig. 12 Time dependency of the temperature

Figure 13 shows the groundwater fluxes and isotherms at the time of 1,000 years after the heat releases under the same condition in Figure 12. Though the groundwater flow is affected by the heat generated from the HLW, the hydraulic gradient within the host rock due to the convection is less than 1/10,000.

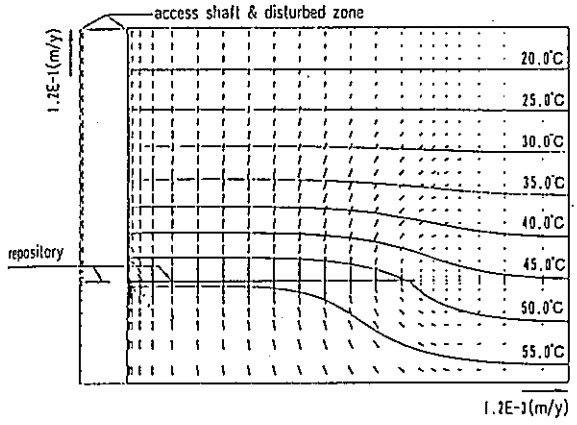

Fig. 13 Groundwater fluxes and isotherms after 1000 years heat release

DISCUSSION

Three kinds of analyses with different analytical methods, were carried out in order to evaluate the temperature effects on the engineered barriers and the surrounding host rock.

Based on the analyses, the increase of the temperature within the engineered barriers is mainly dependent upon the heat release properties of the HLW, the occupied area of the package, and the thermal conductivity of the host rock. If the temperature limit of the buffer material is assumed to be 100 ℃ to minimize the alteration of the chemical properties (ref. 1), it can be achieved by adjusting the occupied area of the waste package. The temperature of the buffer material becomes less than 100℃ in the case of the occupied area of the package with more than 100 m²/package, a 30-years interim storage period, and a thermal conductivity of the buffer material of 0.78 kcal/mh℃ under the dry condition.

For the waste glass, the crystallization of a waste glass is considered if the temperature exceeds a transformation temperature of approximately 500 ℃ (ref. 1). However, the maximum temperature within the waste glass becomes under 150 ℃ in the simulation. Therefore, the crystallization of the waste glass can be negligible.

For the surrounding host rock, granite, clay, and tuff are stable under 300℃, 150℃ and 200℃, respectively (ref. 1). The temperature of the host rock becomes its maximum, approximately 60 to 90℃, in the thermal analyses as shown in Figure 7 and Figure 8. Therefore, the host rock is considered to be stable and the maximum temperature will be adjusted by a repository lay-out. However, the thermal stresses by the heat generated from the HLW, should be considered regardless of whether it is negligible or not.

Figure 14 shows the time dependency of the near-field temperature of both 2D analysis and 3D analysis in the case of the pit disposal at a depth of 1,000 m after a 30 years interim storage period. The occupied area is 100m²/package. From this figure and Figure 7, the results of 2D analysis show a good accordance with those of 3D analysis. Therefore, the 2D analysis can be available for the parameter analysis about the heat transfer.

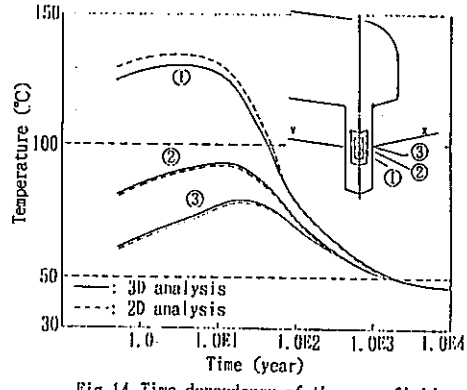

Fig. 14 Time dependency of the near-field temperature of 2D and 3D analysis

Figure 15 shows the temperature distribution of 2D analysis and coupled analysis. From this figure and Figure 12, the temperature distribution and its temporal change around the repository shows a good accordance with the results of coupled thermo-hydraulic analysis. The results show a good agreement with the results of the IAEA technical document (ref. 1). Therefore, an effect of the groundwater on the temperature distribution is considered to be negligible.

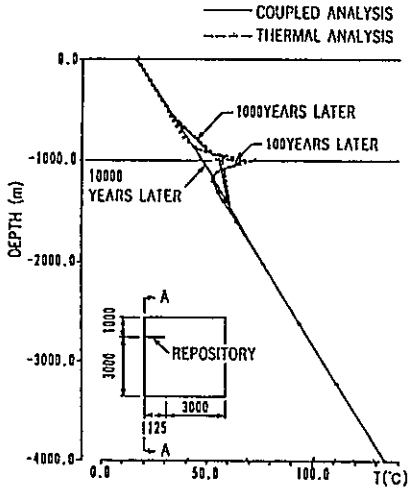

Fig. 15 Temperature distribution of 2D and coupled analysis

CONCLUSIONS

The conclusions obtained from this study are described as follows.

1) The governing factor for sizing the repository is the maximum temperature acceptable to the buffer material. The maximum temperature mainly depends upon the period of the interim storage of the wastes, the occupied area per waste package, the depth of the repository, and the thermal conductivity of the host rock.

2) Crystallization of the vitrified waste can be negligible because the temperature does not exceed the limit for crystallization. The host rock around the repository keeps stable against the heat generated from the HLW. However, the stresses due to the heat should be considered regardless of whether it is negligible or not.

3) The near-field analysis with two dimensional model is considered to be valid for the sensitive analysis of the heat transfer because of the good agreement with the detailed three dimensional analysis. The temperature distribution in the host rock is little affected by the convective flow. Therefore, the effect of the groundwater flow on the heat transfer within the host rock is considered to be negligible.

ACKNOWLEDGMENT

The analyses presented in this paper have been performed in cooperation with Kajima Corp., Taisei Corp., and Shimizu Corp. The authors would like to express gratefulness for their cooperation to accomplish the work.

REFERENCES

1. "EFFECTS OF HEAT FROM HIGH-LEVEL WASTE ON PERFORMANCE OF DEEP GEOLOGICAL REPOSITORY COMPONENTS", IAEA-TECDOC-319, Stockholm, Aug. 28 to Sept. 2, (1983).
2. SASAKI N., ISHIKAWA H., MIYAHARA K., YAMADA K., YUSA Y., "DEVELOPMENT OF THE ENGINEERED BARRIERS FOR THE DEEP GEOLOGICAL DISPOSAL OF HIGH-LEVEL RADIOACTIVE WASTE", Int. High-level Radioactive Waste Management Conf., Las Vegas, Nevada, U.S.A., April 8-12, (1990).
3. HARA K., ARAI T., YUSA Y., SASAKI N., ISHIHARA K.,"Design Concept of Repository Concerning Thermal Stability of Buffer Material", Proc. of 1989 Fall Meeting of Atomic Energy Society of Japan, October 17-19,(1989).
4. HARA K., FUJITA T., SAOTOME A., UCHIDA M., SASAKI N., "CONCEPTUAL DESIGN STUDY OF GEOLOGICAL DISPOSAL SYSTEM", Int. High-level Radioactive Waste Management Conf., Las Vegas, Nevada, U.S.A., April, (1991)
5. OKAMOTO J., ISHIHARA K., SAWAUCHI Y., HARA K., SASAKI N., "COUPLED THERMO-HYDRAULIC BEHAVIOR AROUND ACCESS SHAFT SEALED WITH BACKFILL MATERIAL", Scientific Basis for Nuclear Waste Management X IV, Symposium P at the 1990 MRS Fall Meeting, Boston, U.S.A., November 26-29, (1990).

題　　名	Development of Iodine Removal Technology at the TOKAI Reprocessing Plant		
発表先	RECOD'91		
発表地	仙　　台	発　表 年月日	平成3年　4月14日 ～ 4月18日
発表者 (○印口頭発表者)	所　属　名	再処理　技術課	
	○伊波　慎一，川崎　道隆，立原　富夫，岡本　弘信		

(要旨)

東海再処理工場実廃気に適した，よう素フィルタ（U207)吸着材の選定と最適運転条件の調査を目的として，工場実廃気による吸着材の性能比較試験を行った。

試験に供した吸着材は，ＡｇＸ，ＡｇＺ，ＡｇＳ，ＡｇＡの４種類であり，試験条件はよう素フィルタの実使用条件と同等とした。

試験の結果，ゼオライト吸着材（ＡｇＸ，ＡｇＺ）が硝酸銀添着吸着材(ＡｇＳ，ＡｇＡ)より良い性能を示した。また，保持能力では，各吸着材とも吸着したよう素は安定に固定化していると考えられた。なお，本試験では，NO_x と工場の運転条件との相関も調査した。

以上の内容を供試吸着材，試験装置，方法，条件および得られた結果について報告する。

資料番号

TN8410　91－039

(80－02－251)

資料番号 TN8410 91-039

DEVELOPMENT OF IODINE REMOVAL TECHNOLOGY AT THE TOKAI REPROCESSING PLANT

S. INAMI , M. KAWASAKI , T. TACHIHARA , H. OKAMOTO

Power Reactor and Nuclear Fuel Development Corporation
4-33 Muramatu , Tokai-mura
Naka-gun , Ibaraki-ken , 319-11 , Japan
Telephone : 0292-82-1111 , Telefax : 0292-82-2321

ABSTRACT

In the Tokai Reprocessing Plant (TRP), iodine removal is carried out by alkaline scrubbers and iodine removal filters (AgX) in the ventilation system. The objective of this experiment is to select the adsorbent adequate for the secondary iodine removal filter and examine the optimum operating conditions.

Performance experiments of four types of iodine adsorbents, silver faujasite (AgX), silver mordenite (AgZ), silver nitrate impregnated silicic acid (AgS) and alumina (AgA), were conducted in the ventilation system during the spent fuel reprocessing campaigns of the TRP.

Input gas was the actual off-gas treated by alkaline scrubbers before going to the secondary iodine removal filter at the TRP. Performance experiments were implemented for four weeks with the actual use of that filter. After that room air was flowed through the adsorbents.

The following results were obtained.

(1) In performance, zeorite adsorbents were superior to silver nitrate impregnated materials.

(2) It was believed that the performance is effected by the material characteristics of the adsorbent under the scarce iodine concentration experienced in this test.

(3) Performance of adsorbents were influenced by increases of NOx (NO, NO_2) concentration.

(4) The adsorbed iodine was fixed stably even in air flow.

INTRODUCTION

Radioactive iodine (^{129}I) is a long half-life nuclide ($t_{1/2}=1.57\times10^{7}y$), so it is important to reduce the amount of it released to the environment as much as possible. So reduction of the amount of iodine released to the environment has been the main objective of the TRP since hot operation began in 1977.

In the TRP two ways had been taken to reduce the amount of released iodine. One is to trap gaseous iodine in alkaline solution by the scrubbers, and the other is to install iodine removal filters (AgX) in the ventilation system for back up. These ways had contributed to reducing the radioactive iodine release.

However AgX has poor acid resistance and adsorbents containing 38wt% silver[1] are expensive. Therefor AgX is not always effective for use in a reprocessing plant. Recently other adsorbents, AgZ, AgS and AgA were developed and used in the reprocessing plant[1][2]. The performance of these adsorbents has been reported by works in many laboratories but the use in reprocessing plant is not always effective and also comparison of various synthetic adsorbents are few. Under the actual off-gas conditions in the reprocessing plant, degradation of the filter adsorbent by exposure to NOx (NO, NO_2), water vapor and other influential nuclides is a problem. Moreover, in the removal of iodine from ventilation system, there is often a problem of adsorbed iodine on the adsorbents being released by weathering.

Anyhow, for reducing the amount of radioactive iodine released, it is necessary to select the proper adsorbent for the reprocessing plant and to examine the optimum operating conditions. For these reasons the TRP has been carrying out experiments and investigations on performance of various adsorbents.

This paper describes the results of recent experiments.

ADSORBENTS

Adsorbents for the experiment were four types; silver faujasite (AgX), silver mordenite (AgZ), silver nitrate impregnated silicic acid (AgS) [2] and activated alumina (AgA) [3]

AgX is used in the iodine removal filter of the TRP at present. AgZ holds silver in the same way as AgX with sodium ion exchanged for silver ion on a moleculer sieve mordenite type. AgZ is different from the zeorite structure and has a high ratio of alminosilicate [4]. AgS is amorphous silica impregnated with silver nitrate and marketed under the trade name AC-6120 [2] [5]. AgA is activated alumina impregnated with silver nitrate [3] Specification of these adsorbents are shown in Table 1. Adsorbents of AgX, AgZ, AgS and AgA are shown in Photos 1-4.

Table 1. The Specification of adsorbents

	AgX	AgZ	AgS	AgA
Silver Holding	ion exchanged		impregnated	
Active Ingredient	silver ion (Ag^+)		silver nitrate ($AgNO_3$)	
Silver Content	38.7 wt%	11.4 wt%	12 wt%	24.75 wt%
Density	1.16 g/mℓ	0.67 g/mℓ	0.66 g/mℓ	1.53 g/mℓ
Particle Form	beads	pellets	beads	beads
Particle Size	10～16 MESH	10～16 MESH	1～2 mmφ	10～16 MESH
Specific Surface	315 m^2/g	500 m^2/g	65 m^2/g	9 m^2/g
*Pressure Drop	17.1 mmAq	7.8 mmAq	45 mmAq	no data

The above data are quoted from the catalogs of adsorbents.

* At bed length; 50mm, linear velocity; 20cm/s, temp.; 30 ℃

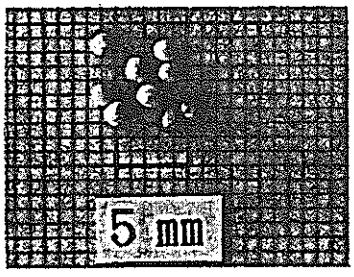

Photo 1. AgX

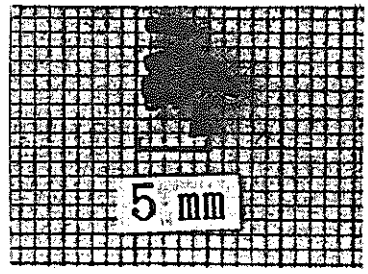

Photo 2. AgZ

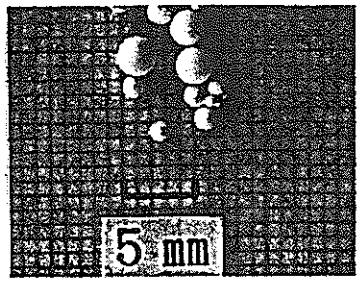

Photo 3. AgS

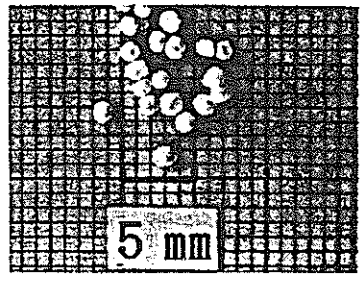

Photo 4. AgA

INPUT OFF-GAS

The actual input off-gas is composed of shearing off-gas (SOG), dissolver off-gas (DOG), HAW vessel off-gas (HAW VOG) and other vessel off-gas (VOG). Each of these is treated by an alkaline scrubber, the other vessel off-gas (VOG) is also treated with an iodine removal filter. As a result, the iodine concentration in the off-gas is very small.

The input off-gas is highly influenced by the chemical form in the process and NOx in high active waste disposal.

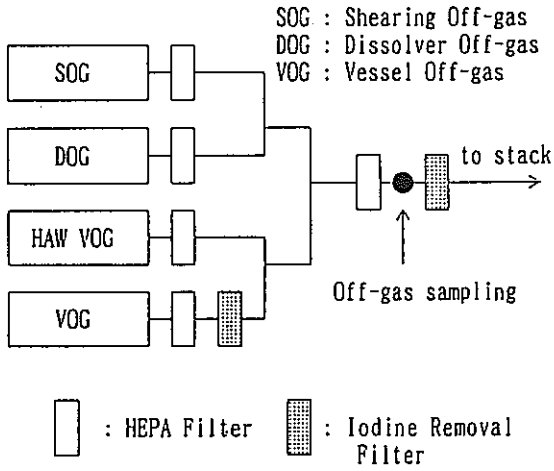

Fig. 1 Flow diagram of the off-gas ventilation system

A flow diagram of the off-gas ventilation system is shown in Fig. 1.

EQUIPMENT

The experimental equipment for adsorption and fixation is shown in Fig. 2.

Each line has an adsorption column with the adsorbent materials, a charcoal sampler to measure the amount of iodine at the exit of adsorbent materials, a pump to suck the sampling off-gas and a flow meter. Temperature and relative humidity indicators are fixed with a heating plate that can control the off-gas temperature for experiment. By setting one paper and two cartridges (a charcoal-soaked paper and two charcoal cartridges) the total iodine discharged to the off-gas was trapped and measured.

ANALYTICAL METHOD

Quantitative analysis of iodine-129 included in sample is possible by measuring γ-rays from iodine-129 in the sample with γ-ray spectrometer. The method for measuring it is to place the materials into the exclusive container. After 3000 seconds the amount of iodine-129 is measured by analysing. This method is only applicable for samples of more than 1.9Bq.

TEDA impregnated charcoal was used for collecting the iodine samples.

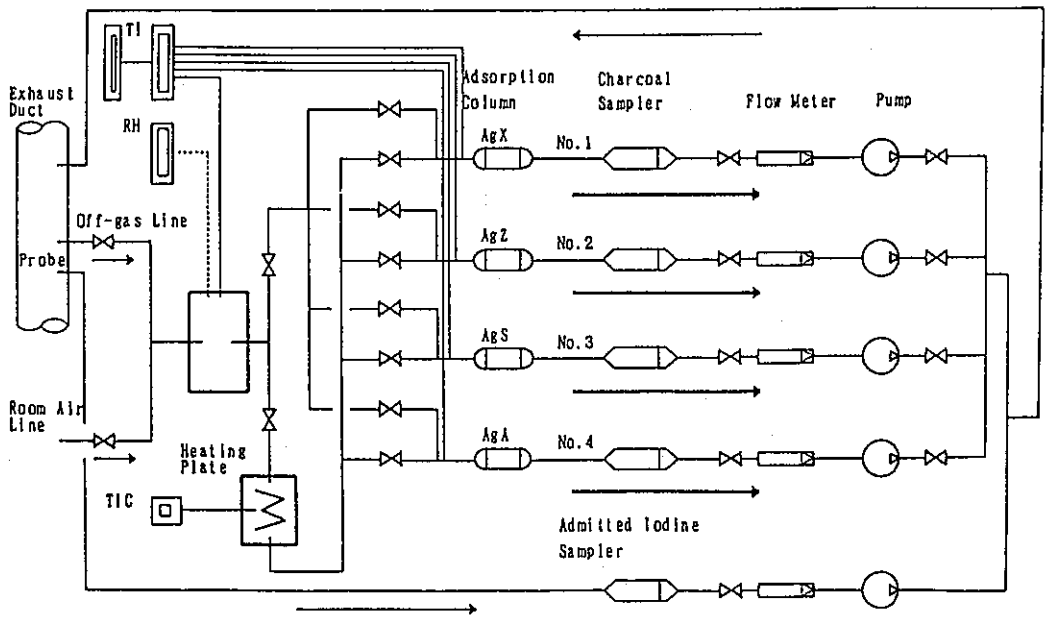

Fig. 2 Schematic Diagram of Equipment

PROCEDURE AND CONDITION

The experiment consisted of adsorption and air flow runs.

Adsorption run operated under conditions that we close to the actual use of a ventilation system. The objective is to select an adsorbent adequate to handle reprocessing plant off-gas.

Therefore the input off-gas was heated to 50℃ and flowed at 10ℓ/min (linear velocity; 17cm/s).

The experiment operating conditions are shown in Table 2.

Table 2. Experimental Operating Conditions

Column Parameter	
Bed Length	50 mm
Diameter	35.5 mm
Input Off-gas Parameter	
Linear Velocity	17 cm/s
Flow Rate	10ℓ/min
Temperature	50℃
Operating period	
Adsorption	28 days
Air flow	12 days
(Room Air	6 days)
(50 ℃ Air	6 days)

The adsorption run was carried out for four weeks (28days) by flowing actual off-gas through four kinds of adsorbent materials. During the experiment time, the DF (amount of iodine entering the adsorbent divided by the amount exiting) was obtained by exchanging charcoal every two days. During the test run of adsorption the related process in the TRP was monitored.

After the experiment the adsorbent materials were removed the equipment and kept in a vinyl sack and preserved for a fixed time, finally the materials were examined for their fixation ability.

The performance of each adsorbent was determined by comparing the decontamination factor (DF) for each material.

$DF=C_0$(admitted iodine)/C(discharged iodine)

The amount of iodine was measured by analyzing the charcoal in the equipment.

RESULTS OF ADSORPTION RUN

Input conditions of the experiment are shown in Table 3.

Iodine concentration was very small with average concentrations of 1.3×10^{-5}Bq/mℓ during the adsorption run.

Table 3. Results of Input Conditions

Input Condition	
Total Time	655.4h
Total Flow	393.4m³
Iodine	
Concentration	av. 1.3×10^{-5}Bq/mℓ
Total Admitted	5.0×10^{3} Bq
Normal Off-gas	
Temperature	av. 29℃
Relative Humidity	av. 30 %

DF data and the amount of adsorption are shown in Table 4. And DF data of every sample along with process operation, input iodine and NOx concentration are shown in Fig. 3.

Table 4. DF of adsorbents

	AgX	AgZ	AgS	AgA
Av. DF	6.6	6.6	3.6	2.6
Max. DF	10.5	9.6	7.9	4.7
Min. DF	4.8	5.8	2.6	2.1
Adsorption Amount ($\times10^{3}$Bq)	4.3	4.3	3.7	3.1
Adsorption Rate (%)	85	85	72	62

The results showed that the performance of zeorite adsorbents AgX and AgZ were better than silver nitrate impregnated AgS and AgA. Also the AgZ showed performance stability during the adsorption runs.

Iodine was adsorbed in larger quantity on AgX and AgZ than on AgS and AgA.

After the experiment, the appearance of the adsorbent materials were carefully observed.

The AgX, AgS and AgA changed color to a reddish light brown in depths of 5-10mm from the front surface and gradually got lighter changing to a yellowish white. The AgZ was colored a blackish brown before the experiment, but it's color changed to a yellowish light brown in depths of 5-7mm from the front surface and then turned to a yellowish white. These changes of color are believed to be the effect of the NOx and iodine adsorbed. However these changes of color were only on the surface. So it is considered that there was little use of the silver.

The NOx concentration was measured by the chemi-luminescence method[6]. However this method is not reliable above 2000ppm because conversion efficiency of NO_2 to NO degrades at high concentrations. NOx data were adopted for reference and plotted on Fig. 3.

After this experiment, the equipment for NOx measurement by the ultraviolet ray[6] adsorption method was set up in the plant. According to this method, NOx (NO, NO_2) was measured to a maximum of 5000ppm in the process. (The NO was 3200ppm and the NO_2 was 1800ppm.) The NO concentration rose to 3200ppm from 300ppm while NO_2 rose to 1800ppm from 500ppm. Thus it appears that the NOx concentration is primarily controled by NO. It is estimated that the DF of all adsorbents degraded with rising NOx concentrations as shown in Fig. 3. Also AgX which has no acid resistance showed performance equal to AgZ. We also believe that the degraded performance of AgS and AgA is caused by the rising concentration of NO in NOx.

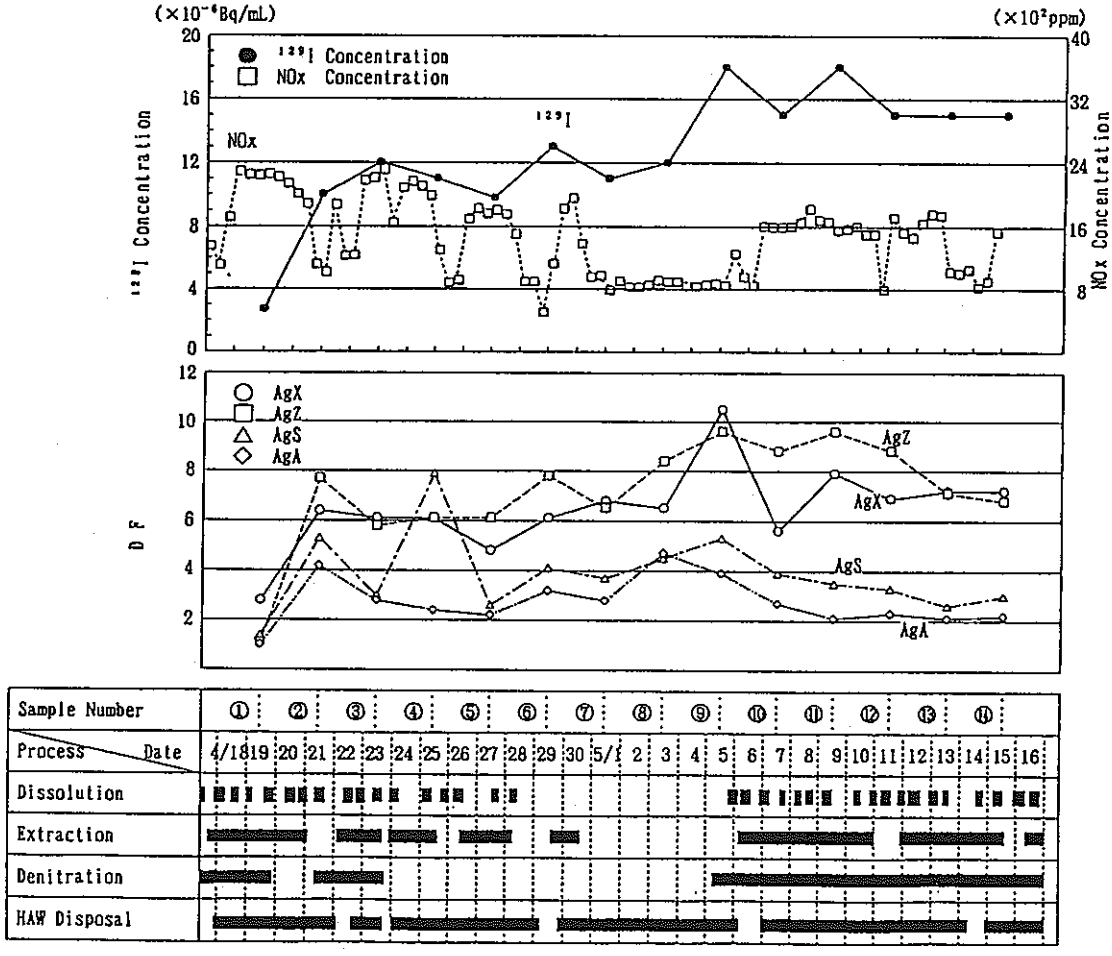

Fig. 3 Performance of Adsorbents and Process Operation in The TRP

The dependency on iodine concentrations could not be shown precisely because of the small amount of iodine in the system.

It was not possible to determine the effects of process operations on the adsorption of iodine on to the materials tested because of the overlap of the process operations.

FIXATION ABILITY

When the same materials were placed in the equipment and room air flowed through it for 12 days. During the first 6 days the air was no heated. The air was heated to 50℃ for the last 6 days. Table 5 shows the result of analysis in charcoal taken every 2 days.

In AgX 5.1Bq (^{129}I) was measured in normal air flow, this is 0.1% of the total amount. In the AgZ and AgS the discharged iodine was below the detection level.

In AgA 11.1Bq (^{129}I) was measured for both normal and hot air, this is 0.4% of the total amount.

These results indicate the following.

(1) The iodine is physically captured by zeorite in AgX.

(2) The discharged iodine from AgA increases at room temperature.

(3) Iodine trapped on silver adsorbents is fixed stably.

Table 5. Iodine of Discharging

(Bq/Sample)

		AgX	AgZ	AgS	AgA
First half	①	2.2	N D	N D	3.0
	②	N D	N D	N D	2.5
	③	2.9	N D	N D	2.9
Second half	④	N D	N D	N D	N D
	⑤	N D	N D	N D	2.7
	⑥	N D	N D	N D	N D
Total		5.1	N D	N D	11.1
Rate of discharge		0.1%	0%	0%	0.4%

N D ; Not Determined
Detection level;1.9Bq

CONCLUSION

The following results from iodine removal experiments of the actual off-gas were obtained.

1. The iodine trapping efficiency of the zeorite adsorbents AgX and AgZ, was superior to silver nitrate impregnated material AgS and AgA.

Under the conditions close to actual use in the TRP and within the limits of these experiments, AgX and AgZ appears to be adequate adsorbents for the secondary iodine removal filters in the ventilation system of the TRP.

2. With the small iodine concentration in these experiments, it is believed that there is an effect of material characteristics on adsorbents, such as specific surface, pore size, pressure drop, silver content etc. However it is necessary to collect more detailed data to verify this.

3. An increase of NOx concentration in the process effected the performance of the adsorbents. It is necessary to investigate the effect of NO and NO_2 respectively in further experiments.

4. After the adsorption run, the result of flowing room air through the adsorbent materials indicated that effluent iodine was hardly detected. It was recognized that the adsorbed iodine was fixed stably by chemisorption.

REFERENCE

(1) L. L. Burger et al. : The Status of Radioiodine Control for Nuclear Fuel Reprocessing Plants: PNL-4689(1983)

(2) IAEA. Technical Reports Series No. 276 : Treatment, Conditioning and Disposal of Iodine-129 : VIENNA, (1987)

(3) S. Hattori et al. : Removal Iodine from Off-gas of Nuclear Fuel Reprocessing Plants with Silver Impregnated Adsorbents : Proc. 18th DOE Nucl. Airborne Waste Management and Air Cleaning Conf., 1343(1985)

(4) D. T. Pence : Science Applications, Inc. SAI-132-80-390-LJ(1980)

(5) J. G. Wolhelm et al. : Head-end Iodine Removal from a Reprocessing Plant with a Solid Sorbent : Proc. 14th ERDA Air Cleaning Conf., 447(1978)

(6) JIS B7982. :Continuous Analyzers for Oxides of Nitrogen in Flue Gas. (1988)

題　　名	Basic Photochemical Study of Plutonium and Neptunium		
発表先	RECOD'91		
発表地	仙　　台	発　表 年月日	平成3年　4月14日 ～ 4月18日
発表者 (○印口頭発表者)	所　属　名	核開部　先端室	
	○和田　幸男，和田　光二，笹尾　信之，榎田　洋一		

(要　旨)

一般に，光化学分離技術の核燃料サイクル技術への適用が期待されている。特に，再処理工程技術への適用によって工程の簡素化，液体廃棄物の低減化及びＴＲＵ元素の分離除去が図られると予想されている。

本報では，光化学分離研究の簡単な系として，プルトニウム精製工程中においてプルトニウム製品側に同伴してくるネプツニウムを除去する目的で，その光化学分離基礎試験を行った。この試験では，まず光による硝酸の分解，亜硝酸発生割合及びプルトニウム，ネプツニウム各々の原子価の光照射挙動を調べた。

その結果，プルトニウムをＰｕ（Ⅳ）に，ネプツニウムをＮｐ（Ｖ）に原子価制御できる可能性のある基礎データを得，これらの相互分離が可能な見通しを得たので報告する。

資　料　番　号
ＴＮ８４１０　９１－０５０ （８０－０２－２７８）

資料番号 TN8410 91-050

BASIC PHOTOCHEMICAL STUDY OF PLUTONIUM AND NEPTUNIUM

Y.WADA*, K.WADA*, S.SASAO*, Y.ENOKIDA**

* Innovation Technology Development Section,
Power Reactor and Nuclear Fuel Development Corporation
3371,Tokai-Mura,Naka-Gun,Ibaraki-Ken
Japan, Zip Code:319-11
Phone:0292-82-1111, Telex:0292-87-0392

** Department of Nuclear Engineering,
University of Tokyo
7-3-1,Hongo,Bunkyo-Ku,
Japan, Zip Code:113
Phone:03-3812-2111

ABSTRACT

Photochemical technologies are generally expected that it will contribute to advanced nuclear fuel reprocessing process technologies by means of using selective excitation of objective elements with photon energy and following redox reactions in solution.

In this work,as the beginning of the basic photochemical studies in the field of nuclear fuel reprocessing,feasibility studies of separation between Pu and Np by using photo-oxidization,reduction reactions have been carried out. The results indicate that there is a possibility of photochemically induced valency adjustment to separate Np from Pu in nitric acid solution.

INTRODUCTION

In the conventional nuclear fuel reprocessing technologies,chemical redox reagents have been used to adjust valencies of U,Pu. For example,U(IV) produced by electrolytic reduction or hydroxylamine(HAN) and sodium nitrite are used to adjust Pu valencies to Pu(III) and Pu(IV) respectively. However,these chemical reagents cause secondary waste solution.

The several studies of redox reaction using photo chemical technologies for nuclear fuel solution as subustitues for these reagents have been reported. In these reports,there are two kinds of studies which are basic photochemical studies of U,Pu and Np[1,2,3] and its application studies to nuclear fuel reprocessing[4,5,6]. The applicabilities of the photochemical technologies have been confirmed from the these studies. However,photo-redox reactions are generally complicated and such as complex reactions which are consist of direct reactions

$$Pu(III) \xrightarrow{\downarrow h\nu} Pu(IV) \xrightarrow{\downarrow h\nu} Pu(VI)$$

and also indirect reactions,

$$NO_3^- \xrightarrow{\downarrow h\nu} NO_2^- + O^\cdot$$

$$Pu(VI) + NO_2^- + O^\cdot \longrightarrow Pu(IV) + NO_3^-$$

are simultaneously occured by photon energy.

Therefore,basic data concerning a variation of the oxidization-reduction potential by photon-excitation,the rate of reaction and other fundamental theories have to be accumulated to control the valencies of objective elements arbitarily.

In this work,the several basic tests of light exposure for Pu and Np in nitric acid solution were carried out to evaluate the photochemical behaviors of their valencies. The valencies of Pu and Np in nitric acid solution are ordinarily Pu(III),Pu(IV), Pu(VI) and Np(IV),Np(V),Np(VI).

The distribution coefficients of their valencies between 30% TBP/dodecane and nitric acid are shown in Fig. 1[7,8]. As shown in this Fig.,Pu(IV),and Np(VI) are easely extracted to TBP. However,Pu(III) and Np(V) which are not shown in it are scarcely extracted and their distribution coefficients are about 10^{-2} and 10^{-3} respectively. Therefore,if their valencies can be controlled into the following like conditions ① Pu(IV)-Np(V) or ② Pu(III)-Np(VI),their elements are effectively mutually separated.

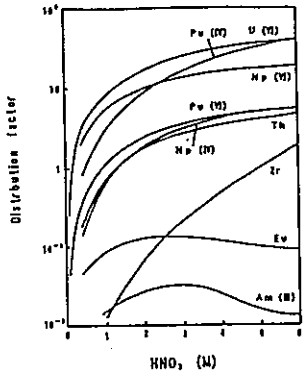

Fig. 1 Plutonium and Neptunium distribution coefficient between 30%TBP/dodecane and nitric acid

EXPERIMENTAL CONDISION

A : Preparation of Test Sample

The concentrations of Pu and Np test nitric acid solutions were adjusted to 1×10^{-4} mol and 1×10^{-3}mol respectively and they were mixed. The purity of α-radioactivity of Np-237 in Np test sample solution was 99.8 %.

Pu test sample solution were prepared by dissolving NBS-949 Pu metal of which abundance ratio of Pu-239 and Pu-241 were about 97 atom % and 0.065 atom % respectively. Therefore,the α-activity contribution of Am-241 compared to the total α-activity of Pu is lower than 1 %.

The valencies of Pu and Np test mixed solution were completely adjusted to Pu(III) and Np(V) with hydroxylamine(NH_2OH) and hydrazine(N_2H_4) as shown in Fig.2 which was the result analyzed by the extraction chromatographic method.

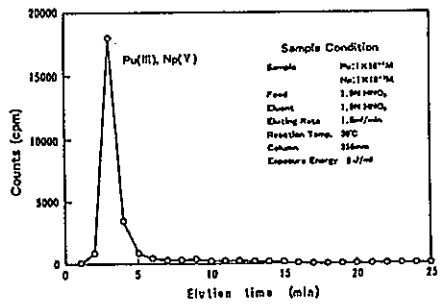

Fig. 2 Valency analysis of mixed solution with Pu and Np by extraction chromatograph

B : Test Instrument

The light exposure instrument system which was used in this work is shown in Fig.3. This system consists of the Hg lamp light source and the part of a sample cell with a temperature stabilizer and a mixing stirrer to stabilize the temparature of the sample solution and to homogenize it during light exposure.

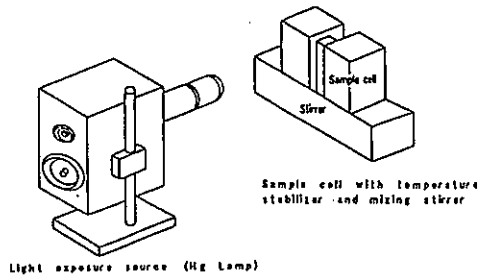

Fig. 3 Outline of instrument of light exposure test

C : Analytical Method

C-1 : Extraction Chromatograph

As a conventional technique of the valency analysis of Pu and Np,colorimetry method has been usually used. However,if concentration of an objective element in a sample solution is less than 10^{-3} mol,the method is not generally applicable.

Therefore,the new method which consisted of the extraction chromatograph and the radioactivity analysis of an each valency fraction was used.

First of all,a sample solution is injected into the extraction chromatograph column which is filled with Gas-Chrom Q made by Applied Science Corp. and impregnated with TBP. Each valency fraction of Pu and Np is obtained according to specific retention time with the fraction collector.

Then, α-radioactivity of the each fraction is measured by α counting system with ZnS detector. Consequently,the extraction chromatograph as shown in Fig.4 is obtained. The horizontal and vertical axis show an elution time and α-radioactivity(CPM) respectively.

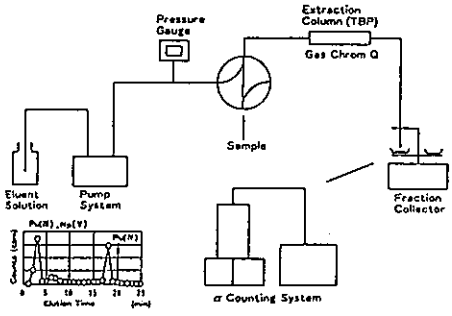

Fig. 4 Schematic diagram of extraction chromatography setup

Fig.5 shows the result of the extraction chromatographic analysis of the Pu,Np mixed solution which contains Pu(Ⅲ),Pu(Ⅳ),Pu(Ⅵ) and Np(Ⅴ). Each valency is eluted in opposite order of an adsorption tendency with TBP.

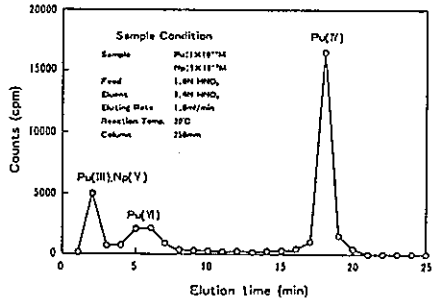

Fig. 5 Valency analysis of mixed solution with Pu and Np by extraction chromatograph

C-2 : Pluse Height Analysis

The fraction of Pu(Ⅲ) and Np(Ⅴ) mixed solution of which valencies are simultaneously eluted as shown in Fig.5 is analyzed by α spectrometry to distinguish between Pu(Ⅲ) and Np(Ⅴ). Fig.6 shows the result of α spectrometric analysis. As shown in this Fig.,Pu and Np are distinguished according to α ray energy from their nuclides and the mixture ratio is quantitatively determined.

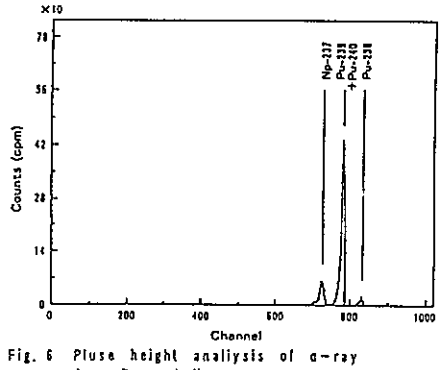

Fig. 6 Pluse height analiysis of α-ray from Pu and Np

RESULTS AND DISCUSSION

Fig.7 shows the step flow of the light exposure tests for Pu and Np in this work. First,the initial valencies condition of Pu,Np mixed sample was adjusted to Pu(Ⅲ),Np(Ⅴ) and their concentrations were 1×10^{-4}mol,1×10^{-3}mol respectively .

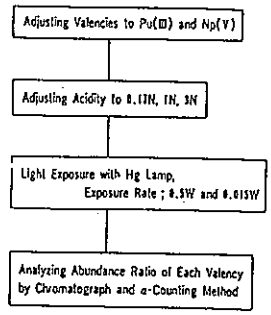

Fig. 7 Step flow of light exposure tests

At the second step,the acidities of several aliquots of the initial sample were adjusted to about 0.2N,1N and 3N.

Next,the light exposure tests were carried out with the exposure rates of 0.5W and 0.015W using the Hg lamp.

At the final step,the radioactive analyses of the each fraction from the extraction chromatograph column were carried out. As shown in this fig.,the parameters of these tests are the acidity of the sample solution and the rate of light exposure.

Fig.8 shows the results of the light exposure tests under the conditions of which the parameters are 3N nitric acid and 0.5W exposure rate.

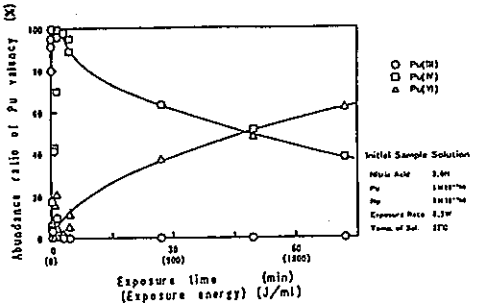

Fig. 8 Redox reaction of Pu by light exposure

The horizontal and the vertical axis in this Fig. show the exposure time(energy) and the abundance ratio(%) of the each valency in the element respectively.

This result indicates that 0.5W of the light exposure rate was too strong so that Pu(III) momentarily decreased untill about zero percent level and Pu(IV) oppositely momentarily increased. After several minutes,Pu(IV) gradually decreased and on the contrary, Pu(VI) gradually increased. In other words,it shows that Pu(III) was momentarily oxidized to Pu(IV) and seemingly,Pu(IV) was gradually oxidized to Pu(VI) under such as the conditions due to the equilibrium of the oxidization-reduction reaction.

Fig.9,10,11 show the results of the light exposure tests under the conditions of the light exposure rates ; 0.015W and of the acidities ; 0.17N,1N,3N. These Fig. show that Pu(III) was more slowly oxidized to Pu(IV) than at the case of Fig.8 and the rates of these oxidizations became faster according to the increase in acidity.

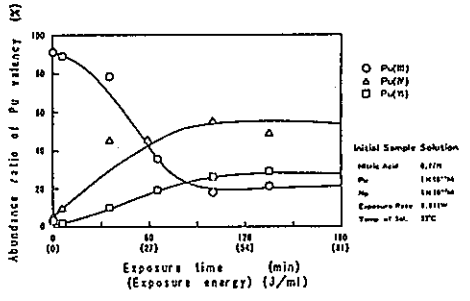

Fig. 9 Redox reaction of Pu by light exposure

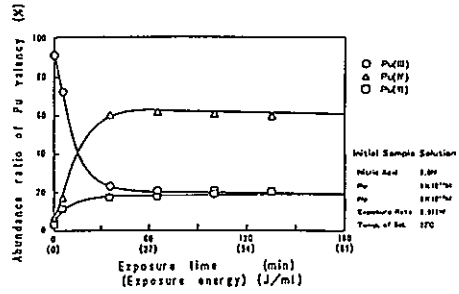

Fig. 10 Redox reaction of Pu by light exposure

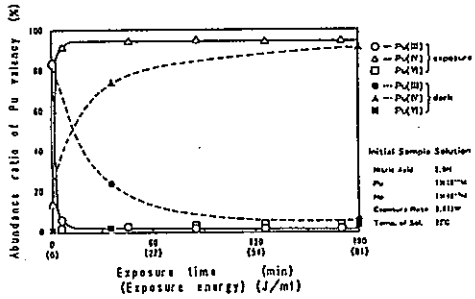

Fig. 11 Redox reaction of Pu by light exposure

Particularly,the results of Fig.11 were characteristic in the redox reaction because Pu(III) was momentally completely oxidized to Pu(IV). Furthermore,there was little Pu(III) and Pu(VI) issued from the oxidization of Pu(IV) and the equilibrium state reached within about 10 minutes after the beginning of light exposure.

The result of the dark test without light exposure was also shown in Fig.11. This result shows that Pu(III) was very slowly oxidized to Pu(IV) and it took about two hours untill the equilibrium state.

Fig.12 shows the result of the extraction chromatographic analysis of the sample at the equilibrium state when the exposure energy was 56 J/ml in Fig.11. From this result,it was also found that the valencies of Pu were controlled to Pu(IV) and there was little Pu(III) and Pu(VI).

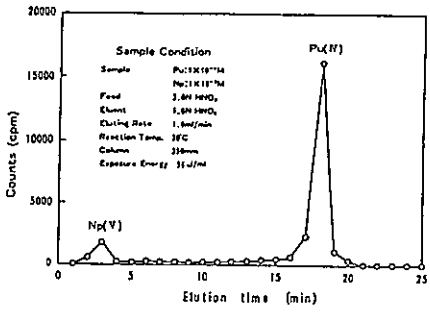

Fig. 12 Valency analysis of mixed solution with Pu and Np by extraction chromatograph

Then,this Fig. shows that Np(V) in the initial sample was not oxidized and also was not reduced by light exposure under these conditions.

Such as controlled valencies condition,Pu(IV)and Np(V),is most suitable for the separation between Pu and Np.

These photochemical behaviors were caused by the direct excitation with photon energy for an objective ion,redox reactions with the photolytic products such as HNO_2,NO_2 from HNO_3 and other excited species.

The supposed theories for these results should be discussed in several aspects of the standard electrode potentials for all of coexisting element species, excitation level by photon energy and wave length characteristic of exposure light,etc on the basis of the data obtained from furthermore detail photochemical tests.

CONCLUSION AND R&D PLAN IN THE NEXT STEP

From this work,following conclusions were obtained

◆ Results of Photochemical Behaviors of Pu and Np

① Pu
- Pu(Ⅲ) is oxidized to Pu(IV) and until Pu(VI) by light exposure.
- As to the oxidization of Pu(Ⅲ)->Pu(IV),the more the acidity of nitric acid solution increase,the more the reaction is easily proceed in the range of 0.1N->3N HNO_3.
- On the other hand,in the case of the reaction of Pu(IV)->PU(VI), the more the acidity decrease,the more the generation rate of Pu(VI) increase in the range of 0.1N->3N HNO_3.

② Np
- Np(V) is not oxidized to Np(VI) and also is not reduced to Np(IV) by light exposure in HNO_3 of 0.1N->3N.

◆ Conclusion
- It is defined that there is a possibility of removal of Np from Pu,Np mixed solution which is adjusted to Np(V) and Pu(Ⅲ) by using photochemical reactions with the adequate rate of light exposure and the adequate acidity of HNO_3.

From above the discussions and conclusions,following R&D of the next step are planed.

◆ R&D Plan in The Next Step
- The continued photochemical studies for the removal technologies of several percent of Np contained in Pu production solution simulating the reprocessing process.
- The studies of photochemical behaviors of U, Pu and Np in a mixed nitric acid solution.
- The studies of selective separation technologies of objective elements(U,PU,TRU and FP) by using photochemical techniques with a selective wave length of laser.
- The development of the quantitative analysis method of trace amounts of an objective element by the laser-induced thermal lensing spectroscopy.

REFERENCES

(1) L.TOTH and H.FRIEDMAN, "The Photochemistry of Neptunium in Aqueous Nitric Acid Solution," Radiochim.Acta,27,173(1980).

(2) H.FRIEDMAN and L.TOTH, "Photochemically Induced Reduction of Trace Np(VI) in U(VI)-HNO Solution," J.Inorg. Nucl. Chem.,43,1811(1981)

(3) Y.ENOKIDA and A.SUZUKI, "Laser Photochemical Neptunium Separation," Proc.Int.Conf.Nuclear Fuel Reprocessing and Waste Management RECOD 87 ,1,475(1987)

(4) T.Gangwer, "Photochemistry Relevant to Nuclear Waste Separations-A Feasibility Study" BNL-50715(1977)

(5) J.BELL and L.TOTH, "Photo and Radiation Chemistry in Nuclear Fuel Reprocessing," Radiochim.Acta,25,225(1978).

(6) Y.ENOKIDA and A.SUZUKI, "Application of Laser Separation Process to Nuclear Fuel Reprocessing" ,NEUT Research Report 87-04(1987).

(7) J.F.FLAGG,:Chemical Processing of Reactor Fuels(Academic Press,1966)

(8) J.T.Long:Engineering for Nuclear Fuel Reprocessing (Gordon & Breach,1967)